EXPANDING OUR CURRENT UNDERSTANDING OF VITAMIN B_6 METABOLISM IN *SALMONELLA ENTERICA*

by

HUONG NGUYEN NHU VU

(Under the Direction of Diana M. Downs)

ABSTRACT

Vitamin B_6 is an essential micronutrient for many biological processes in all three domains of life. Among the six B_6 vitamers, pyridoxal 5′-phosphate (PLP) plays an irreplaceable role in cellular functions as a universal and versatile cofactor. Pathways involving PLP-dependent enzymes permeate the metabolic network, making studying vitamin B_6 a powerful tool to probe the complexity of microbial physiology and metabolism. The research described herein seeks to expand our current knowledge on vitamin B_6 biosynthesis, salvage, and homeostasis using *Salmonella enterica* serovar Typhimurium as a model organism. The first study investigates the unique ability of *S. enterica* to salvage phosphorylated B_6 vitamers and identifies the enzyme responsible for this process. The next study examines the adverse effects of 4-deoxypyridoxine and uncovers a metabolic connection between vitamin B_6 metabolism and synthesis of thiamine and coenzyme A. The last two studies explore the phenotypic and metabolic consequences caused by a mutation in *yggS*, which encodes a PLP-binding protein of unknown function, with a focus on vitamin B_6 homeostasis and aspartate biosynthesis.

INDEX WORDS: Vitamin B_6, Pyridoxal 5′-phosphate, Metabolism, YggS, *Salmonella enterica*

EXPANDING OUR CURRENT UNDERSTANDING OF VITAMIN B_6 METABOLISM IN *SALMONELLA ENTERICA*

by

Huong Nguyen Nhu Vu

B.S., San José State University, 2015

A Dissertation Submitted to the Graduate Faculty of The University of Georgia in Partial Fulfillment of the Requirements for the Degree

DOCTOR OF PHILOSOPHY

ATHENS, GEORGIA

2021

EXPANDING OUR CURRENT UNDERSTANDING OF VITAMIN B_6 METABOLISM IN *SALMONELLA ENTERICA*

by

HUONG NGUYEN NHU VU

Major Professor:	Diana M. Downs
Committee:	Jorge C. Escalante-Semerena
	Zachary A. Lewis
	M. Stephen Trent

Electronic Version Approved:

Ron Walcott
Vice Provost for Graduate Education and Dean of the Graduate School
The University of Georgia
December 2021

ACKNOWLEDGEMENTS

First and foremost, I would like to thank my research advisor, Dr. Diana Downs, for her guidance and patience. She always encouraged me to think outside the box and go beyond simple phenotypic analyses to achieve more sophisticated and testable models. Her enthusiasm and encouragement were integral to shaping my passion for microbial physiology and metabolism. I would also like to thank my committee members, Dr. Jorge Escalante, Dr. Stephen Trent, and Dr. Zachary Lewis, for their constructive feedback regarding my research projects.

I would like to express my gratitude to Dr. Elizabeth Skovran at San José State University. Not only did she welcome me, a junior undergraduate student with no prior research experience, to her laboratory, but she also opened my eyes to the wonders of microbiology and instilled in me the love for bacterial genetics. Without a doubt, Dr. Skovran was the reason why I started and have been pursuing a career in research.

My time at UGA would have been a lonely journey without my friends and colleagues that I have met over the years in Georgia and California. I would like to thank Jessica, for showing me the power of compassion and empathy; Mike, for exchanging crazy ideas and answering my questions about biochemical techniques; Dustin and Kelsey, for mentoring me during my rotation; Brandi and Kailey, for going on walks with me and being my complaint department; Rachael, for sending me care packages; my UGA friends from Vietnam, for organizing dinners to celebrate both American and Vietnamese holidays; current and past members of the Downs and Escalante laboratory, for giving constructive critiques of my research and sharing resources. To the rest of my cohort, we are almost at the finish line!

Last but not least, I would like to dedicate my academic achievements to my parents, Thang and Hoai, for having always been with me since the very start of my education; to my aunt Hoai, uncle Hung, and cousin Hang and Hien, for welcoming me to their family after I moved to the United States to attend college; to my brother Triet and all relatives in my extended family, for making me feel at home at countless family gatherings; and to my husband, Richard, for being my partner in life (and partner in crime) throughout my undergraduate and graduate years. Without their love and support, I could not have become the scientist and the person that I am today.

TABLE OF CONTENTS

Page

ACKNOWLEDGEMENTS iv

CHAPTER

1 INTRODUCTION AND LITERATURE REVIEW 1

2 AN UNEXPECTED ROLE FOR THE PERIPLASMIC PHOSPHATASE PHON IN THE SALVAGE OF B_6 VITAMERS IN *SALMONELLA ENTERICA* 25

3 GENETIC ANALYSIS USING VITAMIN B_6 ANTAGONIST 4-DEOXYPYRIDOXINE DEFINES A CONNECTION BETWEEN PYRIDOXAL 5′-PHOSPHATE AND COENZYME A METABOLISM IN *SALMONELLA ENTERICA* 63

4 THE ROLE OF YGGS IN VITAMIN B_6 HOMEOSTASIS IN *SALMONELLA ENTERICA* IS INFORMED BY HETEROLOGOUS EXPRESSION OF YEAST *SNZ3* 97

5 LOSS OF YGGS (COG0325) IMPACTS ASPARTATE METABOLISM IN *SALMONELLA ENTERICA* 127

6 CONCLUSIONS AND FUTURE DIRECTIONS 163

CHAPTER 1

INTRODUCTION AND LITERATURE REVIEW

Metabolic networks are composed of functional modules integrated in a hierarchical topology. The hierarchical modularity model of cellular metabolism predicts that (i) changes occurring locally in small, highly interconnected modules can affect larger, less cohesive units; and (ii) modules that arose first play a key role in the network due to their complex integration with other subnetworks (1). However, the impacts of metabolic perturbations in a pathway on overall physiology can be minimized or masked by tuning the pathway components via transcriptional regulation, post-translational modification, and/or flux control. Such plasticity and robustness of metabolic networks in nature make studying metabolism a complicated and challenging task. Regardless, there have been tremendous efforts made to understand cellular metabolism, specifically in the research area of vitamins and cofactors.

Vitamin B_6 has been a focal point of research since its discovery almost 90 years ago. Proposed to have emerged before the divergence of species, vitamin B_6 metabolism consists of pathways that are partially conserved, making it a suitable tool to dissect complex interactions among metabolic nodes. Vitamin B_6 is a collective term for six vitamers, including pyridoxal 5′-phosphate (PLP), pyridoxine 5′-phosphate (PNP), pyridoxamine 5′-phosphate (PMP), and their unphosphorylated forms (pyridoxal/PL, pyridoxine/PN, pyridoxamine/PM) (Figure 1.1). Among the six vitamers, PLP is a ubiquitous and versatile cofactor required for cellular functions across domains of life. PLP-dependent enzymes account for more than 140 distinct biochemical activities,

including transamination, decarboxylation, racemization, and elimination (2). Enzymes that rely on PLP for catalysis are classified into seven fold types based on structural similarity (3). In all fold types, PLP is covalently bound to a conserved lysine residue in the active site via a Schiff-base linkage. The reaction mechanism involves transformation from a PLP-enzyme internal aldimine to PLP-substrate external aldimine, which proceeds to a quinonoid intermediate and subsequently specific products, depending on the type of reaction being catalyzed (4). Like many other vitamin cofactors, PLP can be synthesized *de novo* via one of the two biosynthetic routes, or acquired from the environment via the salvage pathway (Figure 1.1).

Given the wealth of knowledge spanning decades of research in different organisms, this chapter summarizes the known and unknown aspects of *de novo* PLP biosynthesis, salvage of B_6 vitamers, connection of vitamin B_6 metabolism with various metabolic processes, vitamin B_6 homeostasis, and finally gives an outline of the dissertation.

1.1 *DE NOVO* PLP BIOSYNTHESIS

Deoxyxylulose-5-phosphate (DXP)-independent pathway. Most organisms capable of synthesizing PLP *de novo* use the DXP-independent pathway (Figure 1.1) (5, 6), which relies on a PLP synthase complex consisting of twelve glutaminase and twelve PLP synthase subunits (7). The glutaminase enzyme (EC 3.5.1.2), which is designated as PdxT in *Bacillus subtilis*, SNOp in *Saccharomyces cerevisiae*, and Pdx2 in higher organisms, converts glutamine to glutamate and ammonia (8-11). The PLP synthase (EC 4.3.3.6), which also has triose/pentose isomerase activity and is designated as PdxS, SNZp, and Pdx1 in *B. subtilis*, *S. cerevisiae*, and higher organisms respectively, combine ammonia with ribose-5-phosphate/ribulose-5-phosphate and glyceraldehyde-3-phosphate (G3P)/dihydroxyacetone phosphate to produce PLP (12, 13). The

activity of Pdx2 was shown to be dependent on Pdx1 (8-11). However, Pdx1 could function without the glutaminase subunit if sufficient ammonium was provided (8, 14, 15). Despite being experimentally discovered later than the DXP-dependent route, the DXP-independent pathway is more widespread among bacteria, archaea, fungi, and plants (5, 6). Along with the salvage pathway, the DXP-independent PLP biosynthesis is thought to have emerged before the divergence of species into three domains of life (6).

DXP-dependent pathway. Alternatively, a subset of bacterial species, primarily γ-proteobacteria, can synthesize PLP *de novo* using the DXP-dependent pathway (5, 6), which consists of two branches and a total of seven catalytic steps (Figure 1.1). The first branch converts erythrose-4-phosphate (E4P), an intermediate from the pentose phosphate pathway, to 3-amino-1-hydroxyacetone 1-phosphate through four consecutive reactions catalyzed by erythrose-4-phosphate dehydrogenase (Epd, EC 1.2.1.72), erythronate-4-phosphate dehydrogenase (PdxB, EC 1.1.1.290), phosphoserine/phosphohydroxythreonine aminotransferase (SerC, EC 2.6.1.52), and 4-hydroxythreonine-4-phosphate dehydrogenase (PdxA, EC 1.1.1.262), respectively (16-18). This branch shares enzymes homologous to the serine biosynthetic pathway and thus is thought to have evolved through gene recruitment (19, 20). One of the biosynthetic enzymes, SerC, requires PLP as a cofactor to function (17), paradoxically making PLP involved in its own synthesis. This observation is consistent with the proposed evolution of vitamin B_6 metabolism, in which the DXP-dependent PLP biosynthesis emerged after the DXP-independent and salvage pathway (6). In the second branch, DXP synthase (Dxs, EC 2.2.1.7) takes G3P and pyruvate to form DXP (21, 22), which PNP synthase (PdxJ, EC 2.6.99.2) subsequently combines with the product of the first branch to produce PNP (23). In the final step of the DXP-dependent PLP biosynthesis, PNP is

oxidized to PLP by PNP/PMP oxidase (PdxH, EC 1.4.3.5), an enzyme that also participates in the salvage pathway of B_6 vitamers (24).

Serendipitous pathways. Previous work in *Escherichia coli* suggests that given a specific genetic/metabolic context, enzymes with promiscuous activities have the potential to form serendipitous pathways that can replace *de novo* DXP-dependent PLP biosynthesis (25). There are at least five serendipitous routes to bypass a block at the PdxB-catalyzed step (Figure 1.1). In the first case, it was reported that ThiG (thiazole synthase, EC 2.8.1.10), whose canonical function is to synthesize the thiazole moiety of thiamine (vitamin B_1), could rescue growth of an *E. coli pdxB* mutant when overexpressed (26). A computational approach in the same study identified structural similarities between *E. coli* ThiG and *B. subtilis* PdxS (PLP synthase, EC 4.3.3.6) (26). However, the putative PLP synthase activity of ThiG has not been reconstituted *in vitro.* If ThiG indeed functions as a promiscuous PLP synthase, overexpression of this enzyme can perhaps replace the entire DXP-dependent pathway, which can be tested using *E. coli* strains carrying a *pdxJ* and/or *pdxH* mutation (Figure 1.1).

Two other serendipitous pathways require multiple promiscuous enzymes and mutations to rescue the PLP auxotrophy of an *E. coli pdxB* mutant (Figure 1.1) (27, 28). One route utilizes NudL (putative hydrolase), LtaE (low-specificity threonine aldolase, EC 4.1.2.48) and ThrB (homoserine kinase, EC 2.7.1.39) to divert 3-phospho-hydroxypyruvate, an intermediate of serine biosynthesis, to 4-phosphohydroxy-L-threonine, the substrate of PdxA in the DXP-dependent pathway (27). The other route recruits SerA (phosphoglycerate dehydrogenase, EC 1.1.1.95/1.1.1.399), SerC, and ThrB to bypass the blocked step catalyzed by PdxB (28). The mechanisms of the remaining two serendipitous pathways, one proceeds via a 3-dehydroquinate

synthase (AroB, EC 4.2.3.4) and the other via an imidazole-glycerol-phosphate dehydratase/histidinol-phosphatase (HisB, EC 4.2.1.19/3.1.3.15), a putative metallohydrolase (Php), and a PF01894 family protein of unknown function (YjbQ), have not been determined (27). Additional mutations to change enzyme levels, metabolite concentrations, and/or flux are necessary for the physiological function of the four pathways (27, 28).

1.2 SALVAGE OF B_6 VITAMERS

Canonical salvage pathway. In addition to *de novo* synthesis, many organisms are equipped with the salvage pathway to obtain PLP from the environment (Figure 1.1). Humans and animals lack the ability to synthesize this cofactor and thus rely exclusively on salvage (5, 6). On the other hand, bioinformatic analysis of available genomes failed to identify signature genes of the salvage pathway in Gram-positive bacteria and archaea (5), suggesting these species depend on *de novo* synthesis as the only source for PLP. In the canonical salvage pathway, unphosphorylated B_6 vitamers are trapped in the cytoplasm/cytosol via phosphorylation by PL/PN/PM kinase (PdxK, EC 2.7.1.35) (29) and/or PL kinase (PdxY, EC 2.7.1.35) (30). For PNP and PMP, one additional step catalyzed by PNP/PMP oxidase (PdxH) is required to convert these vitamers to PLP (24). Besides the conserved salvage components, some organisms also have accessory enzymes to interconvert B_6 vitamers. Homologs of PL reductase (PdxI, EC 1.1.1.65) capable of converting PL to PN have been found in *E. coli*, *Schizosaccharomyces pombe*, *Arabidopsis thalia*, and humans (31-34). The reverse reaction from PN to PL can also be achieved enzymatically with *Mesorhizobium loti* pyridoxine 4′-oxidase (EC 1.1.3.12) (35). In addition, PLP phosphatase (EC 3.1.3.74), such as YbhA in *E. coli* and hPLPP in humans (36-38), has been characterized *in vitro*, although their proposed *in vivo* role in PLP homeostasis needs further investigation.

Catabolism of vitamin B_6. Some microorganisms can use unphosphorylated B_6 vitamers as a sole source of carbon and nitrogen (39). Two distinct pathways, both of which share some common end products, have been characterized (Figure 1.1). The first catabolic route, which proceeds via a 4-pyridoxic acid (4PA) intermediate, was first identified in *Pseudomonas* MA-1 and later in *Mesorhizobium loti* (35, 40). Through a series of eight enzymatic steps, PN is converted to succinic semialdehyde, acetate, ammonia, and carbon dioxide (41). Alternatively, in *Pseudomonas* IA and *Arthrobacter* Cr-7 (40, 42), PN is broken down to 2-(hydroxymethyl)-4-oxobutanoate, acetate, ammonia, and carbon dioxide using the second catabolic pathway, which comprises five catalytic steps and proceeds through a 5-pyridoxic acid (5PA) intermediate (41). In both cases, the degradation products of B_6 vitamers subsequently enter central carbon and nitrogen metabolism. Since all instances of vitamin B_6 catabolism are found in soil bacterial species, it is curious to know if the distribution of these pathways extends beyond environmental isolates.

Uptake of vitamin B_6. As known B_6 salvage enzymes are cytoplasmic/cytosolic, exogenous B_6 vitamers need to be taken up by the cells through transporters. Interestingly, only a few transporters for B_6 vitamers have been described. In some yeasts and plants, unphosphorylated B_6 vitamers are imported via proton symporters, such as Tpn1p in *S. cerevisiae*, Bsu1p in *S. pombe*, PUP1 in *A. thalia*, and NUP1 in *Nicotiana tabacum* (43-46). In bacterial species with identified B_6 transporters, the uptake process is thought to require energy input. Data from mass spectrometry and molecular dynamics simulation suggest that *Lactobacillus brevis* PdxU is an energy-coupling factor transporter for PM (47), though whether this protein complex functions as a *bona fide* B_6 transporter *in vivo* has not been experimentally verified. Notably, it was shown that in the pathogen *Actinobacillus pleuropneumoniae*, a binding protein-dependent ABC transporter system, which

consists of a periplasmic binding protein (P5PA), a permease (P5PB), and an ATPase (AfuC), could transport PLP and rescue PLP auxotrophy when expressed in an *E. coli* strain defective in *de novo* PLP synthesis (48). This recently described system is the only known example of a transporter that can import a phosphorylated form of vitamin B_6. In *Salmonella enterica* and *E. coli*, uptake of unphosphorylated B_6 vitamers is proposed to occur via facilitated diffusion, though specific transporter(s) has not been identified (49-51). Despite not being considered a part of the canonical salvage pathway, components of vitamin B_6 uptake remain crucial in PLP acquisition.

1.3 INTEGRATION OF VITAMIN B_6 METABOLISM IN BIOLOGICAL PROCESSES

Vitamin B_6 metabolism connects with other metabolic subnetworks via shared intermediates and enzymes. The first committed step of the DXP-dependent for *de novo* PLP biosynthesis is catalyzed by Epd and involves E4P (Figure 1.1) (16). E4P is an intermediate derived from the pentose phosphate pathway and a precursor of several aromatic amino acids (tryptophan, phenylalanine, and tyrosine) and chorismate derivatives (4-aminobenzoate, 4-hydroxybenzoate, and 2,3-dihydroxybenzoate). Hints leading to the discovery of this reaction stemmed from a previous report that growth of an *E. coli* mutant carrying lesions in *tktA* and *tktB* (encoding transketolase 1 and 2, EC 2.2.1.1) required PL/PN, in addition to aromatic amino acids and chorismate derivatives (52). It is curious to know if flux perturbations in the pentose phosphate pathway would lead to changes in vitamin B_6 levels, and conversely if changes in vitamin B_6 metabolism would impact the pentose phosphate pathway or biosynthesis of aromatic amino acids. In the second branch of the DXP-dependent PLP synthesis (Figure 1.1), DXP is also a precursor of thiamine and isoprenoids (21). This poses a potential bottleneck for the biosynthesis of these metabolites when flux towards DXP is restricted.

Enzyme promiscuity also links vitamin B_6 metabolism with other metabolic nodes. In the first branch of PLP synthesis, *E. coli* SerC can catalyze the transamination reaction of 3-phosphohydroxypyruvate to 3-phospho-serine, a precursor of serine (20). In addition, PdxK in the salvage pathway was shown to have kinase activity using the pyrimidine moiety of thiamine as a substrate (53). As mentioned above, many enzymes in the serendipitous routes are recruited from other pathways, including thiamine, serine, and threonine biosynthesis (26-28). These connections give support to the idea that new pathways emerge by building upon existing functional components of other metabolic modules.

PLP-dependent enzymes permeate metabolic network. PLP-dependent enzymes, most of which use amino substrates, account for ~4% of all classified activities by the Enzyme Commission (2). Notable examples include aspartate aminotransferase (EC 2.6.1.1) in aspartate synthesis, serine hydroxymethyltransferase (EC 2.1.2.1) in one-carbon unit generation, 5-aminolevulinate synthase (EC 2.3.1.37) in tetrapyrroles biosynthesis, and glycogen phosphorylase (EC 2.4.1.1) in glycogen degradation (54-57). As such, significant perturbations in vitamin B_6 metabolism and/or damages to PLP-dependent enzymes are predicted to affect multiple metabolic nodes, although the degree of impact depends on the plasticity of specific pathways and genetic context (58, 59).

1.4 HOMEOSTASIS OF B_6 VITAMERS

Homeostasis of B_6 vitamers is achieved when input and output of free and enzyme-bound pools are in equilibrium to support normal cellular metabolism. Processes that increase vitamin B_6 levels include *de novo* synthesis and salvage from the environment and/or protein turnover.

Meanwhile, loss of B_6 vitamers can occur through cell division, excretion/leakage, enzymatic/chemical degradation, and nonspecific binding/promiscuous reactions. Interconversion among B_6 vitamers can also affect their intracellular distribution. Among the six vitamers, PLP is the predominant form of vitamin B_6, totaling ~40-50% of intracellular B_6 pool (60, 61). It is estimated that ~40% of endogenous PLP level in *E. coli* exists as free PLP (61). Due to the reactive nature and the biological relevance of this cofactor, PLP has been the focus of vitamin B_6 homeostasis.

Adverse consequences of perturbed PLP levels. With a reactive aldehyde group at the 4′ position (Figure 1.1), PLP can inhibit PLP-independent enzymes *in vitro* (62-64). In addition to direct enzyme modifications, changes in PLP levels can perturb metabolic nodes that rely on PLP-dependent enzymes. In yeast, disruption in mitochondrial PLP trafficking results in lower activity of 5-aminolevulinate synthase (65), a PLP-dependent enzyme in heme biogenesis, leading to reduced mitochondrial heme content (66). In plants, root growth defects have been observed in vitamin B_6-deficient mutants due to decreased levels of the phytohormone auxin (67), the synthesis of which requires a PLP-dependent tryptophan aminotransferase (EC 2.6.1.27) (68). In humans, vitamin B_6 deficiency is associated with various symptoms, such as electroencephalographic abnormalities, microcytic anemia, weakened immune response, and seizures (69-72). The proposed mechanisms underlying some of these conditions are linked to changes in activity of PLP-dependent enzymes involved in neurotransmitter metabolism (73). Taken together, the reactivity of PLP molecule and the overarching involvement of PLP-dependent enzymes in other biological processes highlight a need to control the intracellular concentration of this cofactor.

Transcriptional and allosteric regulation of vitamin B_6 metabolism. Many organisms can regulate the *de novo* biosynthesis and salvage pathways for PLP at the transcriptional level. One interesting class of transcriptional regulators is the bacterial MocR-like subfamily of the GntR transcription factors, which contain an N-terminal helix-turn-helix domain capable of DNA binding linked to a C-terminal aminotransferase-like domain capable of effector binding (74). Some members of the MocR-like subfamily, designated PdxR homologs, activate expression of *pdxST* genes encoding the glutaminase and PLP synthase subunits of the DXP-independent pathway in Gram-positive bacteria (75-78). In these cases, binding of PLP to PdxR reduces the activation of *pdxST* transcripts, and this transcriptional factor also functions as an autorepressor of its own gene expression (75-78). Another example comes from a study of PtsJ, a transcriptional repressor in *S. enterica* (79). Typical of the MocR-like subfamily, the C-terminal domain of PtsJ resembles fold type I of PLP-dependent enzymes and can bind PLP as an effector molecule. Interestingly, PLP binding enhances the binding of PtsJ to the promoter region of *pdxK*, thus controlling the salvage pathway via transcriptional repression (79). In the soil bacterium *M. loti*, expression of several genes encoding enzymes in the 4PA-dependent vitamin B_6 degradation pathway is repressed by PyrR, which belongs to the VanR subgroup of the GntR family (80). Further investigation is necessary to determine if PyrR binds to any B_6 vitamer as an effector.

In addition to transcriptional modulation, allosteric regulation is proposed to play a role in controlling flux towards PLP formation. Kinetic and structural studies suggest that PLP binding to the allosteric site of *E. coli* PNP/PMP oxidase (PdxH), which is involved in both *de novo* synthesis and salvage of PLP, leads to complete inactivation of this enzyme (81, 82). Interestingly, PdxH can transfer the PLP molecule bound to its allosteric site and reactivate another apo-PLP-dependent enzyme *in vitro* (83). The activity of another salvage enzyme, PL/PN/PM kinase

(PdxK), is inhibited by high levels of its substrate (PL) and product (PLP) when assayed *in vitro* (84, 85). However, the physiological relevance of these *in vitro* findings remains to be verified.

Connection between YggS (COG0325) and homeostasis of B_6 vitamers. One potential player in vitamin B_6 homeostasis is YggS, a conserved PLP-binding protein of unknown function. Initially identified using a computational approach, *S. cerevisiae* YggS homolog (Ybl036c) was purified as a monomer and showed structural similarity with alanine racemase and ornithine decarboxylase, two fold type III PLP-dependent enzymes (86). However, alanine racemase activity of YggS was not detected *in vitro* (87) or *in vivo* (88). Subsequent work in *E. coli* reported that YggS binds to PLP via a conserved lysine residue, and PLP binding was essential for the function of this protein (87). Spectral analysis in the same study failed to detect binding of purified YggS to any L- or D-amino acids under the condition tested (87).

Many pleiotropic effects caused by mutations in *yggS* homologs have been documented in different organisms. Lack of YggS altered amino acid, α-keto acid, and CoA levels in *E. coli* (87, 89-92). Patients carrying pathogenic variants of PLPHP, the human homolog of YggS, showed similar perturbations in metabolic pools (93-98). Notably, significant changes in B_6 vitamer levels were observed in all organisms (88, 90-94, 97), implicating YggS in vitamin B_6 homeostasis. To date, a precise mechanism of YggS function has not been determined.

1.5 DISSERTATION OUTLINE

Built upon the foundation of previous research in other organisms, this dissertation describes my efforts in investigating the unknown aspects of vitamin B_6 metabolism using *S. enterica* serovar Typhimurium as a model organism. *S. enterica* is a Gram-negative facultative

anaerobe capable of infecting humans and animals. Like other γ-proteobacteria, this enteric pathogen relies on the DXP-dependent pathway for *de novo* PLP synthesis as well as the salvage pathway to acquire this cofactor from the environment. The work that follows sheds light on the biosynthesis, salvage, integration, and homeostasis of B_6 vitamers in *S. enterica*, the metabolism of which is often mistakenly assumed to be indistinguishable from that of *E. coli.*

Chapter 2 investigates the ability to utilize phosphorylated B_6 vitamers of an *S. enterica* strain defective in *de novo* biosynthesis of PLP. Genetic and biochemical approaches identified PhoN, a class A acid phosphatase (EC 3.1.3.2), as the enzyme responsible for converting PLP and PNP to PL and PN, respectively. The periplasmic localization of PhoN was determined to be essential for its function in salvaging phosphorylated B_6 vitamers. Enzyme promiscuity and conservation of the vitamin B_6 salvage pathway in *S. enterica* and *E. coli* was also discussed.

Chapter 3 employs the sensitivity of an *S. enterica ptsJ* mutant to 4-deoxypyridoxine (dPN), a vitamin B_6 antagonist, to probe the connection between vitamin B_6 metabolism and other metabolic nodes. Analyses of the growth phenotypes and intracellular B_6 profiles of *ptsJ* strains with and without intact *pdxK* (encoding a PL/PN/PM kinase, EC 2.7.1.35) indicated that dPN toxicity was dependent on phosphorylation by PdxK to 4-deoxypyridoxine 5′-phosphate (dPNP), which could interfere with the DXP-dependent PLP biosynthesis. Genetic evidence showed that in the presence of dPNP, thiamine synthesis was compromised, which was an indirect consequence of reduced coenzyme A level. Nutritional supplementation data suggested that GlyA (serine hydroxymethyltransferase, EC 2.1.2.1) and GcvP (glycine decarboxylase, EC 1.4.4.2), two PLP-dependent enzymes involved in generating one-carbon units, were also affected, resulting in lower flux to the CoA precursor pantoate.

Chapter 4 explores the phenotypic and metabolic consequences associated with a mutation in *yggS*, which encodes a PLP-binding protein of unknown function implicated in vitamin B_6 homeostasis. Despite having no significant growth defect, an *S. enterica* strain lacking YggS exhibited dramatic changes in intracellular PNP and extracellular PLP levels, which was also observed in an *E. coli yggS* mutant. The use of a heterologous expression system for PLP biosynthesis in place of the native pathway revealed perturbations in PLP and PMP levels, which were attributed to an epistasis between YggS and PdxH (PNP/PMP oxidase, EC 1.4.3.5). Based on vitamin B_6 profiles in different *yggS*$^+$ and *yggS*$^-$ backgrounds, a general model of YggS placement in modulating PLP→PMP cycling was proposed. This model predicts potential impacts on transamination reactions, which is demonstrated in the subsequent chapter.

Chapter 5 examines a synthetic growth defect of an *S. enterica* strain carrying lesions in *yggS* and *aspC* (encoding a PLP-dependent aspartate aminotransferase, EC 2.6.1.1). Analysis of spontaneous suppressors of *yggS aspC* mutant linked the synthetic aspartate auxotrophy to TyrB, a PLP-dependent aromatic amino acid aminotransferase (EC 2.6.1.57). Genetic and biochemical data suggested that the metabolic consequences caused by a *yggS* mutation, such as accumulation of intracellular PNP and perturbations in α-keto acid levels, inhibited TyrB activity. This chapter provides evidence consistent with the working model of YggS function proposed previously.

Chapter 6 summarizes major conclusions from previous chapters and outlines future directions for this research. Remaining questions about the identity of B_6 transporter(s) in *S. enterica*, the role of chaperone(s) in PLP incorporation into apo-enzymes, and the function of YggS in vitamin B_6 homeostasis await further investigations.

1.6 REFERENCES

1. Ravasz E, Somera AL, Mongru DA, Oltvai ZN, Barabási A-L. 2002. Hierarchical organization of modularity in metabolic networks. Science. 297:1551-1555.

2. Percudani R, Peracchi A. 2003. A genomic overview of pyridoxal-phosphate-dependent enzymes. EMBO Reports. 4:850-854.

3. Percudani R, Peracchi A. 2009. The B_6 database: a tool for the description and classification of vitamin B_6-dependent enzymatic activities and of the corresponding protein families. BMC Bioinformatics. 10:1-8.

4. Di Salvo ML, Budisa N, Contestabile R. 2012. PLP-dependent enzymes: a powerful tool for metabolic synthesis of non-canonical amino acids. Proceedings of the Beilstein Bozen Symposium on Molecular Engineering and Control. 27-66.

5. Mittenhuber G. 2001. Phylogenetic analyses and comparative genomics of vitamin B_6 (pyridoxine) and pyridoxal phosphate biosynthesis pathways. Journal of Molecular Microbiology and Biotechnology. 3:1-20.

6. Tanaka T, Tateno Y, Gojobori T. 2004. Evolution of vitamin B_6 (pyridoxine) metabolism by gain and loss of genes. Molecular Biology and Evolution. 22:243-250.

7. Strohmeier M, Raschle T, Mazurkiewicz J, Rippe K, Sinning I, Fitzpatrick TB, Tews I. 2006. Structure of a bacterial pyridoxal 5′-phosphate synthase complex. Proceedings of the National Academy of Sciences. 103:19284-19289.

8. Belitsky BR. 2004. Physical and enzymological interaction of *Bacillus subtilis* proteins required for *de novo* pyridoxal 5′-phosphate biosynthesis. Journal of Bacteriology. 186:1191-1196.

9. Dong YX, Sueda S, Nikawa JI, Kondo H. 2004. Characterization of the products of the genes *SNO1* and *SNZ1* involved in pyridoxine synthesis in *Saccharomyces cerevisiae*. European Journal of Biochemistry. 271:745-752.

10. Wrenger C, Eschbach M-L, Müller IB, Warnecke D, Walter RD. 2005. Analysis of the vitamin B_6 biosynthesis pathway in the human malaria parasite *Plasmodium falciparum*. Journal of Biological Chemistry. 280:5242-5248.

11. Tambasco-Studart M, Tews I, Amrhein N, Fitzpatrick TB. 2007. Functional analysis of PDX2 from *Arabidopsis*, a glutaminase involved in vitamin B_6 biosynthesis. Plant Physiology. 144:915-925.

12. Burns KE, Xiang Y, Kinsland CL, McLafferty FW, Begley TP. 2005. Reconstitution and biochemical characterization of a new pyridoxal-5′-phosphate biosynthetic pathway. Journal of the American Chemical Society. 127:3682-3683.

13. Raschle T, Amrhein N, Fitzpatrick TB. 2005. On the two components of pyridoxal 5′-phosphate synthase from *Bacillus subtilis*. Journal of Biological Chemistry. 280:32291-32300.

14. Paxhia MD, Downs DM. 2019. *SNZ3* Encodes a PLP synthase involved in thiamine synthesis in *Saccharomyces cerevisiae*. G3: Genes, Genomes, Genetics. 9:335-344.

15. Richts B, Lentes S, Poehlein A, Daniel R, Commichau FM. 2021. A *Bacillus subtilis* Δ*pdxT* mutant suppresses vitamin B_6 limitation by acquiring mutations enhancing *pdxS* gene dosage and ammonium assimilation. Environmental Microbiology Reports. 13:218-233.

16. Zhao G, Pease AJ, Bharani N, Winkler ME. 1995. Biochemical characterization of *gapB*-encoded erythrose 4-phosphate dehydrogenase of *Escherichia coli* K-12 and its possible role in pyridoxal 5′-phosphate biosynthesis. Journal of Bacteriology. 177:2804-2812.

17. Drewke C, Klein M, Clade D, Arenz A, Müller R, Leistner E. 1996. 4-O-phosphoryl-L-threonine, a substrate of the *pdxC* (*serC*) gene product involved in vitamin B_6 biosynthesis. FEBS Letters. 390:179-182.

18. Banks J, Cane DE. 2004. Biosynthesis of vitamin B_6: direct identification of the product of the PdxA-catalyzed oxidation of 4-hydroxy-l-threonine-4-phosphate using electrospray ionization mass spectrometry. Bioorganic and Medicinal Chemistry Letters. 14:1633-1636.

19. Schoenlein PV, Roa B, Winkler ME. 1989. Divergent transcription of *pdxB* and homology between the *pdxB* and *serA* gene products in *Escherichia coli* K-12. Journal of Bacteriology. 171:6084-6092.

20. Lam H, Winkler ME. 1990. Metabolic relationships between pyridoxine (vitamin B_6) and serine biosynthesis in *Escherichia coli* K-12. Journal of Bacteriology. 172:6518-6528.

21. Sprenger GA, Schörken U, Wiegert T, Grolle S, De Graaf AA, Taylor SV, Begley TP, Bringer-Meyer S, Sahm H. 1997. Identification of a thiamin-dependent synthase in *Escherichia coli* required for the formation of the 1-deoxy-D-xylulose 5-phosphate precursor to isoprenoids, thiamin, and pyridoxol. Proceedings of the National Academy of Sciences. 94:12857-12862.

22. Lois LM, Campos N, Putra SR, Danielsen K, Rohmer M, Boronat A. 1998. Cloning and characterization of a gene from *Escherichia coli* encoding a transketolase-like enzyme that catalyzes the synthesis of D-1-deoxyxylulose 5-phosphate, a common precursor for isoprenoid, thiamin, and pyridoxol biosynthesis. Proceedings of the National Academy of Sciences. 95:2105-2110.

23. Laber B, Maurer W, Scharf S, Stepusin K, Schmidt FS. 1999. Vitamin B_6 biosynthesis: formation of pyridoxine 5′-phosphate from 4-(phosphohydroxy)-L-threonine and 1-deoxy-D-xylulose-5-phosphate by PdxA and PdxJ protein. FEBS Letters. 449:45-48.

24. Zhao G, Winkler ME. 1995. Kinetic limitation and cellular amount of pyridoxine (pyridoxamine) 5′-phosphate oxidase of *Escherichia coli* K-12. Journal of Bacteriology. 177:883-891.

25. Richts B, Commichau FM. 2021. Underground metabolism facilitates the evolution of novel pathways for vitamin B_6 biosynthesis. Applied Microbiology and Biotechnology.1-9.

26. Oberhardt MA, Zarecki R, Reshef L, Xia F, Duran-Frigola M, Schreiber R, Henry CS, Ben-Tal N, Dwyer DJ, Gophna U. 2016. Systems-wide prediction of enzyme promiscuity reveals a new underground alternative route for pyridoxal 5′-phosphate production in *E. coli*. PLoS Computational Biology. 12:e1004705.

27. Kim J, Kershner JP, Novikov Y, Shoemaker RK, Copley SD. 2010. Three serendipitous pathways in *E. coli* can bypass a block in pyridoxal-5′-phosphate synthesis. Molecular Systems Biology. 6:436.

28. Kim J, Flood JJ, Kristofich MR, Gidfar C, Morgenthaler AB, Fuhrer T, Sauer U, Snyder D, Cooper VS, Ebmeier CC. 2019. Hidden resources in the *Escherichia coli* genome restore PLP synthesis and robust growth after deletion of the essential gene *pdxB*. Proceedings of the National Academy of Sciences. 116:24164-24173.

29. Yang Y, Zhao G, Winkler ME. 1996. Identification of the *pdxK* gene that encodes pyridoxine (vitamin B_6) kinase in *Escherichia coli* K-12. FEMS Microbiology Letters. 141:89-95.

30. Yang Y, Tsui H-CT, Man T-K, Winkler ME. 1998. Identification and function of the *pdxY* gene, which encodes a novel pyridoxal kinase involved in the salvage pathway of pyridoxal 5′-phosphate biosynthesis in *Escherichia coli* K-12. Journal of Bacteriology. 180:1814-1821.

31. Ito T, Downs DM. 2020. Pyridoxal reductase, PdxI, is critical for salvage of pyridoxal in *Escherichia coli*. Journal of Bacteriology. 202:e00056-20.

32. Nakano M, Morita T, Yamamoto T, Sano H, Ashiuchi M, Masui R, Kuramitsu S, Yagi T. 1999. Purification, molecular cloning, and catalytic activity of *Schizosaccharomyces pombe* pyridoxal reductase: A possible additional family in the aldo-keto reductase superfamily. Journal of Biological Chemistry. 274:23185-23190.

33. Herrero S, González E, Gillikin JW, Vélëz H, Daub ME. 2011. Identification and characterization of a pyridoxal reductase involved in the vitamin B_6 salvage pathway in *Arabidopsis*. Plant Molecular Biology. 76:157-169.

34. Ramos RJ, Albersen M, Vringer E, Bosma M, Zwakenberg S, Zwartkruis F, Jans JJ, Verhoeven-Duif NM. 2019. Discovery of pyridoxal reductase activity as part of human vitamin B_6 metabolism. Biochimica et Biophysica Acta (BBA)-General Subjects. 1863:1088-1097.

35. Yuan B, Yoshikane Y, Yokochi N, Ohnishi K, Yagi T. 2004. The nitrogen-fixing symbiotic bacterium *Mesorhizobium loti* has and expresses the gene encoding pyridoxine 4-oxidase involved in the degradation of vitamin B_6. FEMS Microbiology Letters. 234:225-230.

36. Kuznetsova E, Proudfoot M, Gonzalez CF, Brown G, Omelchenko MV, Borozan I, Carmel L, Wolf YI, Mori H, Savchenko AV. 2006. Genome-wide analysis of substrate specificities of the *Escherichia coli* haloacid dehalogenase-like phosphatase family. Journal of Biological Chemistry. 281:36149-36161.

37. Sugimoto R, Saito N, Shimada T, Tanaka K. 2017. Identification of YbhA as the pyridoxal 5′-phosphate (PLP) phosphatase in *Escherichia coli*: Importance of PLP homeostasis on the bacterial growth. The Journal of General and Applied Microbiology. 63:362–368.

38. Jang YM, Kim DW, Kang T-C, Won MH, Baek N-I, Moon BJ, Choi SY, Kwon O-S. 2003. Human pyridoxal phosphatase: Molecular cloning, functional expression, and tissue distribution. Journal of Biological Chemistry. 278:50040-50046.

39. Rodwell VW, Volcani BE, Ikawa M, Snell EE. 1958. Bacterial oxidation of vitamin B_6: I. Isopyridoxal and 5-pyridoxic acid. Journal of Biological Chemistry. 233:1548-1554.

40. Sundaram T, Snell EE. 1969. The bacterial oxidation of vitamin B_6: V. The enzymatic formation of pyridoxal and isopyridoxal from pyridoxine. Journal of Biological Chemistry. 244:2577-2584.

41. Mukherjee T, Hanes J, Tews I, Ealick SE, Begley TP. 2011. Pyridoxal phosphate: biosynthesis and catabolism. Biochimica et Biophysica Acta (BBA)-Proteins and Proteomics. 1814:1585-1596.

42. Jong Y, Nelson M, Snell E. 1986. Enzymes of vitamin B_6 degradation. Purification and properties of pyridoxine 5′-dehydrogenase (oxidase). Journal of Biological Chemistry. 261:15102-15105.

43. Stolz Jr, Vielreicher M. 2003. Tpn1p, the plasma membrane vitamin B_6 transporter of *Saccharomyces cerevisiae*. Journal of Biological Chemistry. 278:18990-18996.

44. Stolz Jr, Wöhrmann HJ, Vogl C. 2005. Amiloride uptake and toxicity in fission yeast are caused by the pyridoxine transporter encoded by *bsu1*$^+$ (*car1*$^+$). Eukaryotic Cell. 4:319-326.

45. Szydlowski N, Bürkle L, Pourcel L, Moulin M, Stolz J, Fitzpatrick TB. 2013. Recycling of pyridoxine (vitamin B_6) by PUP1 in *Arabidopsis*. The Plant Journal. 75:40-52.

46. Kato K, Shitan N, Shoji T, Hashimoto T. 2015. Tobacco NUP1 transports both tobacco alkaloids and vitamin B_6. Phytochemistry. 113:33-40.

47. Wang T, De Jesus AJ, Shi Y, Yin H. 2015. Pyridoxamine is a substrate of the energy-coupling factor transporter HmpT. Cell Discovery. 1:1-10.

48. Pan C, Zimmer A, Shah M, Huynh MS, Lai CC-L, Sit B, Hooda Y, Curran DM, Moraes TF. 2021. *Actinobacillus* utilizes a binding protein–dependent ABC transporter to acquire the active form of vitamin B_6. Journal of Biological Chemistry. https://doi.org/10.1016/j.jbc.2021.101046.

49. Mulligan JH, Snell E. 1976. Transport and metabolism of vitamin B_6 in *Salmonella typhimurium* LT2. Journal of Biological Chemistry. 251:1052-1056.

50. Yamada R, Tsuji T, Nose Y. 1977. Uptake and utilization of vitamin B_6 and its phosphate esters by *Escherichia coli*. Journal of Nutritional Science and Vitaminology. 23:7-17.

51. Yamada R, Furukawa. 1981. Role of pyridoxal kinase in vitamin B_6 uptake by *Escherichia coli*. Journal of Nutritional Science and Vitaminology. 27:177-191.

52. Zhao G, Winkler ME. 1994. An *Escherichia coli* K-12 *tktA tktB* mutant deficient in transketolase activity requires pyridoxine (vitamin B_6) as well as the aromatic amino acids and vitamins for growth. Journal of Bacteriology. 176:6134-6138.

53. Reddick JJ, Kinsland C, Nicewonger R, Christian T, Downs DM, Winkler ME, Begley TP. 1998. Overexpression, purification and characterization of two pyrimidine kinases involved in the biosynthesis of thiamin: 4-amino-5-hydroxymethyl-2-methylpyrimidine kinase and 4-amino-5-hydroxymethyl-2-methylpyrimidine phosphate kinase. Tetrahedron. 54:15983-15991.

54. Gelfand DH, Steinberg RA. 1977. *Escherichia coli* mutants deficient in the aspartate and aromatic amino acid aminotransferases. Journal of Bacteriology. 130:429-440.

55. Perry C, Yu S, Chen J, Matharu KS, Stover PJ. 2007. Effect of vitamin B_6 availability on serine hydroxymethyltransferase in MCF-7 cells. Archives of Biochemistry and Biophysics. 462:21-27.

56. Volland C, Felix F. 1984. Isolation and properties of 5-aminolevulinate synthase from the yeast *Saccharomyces cerevisiae*. European Journal of Biochemistry. 142:551-557.

57. Palm D, Klein HW, Schinzel R, Buehner M, Helmreich EJ. 1990. The role of pyridoxal 5′-phosphate in glycogen phosphorylase catalysis. Biochemistry. 29:1099-1107.

58. Nijhout HF, Gregory JF, Fitzpatrick C, Cho E, Lamers KY, Ulrich CM, Reed MC. 2009. A mathematical model gives insights into the effects of vitamin B_6 deficiency on 1-carbon and glutathione metabolism. Journal of Nutrition. 139:784-791.

59. Irons JL, Hodge-Hanson K, Downs DM. 2020. RidA proteins protect against metabolic damage by reactive intermediates. Microbiology and Molecular Biology Reviews. 84:e00024-00020.

60. Chrisley BM, Thye FW, McNair HM, Driskell JA. 1988. Plasma B_6 vitamer and 4-pyridoxic acid concentrations of men fed controlled diets. Journal of Chromatography B: Biomedical Sciences and Applications. 428:35-42.

61. Fu T-F, Di Salvo M, Schirch V. 2001. Distribution of B_6 vitamers in *Escherichia coli* as determined by enzymatic assay. Analytical Biochemistry. 298:314-321.

62. Venegas A, Martial J, Valenzuela P. 1973. Active site-directed inhibition of *E. coli* DNA-dependent RNA polymerase by pyridoxal 5′-phosphate. Biochemical and Biophysical Research Communications. 55:1053-1059.

63. Bartzatt R, Beckmann JD. 1994. Inhibition of phenol sulfotransferase by pyridoxal phosphate. Biochemical Pharmacology. 47:2087-2095.

64. Vermeersch JJ, Christmann-Franck S, Karabashyan LV, Fermandjian S, Mirambeau G, Der Garabedian PA. 2004. Pyridoxal 5′-phosphate inactivates DNA topoisomerase IB by modifying the lysine general acid. Nucleic Acids Research. 32:5649-5657.

65. Whittaker MM, Penmatsa A, Whittaker JW. 2015. The Mtm1p carrier and pyridoxal 5′-phosphate cofactor trafficking in yeast mitochondria. Archives of Biochemistry and Biophysics. 568:64-70.

66. Park J, McCormick SP, Chakrabarti M, Lindahl PA. 2013. Insights into the iron-ome and manganese-ome of Δ*mtm1 Saccharomyces cerevisiae* mitochondria. Metallomics. 5:656-672.

67. Boycheva S, Dominguez A, Rolcik J, Boller T, Fitzpatrick TB. 2015. Consequences of a deficit in vitamin B_6 biosynthesis *de novo* for hormone homeostasis and root development in *Arabidopsis*. Plant physiology. 167:102-117.

68. Stepanova AN, Robertson-Hoyt J, Yun J, Benavente LM, Xie D-Y, Doležal K, Schlereth A, Jürgens G, Alonso JM. 2008. TAA1-mediated auxin biosynthesis is essential for hormone crosstalk and plant development. Cell. 133:177-191.

69. Del Giudice E, Striano S, Andria G. 1983. Electroencephalographic abnormalities in homocystinuria due to cystathionine synthase deficiency. Clinical Neurology and Neurosurgery. 85:165-168.

70. Toriyama T, Matsuo S, Fukatsu A, Takahashi H, Sato K, Mimuro N, Kawahara H. 1993. Effects of high-dose vitamin B_6 therapy on microcytic and hypochromic anemia in hemodialysis patients. Japanese Journal of Nephrology. 35:975-980.

71. Qian B, Shen S, Zhang J, Jing P. 2017. Effects of vitamin B_6 deficiency on the composition and functional potential of T cell populations. Journal of Immunology Research. doi: 10.1155/2017/2197975.

72. Tong Y. 2014. Seizures caused by pyridoxine (vitamin B_6) deficiency in adults: A case report and literature review. Intractable and Rare Diseases Research. 3:52-56.

73. Clayton PT. 2006. B_6-responsive disorders: a model of vitamin dependency. Journal of Inherited Metabolic Disease. 29:317-326.

74. Tramonti A, Nardella C, di Salvo ML, Pascarella S, Contestabile R. 2018. The MocR-like transcription factors: pyridoxal 5′-phosphate-dependent regulators of bacterial metabolism. The FEBS Journal. 285:3925-3944.

75. Jochmann N, Götker S, Tauch A. 2011. Positive transcriptional control of the pyridoxal phosphate biosynthesis genes *pdxST* by the MocR-type regulator PdxR of *Corynebacterium glutamicum* ATCC 13032. Microbiology. 157:77-88.

76. El Qaidi S, Yang J, Zhang J-R, Metzger DW, Bai G. 2013. The vitamin B_6 biosynthesis pathway in *Streptococcus pneumoniae* is controlled by pyridoxal 5′-phosphate and the transcription factor PdxR and has an impact on ear infection. Journal of Bacteriology. 195:2187-2196.

77. Belitsky BR. 2014. Role of PdxR in the activation of vitamin B_6 biosynthesis in *Listeria monocytogenes*. Molecular Microbiology. 92:1113-1128.

78. Tramonti A, Fiascarelli A, Milano T, di Salvo ML, Nogués I, Pascarella S, Contestabile R. 2015. Molecular mechanism of PdxR–a transcriptional activator involved in the regulation of vitamin B_6 biosynthesis in the probiotic bacterium *Bacillus clausii*. The FEBS Journal. 282:2966-2984.

79. Tramonti A, Milano T, Nardella C, di Salvo ML, Pascarella S, Contestabile R. 2017. *Salmonella typhimurium* PtsJ is a novel MocR-like transcriptional repressor involved in regulating the vitamin B_6 salvage pathway. The FEBS Journal. 284:466-484.

80. Nagase T, Mugo AN, Chu HN, Yoshikane Y, Ohnishi K, Yagi T. 2012. The *mll6786* gene encodes a repressor protein controlling the degradation pathway for vitamin B_6 in *Mesorhizobium loti*. FEMS Microbiology Letters. 329:116-122.

81. Barile A, Tramonti A, di Salvo ML, Nogués I, Nardella C, Malatesta F, Contestabile R. 2019. Allosteric feedback inhibition of pyridoxine 5′-phosphate oxidase from *Escherichia coli.* Journal of Biological Chemistry. 294:15593-15603.

82. Safo MK, Mathews I, Musayev FN, di Salvo ML, Thiel DJ, Abraham DJ, Schirch V. 2000. X-ray structure of *Escherichia coli* pyridoxine 5′-phosphate oxidase complexed with FMN at 1.8 Å resolution. Structure. 8:751-762.

83. Yang ES, Schirch V. 2000. Tight binding of pyridoxal 5′-phosphate to recombinant *Escherichia coli* pyridoxine 5′-phosphate oxidase. Archives of Biochemistry and Biophysics. 377:109-114.

84. Ghatge MS, Contestabile R, di Salvo ML, Desai JV, Gandhi AK, Camara CM, Florio R, González IN, Parroni A, Schirch V. 2012. Pyridoxal 5′-phosphate is a slow tight binding inhibitor of *E. coli* pyridoxal kinase. PLoS One. 7:e41680.

85. di Salvo ML, Nogués I, Parroni A, Tramonti A, Milano T, Pascarella S, Contestabile R. 2015. On the mechanism of *Escherichia coli* pyridoxal kinase inhibition by pyridoxal and pyridoxal 5′-phosphate. Biochimica et Biophysica Acta (BBA)-Proteins and Proteomics. 1854:1160-1166.

86. Eswaramoorthy S, Gerchman S, Graziano V, Kycia H, Studier F, Swaminathan S. 2003. Structure of a yeast hypothetical protein selected by a structural genomics approach. Acta Crystallographica Section D: Biological Crystallography. 59:127-135.

87. Ito T, Iimori J, Takayama S, Moriyama A, Yamauchi A, Hemmi H, Yoshimura T. 2013. Conserved pyridoxal protein that regulates Ile and Val metabolism. Journal of Bacteriology. 195:5439-5449.

88. Labella JI, Cantos R, Espinosa J, Forcada-Nadal A, Rubio V, Contreras A. 2017. PipY, a member of the conserved COG0325 family of PLP-binding proteins, expands the cyanobacterial nitrogen regulatory network. Frontiers in Microbiology. 8:1244.

89. Ito T, Yamauchi A, Hemmi H, Yoshimura T. 2016. Ophthalmic acid accumulation in an *Escherichia coli* mutant lacking the conserved pyridoxal 5′-phosphate-binding protein YggS. Journal of Bioscience and Bioengineering. 122:689-693.

90. Prunetti L, El Yacoubi B, Schiavon CR, Kirkpatrick E, Huang L, Bailly M, El Badawi-Sidhu M, Harrison K, Gregory 3rd JF, Fiehn O. 2016. Evidence that COG0325 proteins are involved in PLP homeostasis. Microbiology. 162:694-706.

91. Ito T, Yamamoto K, Hori R, Yamauchi A, Downs DM, Hemmi H, Yoshimura T. 2019. Conserved pyridoxal 5′-phosphate-binding protein YggS impacts amino acid metabolism through pyridoxine 5′-phosphate in *Escherichia coli*. Applied and environmental microbiology. 85:e00430-19.

92. Ito T, Hori R, Hemmi H, Downs DM, Yoshimura T. 2020. Inhibition of glycine cleavage system by pyridoxine 5′-phosphate causes synthetic lethality in *glyA yggS* and *serA yggS* in *Escherichia coli*. Molecular Microbiology. 113:270-284.

93. Darin N, Reid E, Prunetti L, Samuelsson L, Husain RA, Wilson M, El Yacoubi B, Footitt E, Chong WK, Wilson LC. 2016. Mutations in *PROSC* disrupt cellular pyridoxal phosphate homeostasis and cause vitamin-B_6-dependent epilepsy. The American Journal of Human Genetics. 99:1325-1337.

94. Plecko B, Zweier M, Begemann A, Mathis D, Schmitt B, Striano P, Baethmann M, Vari MS, Beccaria F, Zara F. 2017. Confirmation of mutations in *PROSC* as a novel cause of vitamin B_6-dependent epilepsy. Journal of Medical Genetics. 54:809-814.

95. Shiraku H, Nakashima M, Takeshita S, Khoo CS, Haniffa M, Ch'ng GS, Takada K, Nakajima K, Ohta M, Okanishi T. 2018. *PLPBP* mutations cause variable phenotypes of developmental and epileptic encephalopathy. Epilepsia Open. 3:495-502.

96. Tremiño L, Forcada-Nadal A, Rubio V. 2018. Insight into vitamin B_6-dependent epilepsy due to *PLPBP* (previously *PROSC*) missense mutations. Human Mutation. 39:1002-1013.

97. Johnstone DL, Al-Shekaili HH, Tarailo-Graovac M, Wolf NI, Ivy AS, Demarest S, Roussel Y, Ciapaite J, van Roermund CW, Kernohan KD. 2019. PLPHP deficiency: clinical, genetic, biochemical, and mechanistic insights. Brain. 142:542-559.

98. Heath O, Pitt J, Mandelstam S, Kuschel C, Vasudevan A, Donoghue S. 2020. Early-onset vitamin B_6-dependent epilepsy due to pathogenic PLPBP variants in a premature infant: A case report and review of the literature. JIMD Reports. 58: 3-11.

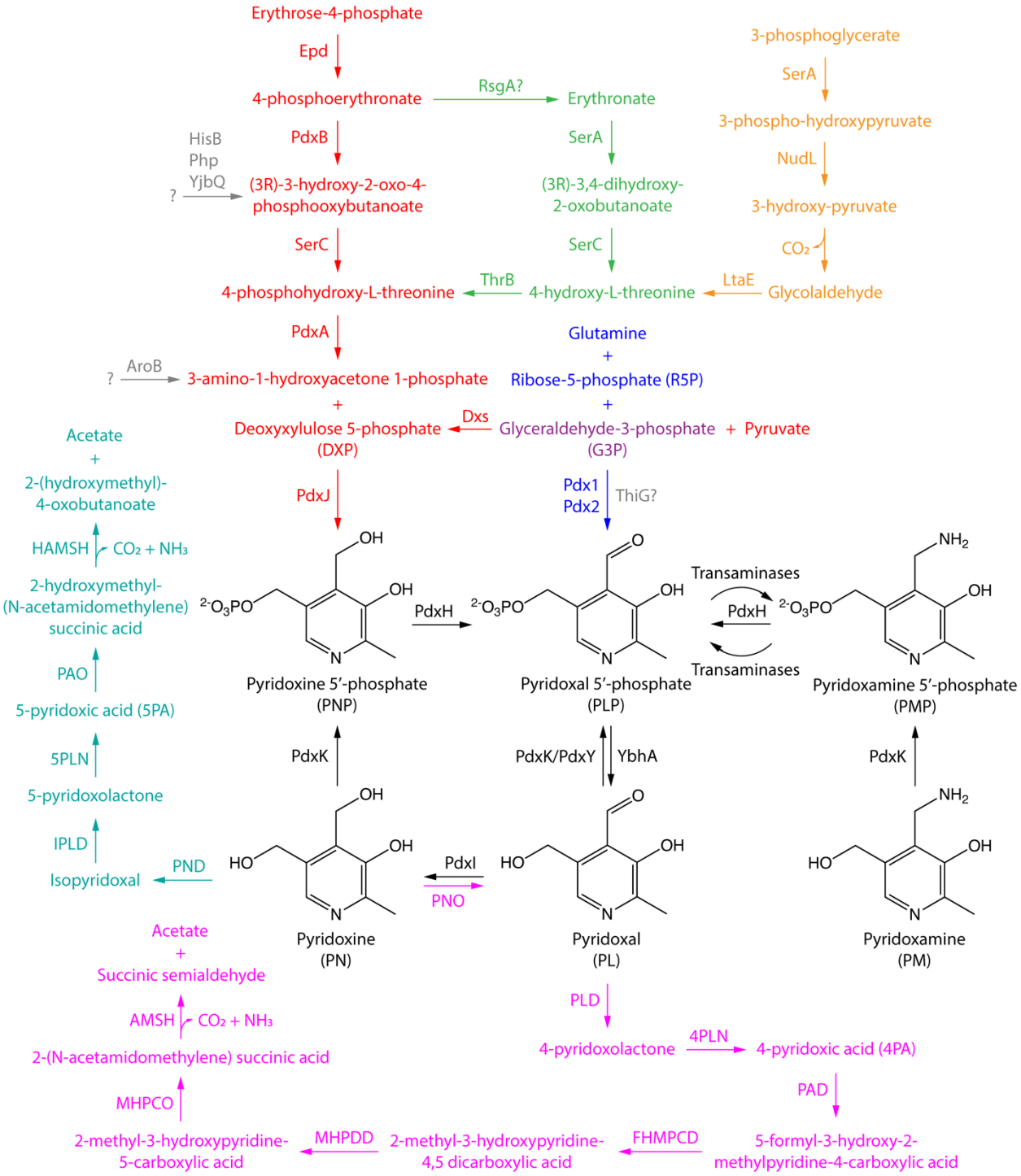

Figure 1.1 – Biosynthesis and salvage of B_6 vitamers. G3P (purple) is a substrate in both DXP-dependent (red highlight) and DXP-independent (blue highlight) pathway. The canonical salvage route for PLP is indicated in black. Putative serendipitous pathways in *E. coli* are highlighted in

gray, whereas those that have been described are highlighted in green and orange. The 4PA-dependent (pink highlight) and 5PA-dependent (teal highlight) pathways for vitamin B6 catabolism have also been characterized. Abbreviations: 4PA, 4-pyridoxic acid; 5PA, 5-pyridoxic acid; PNO, pyridoxine 4′-oxidase; PLD, pyridoxal dehydrogenase; 4PLN, 4′-pyridoxo 4′-lactonase; PAD, pyridoxic acid 4′-dehydrogenase; FHMPCD, 5-formyl-3-hydroxy-2-methylpyridine-4-carboxylic acid dehydrogenase; MHPDD, 2-methyl-3-hydroxypyridine-4,5-dicarboxylic acid decarboxylase; MHPCO, 2-methyl-3-hydroxypyridine-5-carboxylic acid oxygenase; AMSH, 2-(N-acetamidomethylene) succinic acid hydrolase; PND, pyridoxine-5-dehydrogenase; IPLD, isopyridoxal dehydrogenase; 5PLN, pyridoxo 5′-lactonase; PAO, 5-pyridoxic acid oxygenase; HAMSH, 2-hydroxymethyl-(N-acetamidomethylene) succinic acid hydrolase.

CHAPTER 2

AN UNEXPECTED ROLE FOR THE PERIPLASMIC PHOSPHATASE PHON IN THE SALVAGE OF B_6 VITAMERS IN *SALMONELLA ENTERICA* [1]

[1] Vu HN, Downs DM. 2020. *Applied and Environmental Microbiology*. 87(3):e02300-20. Reprinted here with permission of the publisher.

2.1 ABSTRACT

Pyridoxal 5′-phosphate (PLP) is the biologically active form of vitamin B_6, essential for cellular function in all domains of life. In many organisms, such as *Salmonella enterica* serovar Typhimurium and *Escherichia coli*, this cofactor can be synthesized *de novo* or salvaged from B_6 vitamers in the environment. Unexpectedly, *S. enterica* strains blocked in PLP biosynthesis were able to use exogenous PLP and pyridoxine 5′-phosphate (PNP) as the source of this required cofactor, while *E. coli* strains of the same genotype could not. Transposon mutagenesis found that *phoN* was essential for the salvage of PLP and PNP under the conditions tested. *phoN* encodes a class A nonspecific acid phosphatase (EC 3.1.3.2) that is transcriptionally regulated by the PhoPQ two-component system. The periplasmic location of PhoN was essential for PLP and PNP salvage, and *in vitro* assays confirmed PhoN has phosphatase activity with PLP and PNP as substrates. The data suggest that PhoN dephosphorylates B_6 vitamers, after which they enter the cytoplasm and are phosphorylated by kinases of the canonical PLP salvage pathway. The connection of *phoN* with PhoPQ and the broad specificity of the gene product suggest *S. enterica* is exploiting a moonlighting activity of PhoN for PLP salvage.

IMPORTANCE

Nutrient salvage is a strategy used by species across domains of life to conserve energy. Many organisms are unable to synthesize all required metabolites *de novo* and must rely exclusively on salvage. Others supplement *de novo* synthesis with the ability to salvage. This study identified an unexpected mechanism present in *S. enterica* that allows salvage of phosphorylated B_6 vitamers. *In vivo* and *in vitro* data herein determined that the periplasmic phosphatase PhoN can facilitate the salvage of PLP and PNP. We suggest a mechanistic working model of PhoN-

dependent utilization of PLP and PNP and discuss the general role of promiscuous phosphatases and kinases in organismal fitness.

2.2 INTRODUCTION

Vitamin B_6 is a collective term for six compounds, including pyridoxal (PL), pyridoxine (PN), pyridoxamine (PM), pyridoxal 5′-phosphate (PLP), pyridoxine 5′-phosphate (PNP), and pyridoxamine 5′-phosphate (PMP) (Figure 2.1). Among the six vitamers, PLP is the biologically active form that plays a critical role in prokaryotic, eukaryotic and archaeal metabolism. PLP can be synthesized *de novo* via the deoxyxylulose 5′-phosphate (DXP)-independent pathway, which exists in *Saccharomyces cerevisiae* and *Bacillus subtilis* among other organisms (1, 2). Alternatively, the DXP-dependent pathway is used to synthesize PLP (Figure 2.1) in gamma-proteobacteria such as *Salmonella enterica* serovar Typhimurium (referred hereafter as *S. enterica*) and *Escherichia coli*. In addition to *de novo* synthesis, PLP can be salvaged from exogenous pyridoxal (PL), pyridoxine (PN), and pyridoxamine (PM) from the environment (Figure 2.1). Further, some *Pseudomonas*, *Arthrobacter*, and *Mesorhizobium loti* species can utilize PN or PL as a sole source of carbon and nitrogen using two different catabolic pathways (3).

For organisms relying on the DXP-dependent pathway, a mutation in *pdxJ* (encoding a PNP synthase, EC 2.6.99.2) blocks *de novo* PLP biosynthesis and prevents growth in the absence of an exogenous B_6 vitamer (Figure 2.1). In contrast, a lesion in *pdxB* (encoding an erythronate-4-phosphate dehydrogenase, EC 1.1.1.290) in *E. coli* can be bypassed by at least three mechanisms, one of which utilizes glycolaldehyde (GA) (4). Many organisms, including humans, lack the ability to synthesize PLP *de novo* and depend on salvage to obtain this cofactor (1, 2). The canonical vitamin B_6 salvage pathway includes a PNP/PMP oxidase (PdxH, EC 1.4.3.5), which also

catalyzes the final step of DXP-dependent PLP biosynthesis (Figure 2.1) and is conserved among many bacteria and eukaryotes (1, 2). Although both PNP and PMP can serve as substrates for this enzyme, PdxH from *E. coli* was reported to prefer PNP to PMP (5), while the PdxH homolog from rabbit liver was shown to not favor one over the other (6). Additional enzymes ascribed a role in vitamin B_6 salvage include PdxK (PN/PL/PM kinase, EC 2.7.1.35) (7) and PdxY (PL kinase, EC 2.7.1.35) (8). *In vitro*, PdxK from *E. coli* phosphorylated the three unphosphorylated B_6 vitamer substrates, while PdxY had low activity and was specific for PL (8, 9). In addition, PdxK could act on 4-amino-5-hydroxymethyl-2-methylpyrimidine, a precursor of thiamine (vitamin B_1) (10), highlighting the promiscuity often found in kinase and phosphatase enzymes.

S. enterica and *E. coli* synthesize PLP *de novo* via the DXP-dependent pathway and share most enzymes attributed to vitamin B_6 salvage (Figure 2.1). In addition to PdxK and PdxY, both species have a cytoplasmic PLP phosphatase (EC 3.1.3.74) encoded by *ybhA* (11). Mutations in YbhA were identified in *E. coli* strains evolved to overcome a defect in *de novo* PLP synthesis (12), suggesting a possible role of this enzyme in maintaining intracellular PLP pools. Beyond these enzymes, there are marked differences between *S. enterica* and *E. coli* in vitamin B_6 salvage. For instance, the *E. coli* genome encodes a PL reductase (PdxI, EC 1.1.1.65), which has the ability to convert PL to PN and is absent in *S. enterica* (13). Further, expression of *pdxK* in *S. enterica* is controlled by PtsJ, a MocR-like repressor that is not present in *E. coli* (14). These differences at a genomic level may provide insights into diverse environmental conditions encountered by *S. enterica* and *E. coli* as well as their distinct metabolic strategies to thrive. Adding to the differences between these species, this study uncovered an unexpected role for the periplasmic phosphatase PhoN, which is unique to *S. enterica*, in the salvage of phosphorylated B_6 vitamers.

2.3 RESULTS

***S. enterica* salvages diverse B_6 vitamers.** The capacity of *S. enterica* to salvage B_6 vitamers and the contribution of the known salvage enzymes was assessed. Strains defective in *de novo* PLP synthesis (*pdxJ*) and derivatives lacking either *pdxK*, *pdxY*, or *pdxH* were grown in minimal NCE glucose supplemented with PL, PN, or PM to a final concentration of 1 μM (Figure 2.2). As expected, none of the strains grew in the absence of a B_6 vitamer (data not shown). Addition of PL allowed growth of all mutants (Figure 2.2A), consistent with phenotypes reported for *E. coli* strains defective in PLP synthesis (7, 8). Further, strains lacking *pdxK* or *pdxH* failed to grow when PN was provided (Figure 2.2B). PM allowed growth of the *pdxJ pdxH* mutant, but not the *pdxJ pdxK* strain (Figure 2.2C), a feature attributed to PLP formation via transamination reactions (15).

Unexpectedly, exogenous PLP and PNP (at 1 μM) allowed growth of *S. enterica* strains lacking *de novo* PLP synthesis (Figure 2.3). At physiological pH, the phosphate group of these vitamers carries a -2 net charge, suggesting a transporter and/or facilitated diffusion would be needed for them to cross the outer and/or inner membrane of Gram-negative bacteria. If transported to the cytoplasm, PLP would be available for immediate use, while PNP must be oxidized by PdxH to generate the active cofactor. This simple scenario, in which salvage of PNP would be independent of PdxK and PdxY, was eliminated by assessing growth of the multiple mutant strains described above. Four strains lacking *pdxJ* grew to full density with PLP (Figure 2.3A). In contrast, growth of the *pdxJ pdxK* and *pdxJ pdxH* strains was compromised when PNP was provided as a source of vitamin B_6 (Figure 2.3B). The *pdxJ pdxK* mutant strain had an extended lag before growth resumed, while the *pdxJ pdxH* strain failed to grow. PMP was not able to support growth of any of the PLP-requiring strains (Figure 2.3C), and was not considered for subsequent experiments. In medium supplemented with PMP, all strains displayed initial growth similar to

that of the *pdxJ pdxK* and *pdxJ pdxH* strains in medium with PNP (Figure 2.3B), suggesting that some amount of vitamin B_6 from preculture medium was carried over to the minimal NCE medium.

The growth phenotypes presented above suggested that PdxK and/or PdxY, in addition to PdxH, played a role in the salvage of PLP/PNP. The redundancy of PdxK and PdxY could not be tested in a *pdxJ* background, since the triple mutant would be unable to synthesize or salvage PLP (Figure 2.1). Instead, *pdxB* strains lacking one or both kinases were grown in minimal NCE glucose with supplementation of PLP/PNP (Figure 2.3D-E). As expected, the growth phenotypes of the *pdxB pdxK* and *pdxB pdxY* strains with exogenous PLP or PNP were similar to those of the *pdxJ pdxK* and *pdxJ pdxY* strains, respectively. Importantly, *pdxB* strain carrying mutations in both kinases was not viable when PLP (Figure 2.3D) or PNP (Figure 2.3E) was provided. *S. enterica pdxB* strains were able to utilize GA for growth (Figure 2.3F) as shown in *E. coli* (4). Taken together, the data suggest that under the conditions tested, i) the salvage of PLP/PNP requires at least one functional kinase, and ii) *S. enterica* encodes a GA-dependent mechanism to bypass part of the DXP-dependent pathway for PLP biosynthesis (Figure 2.1).

PhoN facilitates salvage of PLP and PNP. Transposon mutagenesis identified two loci that were necessary for a *pdxJ* mutant to use exogenous phosphorylated B_6 vitamers as a source of PLP. Approximately 20,000 colonies of a *pdxJ* mutant, each carrying a randomly located Tn*10*(d)Tc insertion, were screened for growth with exogenous PL coupled with the inability to use exogenous PLP. Insertions in colonies with the appropriate growth response were transduced into a fresh genetic background, and the original phenotype was confirmed. Sanger sequencing of nine reconstructed isolates found that eight carried insertions in *phoN* and one had an insertion in *phoP*.

The *phoN* gene encodes a nonspecific acid phosphatase (EC 3.1.3.2) in the periplasm and is regulated by the PhoPQ two-component system (16-18). *phoQ* encodes a histidine sensor kinase (EC 2.7.13.3) in an operon and is located downstream of *phoP*, which encodes a transcriptional response regulator. Deletions of *phoN*, *phoP*, and *phoQ* were individually placed in a *pdxJ* background and growth phenotypes with PLP and PNP were assessed (Table 2.1). Growth of the *pdxJ* strain with phosphorylated B_6 vitamers was eliminated by each of the three deletions. Significantly, providing *phoN in trans* restored growth of all of the double mutants (*pdxJ phoN*, *pdxJ phoP*, *pdxJ phoQ*) when exogenous PLP or PNP was added to the medium. Growth of the *pdxJ phoQ* mutant was also restored by expressing *phoQ in trans*. In contrast, expression of *phoP in trans* failed to allow growth of the *pdxJ phoP* mutant with PLP and PNP, while expressing both *phoP* and *phoQ* restored growth. In total, these data supported the conclusions that i) PhoN was necessary and sufficient for salvage of PLP or PNP, ii) the *phoP* mutation was polar on *phoQ,* and iii) the role of *phoPQ* was regulatory. Consistently, heterologous expression of *phoN* (pDM1603, Figure 2.4A) in an *E. coli pdxJ* mutant conferred growth on both phosphorylated B_6 vitamers, while the strain with the vector only control failed to grow (Figure 2.4B-C). This result emphasized a critical role for PhoN, which is not encoded in the *E. coli* genome (19), in the salvage of PLP/PNP under the conditions tested.

A periplasmic location is required for PhoN function *in vivo*. The first 20 amino acids of PhoN make up a putative Sec-dependent signal sequence directing PhoN to the periplasm as predicted by SignalP 5.0 (20). The DNA sequence encoding these 20 codons was removed to generate a plasmid that expressed the mature PhoN (pDM1606, Figure 2.4A). Plasmid pDM1606 did not support growth of a *pdxJ* mutant of *E. coli*, or a *pdxJ phoN* mutant of *S. enterica* on PLP or PNP

(Figure 2.4B-E). Sequence encoding the Tat-dependent signal peptide from *E. coli* TorA (trimethylamine-N-oxide reductase 1, EC 1.7.2.3) (21) was fused to *phoN* lacking the Sec-dependent signal sequence to generate plasmid pDM1607 (Figure 2.4A). Plasmid pDM1607 supported growth of the *E. coli pdxJ* and *S. enterica pdxJ phoN* strain in minimal medium with added PLP or PNP to a similar extent as the wild-type PhoN (Figure 2.4B-E). Taken together, these results demonstrated the periplasmic location of PhoN was required for function *in vivo* under the conditions tested.

PhoN has phosphatase activity on PLP and PNP *in vitro*. PhoN was previously characterized for its phosphatase activity on the non-physiological substrate *p*-nitrophenyl phosphate (*p*-NPP) (22). Results above suggested PhoN would act on phosphorylated B_6 vitamers. PhoN-6xHis was overexpressed in *E. coli* and purified by nickel-affinity and size-exclusion column chromatography. Purified PhoN-6xHis ran as two major bands in the range of ~30 kDa on SDS-PAGE gel (Figure 2.5A), which agrees with the predicted molecular mass of pre- (30.1 kDa) and mature-PhoN (27.7 kDa). Peptide mass fingerprinting identified both protein bands as *S. enterica* PhoN. The protein characterized was 89% pure and contained both pre-PhoN and mature-PhoN present at a ratio of ~3:1.

PhoN was assayed with PLP as a substrate by monitoring the disappearance of PLP over time as a decrease in absorbance at 390 nm. The initial velocity of each reaction was determined with PLP concentrations from 0 to 1.5 mM (Figure 2.S1). The K_m and k_{cat} for PLP, derived from the Michaelis-Menten saturation curves, was 0.35 ± 0.03 mM and 27.19 ± 0.71 s^{-1} respectively (Figure 2.5B). As reference, another PLP phosphatase, YbhA (Figure 2.1), has similar binding affinity for PLP (K_m = 0.37 ± 0.05 mM), while its catalytic turnover (k_{cat} = 1.0 ± 0.04 s^{-1}) is ~27

times slower than that of PhoN (23). Unlike PLP, hydrolysis of PNP and PMP cannot be easily monitored spectrophotometrically. The ability of PhoN to hydrolyze these vitamers was determined by end point assays using 50 nM PhoN with PLP, PNP, PMP, and *p*-NPP provided as substrates at 0.1 mM. PhoN had significant activity on each of the provided substrates with the exception of PMP (Table 2.2). PhoN had the highest specific activity with the generic phosphatase substrate *p*-NPP, followed by PLP and PNP. Under the conditions tested, PhoN exhibited only low activity with PMP, consistent with the inability of PMP to support growth of a *pdxJ* mutant (Figure 2.3C).

How does a phosphatase contribute to generating PLP required for growth? The combination of growth phenotypes and *in vitro* assays convincingly showed that PhoN can participate in the salvage of PLP and PNP in *S. enterica* and *E. coli*. The requirement for characterized kinases in PhoN-dependent salvage suggested that the phosphorylated vitamers were not transported across the inner membrane. A working model depicting incorporation of exogenous PLP is shown in Figure 2.6. The model has several tenets based on the data, i) PhoP and PhoQ are required (likely indirectly (24)) for expression of *phoN,* (Figure 2.6A), ii) the Sec-dependent system translocates PhoN to the periplasm (Figure 2.6B) where it is folded to the mature form (Figure 2.6C), iii) PLP crosses the outer membrane, perhaps through a porin (Figure 2.6D), iv) PL produced by PhoN (Figure 2.6E) crosses the inner membrane (Figure 2.6F) and, v) PdxK and/or PdxY generate PLP to complete salvage (Figure 2.6G). Salvage of PNP is viewed as similar with an additional step of converting PNP to PLP by PdxH (Figure 2.1).

Promiscuous phosphatases and kinases permeate vitamin B_6 salvage. Although PhoN was required to utilize PLP or PNP in the experiments above, growth of both *E. coli* and *S. enterica* *pdxJ* mutants were independent of PhoN when the vitamers were provided at ten-fold higher levels (10 μM) (Figure 2.7). There are a number of formal possibilities that could explain this result. At high concentrations, i) PLP and PNP may trickle into the cytoplasm, ii) PLP and PNP may be dephosphorylated by other promiscuous, but low-efficiency phosphatases, and/or iii) sufficient spontaneous hydrolysis to PL and PN occurs to support growth. These possibilities were not distinguished by the work described here, as they were thought to be less relevant to physiological conditions that would be encountered by the enteric bacteria than the lower concentrations.

Substrate promiscuity was also observed for kinases in the vitamin B_6 salvage pathway. An *S. enterica pdxJ pdxK* mutant was able to grow when 10 μM PN was provided (Figure 2.8A), while 10 μM PM had no effect (data not shown). No traces of other B_6 vitamers in minimal medium supplemented with 10 μM PN were detected by HPLC (data not shown), suggesting that another kinase(s) can phosphorylate PN, but not PM. Growth with 10 μM PN was eliminated in a *pdxB* background with mutations in both PdxK and PdxY (Figure 2.8B), indicating the promiscuous activity was due to the latter. It was not established if *E. coli* PdxY exhibits similar substrate promiscuity, since this enzyme only showed low kinase activity toward PN (9), and interpretation of *in vivo* function of PdxY was complicated by possible contamination of PL in growth medium supplemented with high PN concentration (100 μM) (8).

2.4 DISCUSSION

PhoN was first characterized as a periplasmic nonspecific acid phosphatase in *S. enterica* (16). PhoN activity increased in cells grown with limiting carbon, nitrogen, phosphorus, or sulfur

(17), and expression of *phoN* was indirectly regulated by the PhoPQ two-component system (18, 24). Prior to this study, the sole phenotype of a *phoN* mutant was slight growth defect when α-naphthyl phosphate or phenyl phosphate was used in phosphorus-limiting minimal glucose medium (18).

Results herein showed that PhoN, in combination with the relevant kinases, allowed *S. enterica* to salvage PLP and PNP. When vitamin B_6 homeostasis is perturbed, some bacteria such as *E. coli* and *S. enterica* can export excess phosphorylated B_6 vitamers into the environment (25). From an ecological standpoint, the ability to salvage phosphorylated forms of vitamin B_6 excreted from other community members may provide a fitness advantage to *S. enterica*. Counterintuitively, salvage of PLP and PNP required a phosphatase and a kinase, which resulted a working model described in Figure 2.6. This model is based on data that i) cells were unable to efficiently uptake phosphorylated forms of vitamin B_6 (26), ii) PhoN dephosphorylated PLP and PNP *in vitro* (Table 2.2), and iii) utilization of PLP/PNP required a functional kinase (PdxK or PdxY) (Figure 2.3D-E). Heterologous expression of *phoN* allowed an *E. coli pdxJ* mutant to grow with PLP/PNP, making it unlikely that there is a dedicated transport system for PLP/PNP (Figure 2.6D). Unphosphorylated B_6 vitamers were suggested to be taken up via facilitated diffusion (Figure 2.6F) followed by phosphorylation to trap the molecule (26-28) (Figure 2.6G). Additional work is required to rigorously define the mechanism of transport and the transporter(s)/porin(s).

An *S. enterica pdxJ pdxK* mutant grew with 1 μM PNP (Figure 2.3B) but not PN (Figure 2.2B) as a source of PLP. In the context of our working model, this result was unexpected, since the salvage of PNP goes through a PN intermediate. In the absence of PdxK, salvage of both PN and PNP is dependent on PdxY (Figure 2.8B and Figure 2.3E), thus a simple scenario suggests that expression of *pdxY* is higher in the presence of PNP than PN. Additional experiments are

needed to address this hypothesis. It was noted that the growth data herein appeared inconsistent with an ^{3}H-labeling study showing that *S. enterica* did not take up PM (27). A likely explanation for the two results is that the labeling experiment was done at low concentration of PM (0.1 μM) over a period of 10 minutes, while the *pdxJ* mutant strains showed exponential growth with ten-fold more PM (1 μM PM). This interpretation was supported by the finding that PM at 0.1 μM did not support growth of a *pdxJ* mutant (data not shown).

Substrate promiscuity is a common theme in vitamin B_6 metabolism, where it has been demonstrated for enzymes including PhoN (herein) (16), PdxH (5, 6), PdxK (9, 10), and YbhA (23). PhoN, specifically, had varying degrees of activity toward *p*-NPP, glucose 6-phosphate, β-glycerophosphate, adenosine monophosphate (16), PLP, and PNP (Table 2.2). It is notable that while both PhoN and YbhA are phosphatases that have the ability to hydrolyze PLP to PL, different cellular localization impacts their respective physiological roles: periplasmic PhoN in salvage and cytoplasmic YbhA in homeostasis of PLP (11, 12). Lack of substrate specificity, and unclear regulation suggests that PhoN is not a dedicated salvage enzyme, but rather participates when PLP or PNP is in the environment. When PLP or PNP is present at high level, other promiscuous phosphatases such as alkaline phosphatase (encoded by *phoA* in *E. coli*) (26) can replace PhoN in salvage (Figure 2.7). In addition, we provided evidence supporting PdxY, previously designated as a PL kinase, can also use PN as substrate at high concentration (Figure 2.8). In total, the contribution of PhoN to PLP/PNP salvage defined herein highlights how enzymes can be recruited to contribute to a robust and adaptive metabolism that allows microbes to thrive in different environments.

2.5 MATERIALS AND METHODS

Strains, media, and chemicals. Strains and plasmids used in this study are shown in Table 2.3. All strains are derivatives of *S. enterica* Typhimurium LT2 or *E. coli* BW25113. Plasmids were propagated in *E. coli* DH5α (Invitrogen, Carlsbad, CA). Recombinant protein was purified from *E. coli* BL21AI (Invitrogen, Carlsbad, CA).

Strains were routinely grown at 37°C on rich media (nutrient broth for *S. enterica*, 8 g/l Difco mix, 5 g/l NaCl; lysogeny broth for *E. coli*, 10 g/l Bacto tryptone, 5 g/l yeast extract, 5 g/l NaCl) or minimal no-carbon E (NCE) medium supplemented with $MgSO_4$ (1 mM), trace elements (29), and glucose (11 mM) as a sole carbon source. Super broth (32 g/l Bacto tryptone, 20 g/l yeast extract, 5 g/l NaCl, 5 mM NaOH) was used for protein purification. Agar was added to 1.5% wt/vol for solid media. B_6 vitamers in chloride form were supplemented to a final concentration of 1 μM or 10 μM as indicated in text. Glycolaldehyde (GA) was added to rich and minimal media at 0.1 mM and 1 mM, respectively (8). When appropriate, antibiotics were added as followed: kanamycin (Km, 50 μg/ml), chloramphenicol (Cm, 20 μg/ml), ampicillin (Am, 150 μg/ml in rich and 15 μg/ml in minimal media), and tetracycline (Tc, 20 μg/ml in rich and 5 μg/ml in minimal media).

Chemicals were purchased from MilliporeSigma (formerly Sigma-Aldrich, St. Louis, MO) unless otherwise stated. *p*-NPP was obtained from Thermo Fisher Scientific (Waltham, MA). Restriction enzymes and *Taq* polymerase were purchased from New England BioLabs (Ipswich, MA). Primers were synthesized by Eton Bioscience (San Diego, CA).

Purification of PNP. PNP was purified as described (30) except Dowex 1×8 was used in place of Amberlite IRC84. Briefly, Amberlite IRA743 resins were washed following published protocol, while Dowex 1×8 resins were washed sequentially with 200 ml (10 bed volumes, BV) water, 100

ml (5 BV) 1 M HCl, and 200 ml (10 BV) water. After a 15-minute incubation with NaOH to allow dissociation of the borate-PNP complex, the solution was adsorbed onto Amberlite IRA743 (10 ml in a 1.0 × 20 cm column) and washed with 10 ml (1 BV) water at a flow rate of 1 ml/min. Fractions containing PNP (detected spectrophotometrically at 325 nm) were pooled, and the pH was adjusted to 8.5 with 1 M HCl. The solution was adsorbed onto Dowex 1×8 (20 ml in 1.5 × 15 cm column), washed with 100 ml (5 BV) water, and eluted with 100 ml (5 BV) 1 M HCl. The eluate containing PNP was pooled and analyzed using HPLC as described (25) to determine the purity and concentration of PNP. The purified PNP solution was lyophilized and stored at -20°C for subsequent use.

Strain and plasmid construction. Primers for strain and plasmid construction are listed in Table 2.4. In-frame deletions of *pdx* genes (except *pdxK*) were generated using the λ Red recombinase system (31) adapted for *S. enterica*. Phage P22 *HT105/1 int-201* (32) carrying donor DNA was propagated in *S. enterica* Typhimurium 14028s *pdxK* and *pho* mutants from the SGD-K collection (33). All mutations were reconstructed in appropriate *S. enterica* Typhimurium LT2 strains via P22 transduction, and phage-free transductants were isolated as described (34). Antibiotic markers were resolved using pCP20 (35) when necessary. *E. coli* BW25113 strains were generated by electroporating different expression plasmids into the parental *pdxJ736*::*Km* mutant from the Keio collection (36).

Plasmids were constructed by cloning *S. enterica pho* genes into pCV1 or pTEV20 (37) at BspQI sites following described protocol (38). Splicing by Overlap Extension (SOE) PCR method (39) was used with slight modifications to create ssTorA-Δ(1-20)PhoN fusion. Briefly, chromosomal DNA segment encoding the signal sequence of *E. coli* TorA was amplified for 30

cycles with PR1329-PR1330 primer pair. A parallel PCR reaction was performed with *S. enterica* DNA encoding the mature sequence of PhoN using PR1331-PR1332 primers. The generated products had a ~30-bp overlap and were used as DNA templates for a subsequent round of amplification. The PCR reaction was initiated without primers to allow annealing of the two DNA fragments and enrichment of the fused product. After 5 cycles, PR1329-PR1332 primers were added and the reaction proceeded for another 25 cycles. The fused DNA product was purified using a QIAquick gel extraction kit (Qiagen, Germantown, MD) and cloned into pCV1 as described.

Transposon mutagenesis. A P22 *HT105/1 int-201* lysate was generated on a pool of *S. enterica* cells carrying ~10,000 independent Tn*10d*(Tc) insertions and used to transduce a *pdxJ662*::*Km* mutant (DM15906) to tetracycline resistant. Tc^R colonies that arose on nutrient agar were replica-printed onto minimal NCE glucose plates containing 1 μM PLP or PL as a sole source of vitamin B_6. Colonies that could grow on PL but not PLP were isolated and made phage-free using green indicator agar (34) supplemented with 1 μM PL. Of ~20,000 colonies screened, 14 putative mutants were identified. The Tn*10d*(Tc) insertion from each isolate was transduced into the parental *pdxJ662*::*Km* background to confirm that the insertion was causative of the growth phenotype. Nine reconstructed mutants showed the expected phenotype and were further analyzed.

Nested colony PCR using degenerate primers (40, 41) (Table 2.4) was performed to amplify the DNA regions from both ends of the transposon in each reconstructed mutant. PCR products were purified with a QIAquick PCR purification kit (Qiagen, Germantown, MD) and subjected to Sanger sequencing (Eurofins, Louisville, KY). The locations of Tn*10d*(Tc) insertions were determined by aligning the sequencing results to *S. enterica* genome using SnapGene 5.1.4.1

(GSL Biotech LLC, San Diego, CA). Eight insertions were located in *phoN* (three insertions located at V14, two at Y17, two at G115, and one at A118 of the coding sequence) and one was in *phoP* between residues Q203 and Y206 of the translated product.

Growth analysis. *S. enterica* and *E. coli* strains were precultured in 2 ml rich media (supplemented with 1 μM PL for *S. enterica pdxJ* strains lacking plasmids and 0.1 mM GA for *pdxB* strains) in an Innova 43 shaker (New Brunswick Scientific, Edison, NJ) at 250 rpm for 6-8 hours. Cells were pelleted, resuspended in equal volume of 0.85% NaCl, and inoculated at a 40-fold dilution into minimal NCE glucose medium with or without vitamin B_6 supplementation. *In trans* expression of *pho* genes from pCV1 was induced by addition of 0.02% (wt/vol) arabinose as indicated in text. Growth was monitored in a 96-well plate as a function of optical density at 650 nm (OD_{650}) using a BioTek Elx808 model (BioTek Instruments, Winooski, VT). Data were graphed using GraphPad Prism 7.0c (GraphPad Software, La Jolla, CA). Vitamin B_6 concentrations in growth media were analyzed with HPLC as described (25).

Purification of recombinant PhoN. Freshly transformed *E. coli* BL21AI / pDM1623 cells were precultured in 10 ml lysogeny broth at 37°C in replicates. The overnight cultures were used to inoculate four flasks, each of which contained 1.5 liters of super broth. Growth was monitored until cells reached an OD_{650} of ~0.8 as determined by a Spectronic 20D+ instrument (Thermo Fisher Scientific, Waltham, MA). Expression of *phoN* was induced with 0.02% (wt/vol) arabinose and 0.5 mM IPTG (isopropyl-β-D-thiogalactopyranoside), and the temperature was shifted to 30°C in an Innova 44 shaker (New Brunswick Scientific, Edison, NJ) at 200 rpm. After incubation for 19h, cells were pelleted (7,000 × g – 15 min, 4°C) and stored at -80°C until purification. All

purification and buffer exchange steps were performed at 4°C. Buffer A (50 mM Tris-HCl, 100 mM NaCl, 10 mM imidazole, pH 7.4) containing lysozyme (1 mg/ml), DNase (0.1 mg/ml), and phenylmethylsulfonyl fluoride (1.5 mM) was added to the cell pellet (2.5 ml/g wet weight). Cells were lysed at 20,000 psi using a Constant Systems Limited One Shot cell disruptor (Northants, United Kingdom). Cell lysate was centrifuged (48,000 × g – 1 h, 4°C) and filtered (0.45-µm PVDF) before loading onto a pre-equilibrated 5-ml HisTrap HP Ni-sepharose column (GE Healthcare, Chicago, IL) attached to an NGC Quest 10 Chromatography System (Bio-Rad, Hercules, CA). The loaded column was washed with 10 column volumes (CV) of buffer A, followed by a 5 CV of 4% buffer B (50 mM Tris-HCl, 100 mM NaCl, 250 mM imidazole, pH 7.4) and eluted with a 20-CV gradient of 4-100% buffer B at a flow rate of 2 ml/min. Fractions containing recombinant PhoN was confirmed on 14% SDS-PAGE gel and pooled. The protein solution was concentrated using an Amicon Ultra-15 10K centrifugal filter unit (MilliporeSigma, St. Louis, MO) and exchanged into buffer C (50 mM Tris-HCl, 100 mM NaCl, pH 7.4) using a PD-10 desalting column (GE Healthcare, Chicago, IL). The concentrated protein solution was applied onto an ENrich SEC 650 (10 × 300 mm) column (Bio-Rad, Hercules, CA), which was pre-equilibrated with buffer C. Size-exclusion purification was carried out with buffer C according to manufacturer's protocol. Fractions containing PhoN (determined by SDS-PAGE gel electrophoresis) were pooled. The protein solution was exchanged into buffer D (50 mM Tris-HCl, 100 mM NaCl, 10% glycerol, pH 7.4) using a PD-10 desalting column, flash-frozen with liquid nitrogen, and stored at -80°C until use. Protein concentration was determined using a Pierce BCA protein assay kit (Thermo Fisher Scientific, Waltham, MA) with bovine serum albumin as a standard.

In vitro **phosphatase assays.** Purified PhoN was thawed from frozen pellets and diluted in assay buffer before each use. Substrates were freshly prepared in assay buffer prior to each experiment. Enzyme assays were performed in two independent experiments with at least three replicates according to published protocol (42) with modifications. Briefly, reactions contained 50 mM triethanolamine-HCl (pH 7.4), 50 nM PhoN, and 0-1.5 mM PLP in a total volume of 100 µl. The rate of PL formation was inferred by spectrophotometrically following the decrease in absorbance at 390 nm normalized to 1-cm pathlength using a Spectramax 398 Plus plate reader (Molecular Devices, Sunnyvale, CA). The extinction coefficient of PLP was 5.23×10^3 M^{-1} cm^{-1} as determined from a 10-point standard curve with 0-2 mM PLP in triplicates. Initial velocity was determined at 37°C for the first 100-150 sec after adding PhoN protein to initiate the reactions. Kinetic parameters were estimated by fitting the data to the Michaelis-Menten equation using GraphPad Prism 7.0c (GraphPad Software, La Jolla, CA).

Specific activity was determined after incubating the enzyme reactions containing 50 mM triethanolamine-HCl (pH 7.4), 50 nM PhoN, and 0.1 mM PLP, PNP, PMP, or *p*-NPP at 37°C for 2.5 min. Hydrolysis of PLP was measured as described above. PN and PM formation was quantified using HPLC following extraction with 7M $HClO_4$ containing 15 µM 4-deoxypyridoxine as an internal standard (25). Production of *p*-nitrophenylate (*p*-NP) was measured spectrophotometrically at 410 nm with a Spectramax 398 Plus plate reader (Molecular Devices, Sunnyvale, CA), after addition of 100 µl 0.4 M NaOH to the enzyme reactions (22). The extinction coefficient of *p*-NP in assay buffer was 12.75×10^3 M^{-1} cm^{-1} as determined from a 9-point standard curve with 0-0.4 mM *p*-NP in triplicates. No enzyme control was used to account for spontaneous hydrolysis of substrates, which was subtracted from the reported activity.

ACKNOWLEDGEMENTS

The authors thank Dr. Tomokazu Ito at the Nagoya University (Nagoya, Japan) for sharing his expertise in the synthesis of PNP. Dr. Anna Karls and Dr. Jorge C. Escalante-Semerena at the University of Georgia (Athens, GA) are recognized for access to their laboratory strain collections. We acknowledge Michael D. Paxhia for the construction of *pdxH* and *pdxB* mutations in *S. enterica*. This work was supported by competitive grant GM095837 from the National Institutes of Health (DMD).

2.6 REFERENCES

1. Mittenhuber G. 2001. Phylogenetic analyses and comparative genomics of vitamin B_6 (pyridoxine) and pyridoxal phosphate biosynthesis pathways. J Mol Microbiol Biotechnol 3:1-20.

2. Tanaka T, Tateno Y, Gojobori T. 2004. Evolution of vitamin B_6 (pyridoxine) metabolism by gain and loss of genes. Mol Biol Evol 22:243-250.

3. Mukherjee T, Hanes J, Tews I, Ealick SE, Begley TP. 2011. Pyridoxal phosphate: biosynthesis and catabolism. Biochim Biophys Acta Proteins Proteom 1814:1585-1596.

4. Kim J, Kershner JP, Novikov Y, Shoemaker RK, Copley SD. 2010. Three serendipitous pathways in *E. coli* can bypass a block in pyridoxal-5′-phosphate synthesis. Mol Syst Biol 6:436.

5. Zhao G, Winkler ME. 1995. Kinetic limitation and cellular amount of pyridoxine (pyridoxamine) 5′-phosphate oxidase of *Escherichia coli* K-12. J Bacteriol 177:883-891.

6. Choi J-D, Bowers-Komro M, Davis MD, Edmondson D, McCormick D. 1983. Kinetic properties of pyridoxamine (pyridoxine)-5′-phosphate oxidase from rabbit liver. J Biol Chem 258:840-845.

7. Yang Y, Zhao G, Winkler ME. 1996. Identification of the *pdxK* gene that encodes pyridoxine (vitamin B_6) kinase in *Escherichia coli* K-12. FEMS Microbiol Lett 141:89-95.

8. Yang Y, Tsui H-CT, Man T-K, Winkler ME. 1998. Identification and function of the *pdxY* gene, which encodes a novel pyridoxal kinase involved in the salvage pathway of pyridoxal 5′-phosphate biosynthesis in *Escherichia coli* K-12. J Bacteriol 180:1814-1821.

9. di Salvo ML, Hunt S, Schirch V. 2004. Expression, purification, and kinetic constants for human and *Escherichia coli* pyridoxal kinases. Protein Expr Purif 36:300-306.

10. Reddick JJ, Kinsland C, Nicewonger R, Christian T, Downs DM, Winkler ME, Begley TP. 1998. Overexpression, purification and characterization of two pyrimidine kinases involved in the biosynthesis of thiamin: 4-amino-5-hydroxymethyl-2-methylpyrimidine kinase and 4-amino-5-hydroxymethyl-2-methylpyrimidine phosphate kinase. Tetrahedron 54:15983-15991.

11. Sugimoto R, Saito N, Shimada T, Tanaka K. 2017. Identification of YbhA as the pyridoxal 5′-phosphate (PLP) phosphatase in *Escherichia coli*: Importance of PLP homeostasis on the bacterial growth. J Gen Appl Microbiol 63:362-368.

12. Kim J, Flood JJ, Kristofich MR, Gidfar C, Morgenthaler AB, Fuhrer T, Sauer U, Snyder D, Cooper VS, Ebmeier CC. 2019. Hidden resources in the *Escherichia coli* genome restore PLP synthesis and robust growth after deletion of the essential gene *pdxB*. Proc Natl Acad Sci U S A 116:24164-24173.

13. Ito T, Downs DM. 2020. Pyridoxal reductase, PdxI, is critical for salvage of pyridoxal in *Escherichia coli*. J Bacteriol 202:e00056-20.

14. Tramonti A, Milano T, Nardella C, di Salvo ML, Pascarella S, Contestabile R. 2017. *Salmonella typhimurium* PtsJ is a novel MocR-like transcriptional repressor involved in regulating the vitamin B_6 salvage pathway. FEBS J 284:466-484.

15. Dempsey W. 1987. Synthesis of pyridoxal phosphate. *Escherichia coli* and *Salmonella typhimurium*: Cellular and Molecular Biology 1:539-543.

16. Kier LD, Weppelman R, Ames BN. 1977. Resolution and purification of three periplasmic phosphatases of *Salmonella typhimurium*. J Bacteriol 130:399-410.

17. Kier LD, Weppelman R, Ames BN. 1977. Regulation of two phosphatases and a cyclic phosphodiesterase of *Salmonella typhimurium*. J Bacteriol 130:420-428.

18. Kier L, Weppelman R, Ames B. 1979. Regulation of nonspecific acid phosphatase in *Salmonella*: *phoN* and *phoP* genes. J Bacteriol 138:155-161.

19. Kasahara M, Nakata A, Shinagawa H. 1991. Molecular analysis of the *Salmonella typhimurium phoN* gene, which encodes nonspecific acid phosphatase. J Bacteriol 173:6760-6765.

20. Armenteros JJA, Tsirigos KD, Sønderby CK, Petersen TN, Winther O, Brunak S, von Heijne G, Nielsen H. 2019. SignalP 5.0 improves signal peptide predictions using deep neural networks. Nat Biotechnol 37:420-423.

21. DeLisa MP, Tullman D, Georgiou G. 2003. Folding quality control in the export of proteins by the bacterial twin-arginine translocation pathway. Proc Natl Acad Sci U S A 100:6115-6120.

22. Makde RD, Dikshit K, Kumar V. 2006. Protein engineering of class-A non-specific acid phosphatase (PhoN) of *Salmonella typhimurium*: modulation of the pH-activity profile. Biomol Eng 23:247-251.

23. Kuznetsova E, Proudfoot M, Gonzalez CF, Brown G, Omelchenko MV, Borozan I, Carmel L, Wolf YI, Mori H, Savchenko AV. 2006. Genome-wide analysis of substrate specificities of the *Escherichia coli* haloacid dehalogenase-like phosphatase family. J Biol Chem 281:36149-36161.

24. Lejona S, Aguirre A, Cabeza ML, Véscovi EG, Soncini FC. 2003. Molecular characterization of the Mg^{2+}-responsive PhoP-PhoQ regulon in *Salmonella enterica*. J Bacteriol 185:6287-6294.

25. Vu HN, Ito T, Downs DM. 2020. The role of YggS in vitamin B_6 homeostasis in *Salmonella enterica* is informed by heterologous expression of yeast *SNZ3*. J Bacteriol 202:00383-20.

26. Yamada R, Tsuji T, Nose Y. 1977. Uptake and utilization of vitamin B_6 and its phosphate esters by *Escherichia coli*. J Nutr Sci Vitaminol 23:7-17.

27. Mulligan JH, Snell E. 1976. Transport and metabolism of vitamin B_6 in *Salmonella typhimurium* LT2. J Biol Chem 251:1052-1056.

28. Yamada R, Furukawa Y. 1981. Role of pyridoxal kinase in vitamin B_6 uptake by *Escherichia coli*. J Nutr Sci Vitaminol 27:177-191.

29. Davis R, Botstein D, Roth J. 1980. Advanced bacterial genetics. Cold Spring Harbor Laboratory Press. Cold Spring Harbor, New York.

30. Argoudelis CJ. 1986. Preparation of crystalline pyridoxine 5′phosphate and some of its properties. J Agric Food Chem 34:995-998.

31. Datsenko KA, Wanner BL. 2000. One-step inactivation of chromosomal genes in *Escherichia coli* K-12 using PCR products. Proc Natl Acad Sci U S A 97:6640-6645.

32. Schmieger H. 1971. A method for detection of phage mutants with altered transducing ability. Mol Gen Genet 110:378-381.

33. Porwollik S, Santiviago CA, Cheng P, Long F, Desai P, Fredlund J, Srikumar S, Silva CA, Chu W, Chen X. 2014. Defined single-gene and multi-gene deletion mutant collections in *Salmonella enterica* sv Typhimurium. PloS One 9:e99820.

34. Chan RK, Botstein D, Watanabe T, Ogata Y. 1972. Specialized transduction of tetracycline resistance by phage P22 in *Salmonella typhimurium*: II. Properties of a high-frequency-transducing lysate. Virology 50:883-898.

35. Cherepanov PP, Wackernagel W. 1995. Gene disruption in *Escherichia coli*: Tc^R and Km^R cassettes with the option of Flp-catalyzed excision of the antibiotic-resistance determinant. Gene 158:9-14.

36. Baba T, Ara T, Hasegawa M, Takai Y, Okumura Y, Baba M, Datsenko KA, Tomita M, Wanner BL, Mori H. 2006. Construction of *Escherichia coli* K-12 in-frame, single-gene knockout mutants: the Keio collection. Mol Syst Biol 2:2006.0008.

37. VanDrisse C, Escalante-Semerena J. 2016. New high-cloning-efficiency vectors for complementation studies and recombinant protein overproduction in *Escherichia coli* and *Salmonella enterica*. Plasmid 86:1-6.

38. Galloway NR, Toutkoushian H, Nune M, Bose N, Momany C. 2013. Rapid cloning for protein crystallography using type IIS restriction enzymes. Cryst Growth Des 13:2833-2839.

39. Horton RM, Cai Z, Ho SN, Pease LR. 2013. Gene splicing by overlap extension: tailor-made genes using the polymerase chain reaction. Biotechniques 54:129-133.

40. Chen P, Ailion M, Bobik T, Stormo G, Roth J. 1995. Five promoters integrate control of the *cob*/*pdu* regulon in *Salmonella typhimurium*. J Bacteriol 177:5401-5410.

41. Sun S, Berg OG, Roth JR, Andersson DI. 2009. Contribution of gene amplification to evolution of increased antibiotic resistance in *Salmonella typhimurium*. Genetics 182:1183-1195.

42. Jang YM, Kim DW, Kang T-C, Won MH, Baek N-I, Moon BJ, Choi SY, Kwon O-S. 2003. Human pyridoxal phosphatase: Molecular cloning, functional expression, and tissue distribution. J Biol Chem 278:50040-50046.

Table 2.1 – Growth of *pdxJ* mutant derivatives.

Strain	pCV1	Final OD_{650}*	
		PLP	PNP
pdxJ	VOC	0.60 ± 0.01	0.62 ± 0.02
pdxJ phoN	VOC	0.10 ± ≤0.01	0.08 ± ≤0.01
	phoN	0.61 ± ≤0.01	0.58 ± 0.01
pdxJ phoP	VOC	0.09 ± ≤0.01	0.08 ± ≤0.01
	phoN	0.58 ± ≤0.01	0.57 ± 0.01
	phoP	0.13 ± 0.01	0.08 ± ≤0.01
	phoQ	0.09 ± ≤0.01	0.08 ± ≤0.01
	phoPQ	0.60 ± ≤0.01	0.25 ± 0.14
pdxJ phoQ	VOC	0.09 ± ≤0.01	0.08 ± ≤0.01
	phoN	0.58 ± 0.01	0.57 ± 0.01
	phoQ	0.50 ± 0.01	0.44 ± 0.12
	phoPQ	0.55 ± 0.02	0.52 ± 0.03

S. enterica pdxJ strains carrying an empty pCV1 vector control (VOC) or pCV1 expressing different gene constructs were grown in minimal NCE glucose supplemented with 1 μM PLP or PNP and induced with 0.02% arabinose. The final growth yield is shown.

*Final optical density at 650 nm (OD_{650}) was determined after 24-hour incubation at 37°C. Data were obtained from two independent experiments with three biological replicates each. Representative result from one experiment is shown. Abbreviations: PLP, pyridoxal 5′-phosphate, PNP, pyridoxine 5′-phosphate.

Table 2.2 – Phosphatase activity of PhoN.

Substrate[*]	Specific activity[#] (μmol min^{-1} mg^{-1})	*P*-value[£]
PLP	9.40 ± 1.52	<0.0001
PNP	2.93 ± 0.52	<0.0001
PMP	0.034 ± 0.004	0.04
p-NPP	18.43 ± 1.50	<0.0001

[*]Abbreviations: PLP, pyridoxal 5′-phosphate; PNP, pyridoxine 5′-phosphate; PMP, pyridoxamine 5′-phosphate; *p*-NPP, *p*-nitrophenyl phosphate.

[#]Activity was measured in 50 mM triethanolamine-HCl (pH 7.4) at 37°C. Data were obtained from two independent experiments with at least three technical replicates each.

[£]Statistical significance with respect to no enzyme control was determined by two-tailed unpaired Student *t*-test using GraphPad Prism 7.0c (GraphPad Software, La Jolla, CA).

Table 2.3 – Strains and plasmids.

Strain or plasmid	Description	Source*
***S. enterica* LT2**		
DM15906	*pdxJ662*::*Km*	This study
DM15964	*pdxJ664*	This study
DM16354	*pdxJ664 pdxH669*::*Km*	This study
DM17013	*pdxJ664 pdxY667*::*Cm*	This study
DM17017	*pdxJ664 pdxK672*::*Km*	This study
DM17067	*pdxB680*	This study
DM17068	*pdxB680 pdxY667*::*Cm*	This study
DM17069	*pdxB680 pdxK672*::*Km*	This study
DM17080	*pdxB680 pdxK672*::*Km pdxY667*::*Cm*	This study
DM16983	*pdxJ664* / pCV1	This study
DM16943	*pdxJ664 phoN247*::*Km* / pCV1	This study
DM16944	*pdxJ664 phoN247*::*Km* / pDM1603	This study
DM16945	*pdxJ664 phoP248*::*Km* / pCV1	This study
DM16946	*pdxJ664 phoP248*::*Km* / pDM1603	This study
DM16947	*pdxJ664 phoP248*::*Km* / pDM1604	This study
DM17007	*pdxJ664 phoP24i*::*Km* / pDM1605	This study
DM17008	*pdxJ664 phoP248*::*Km* / pDM1620	This study
DM16904	*pdxJ664 phoQ245*::*Km* / pCV1	This study
DM16905	*pdxJ664 phoQ245*::*Km* / pDM1603	This study
DM16906	*pdxJ664 phoQ245*::*Km* / pDM1605	This study
DM17006	*pdxJ664 phoQ245*::*Km* / pDM1620	This study
***E. coli* BW25113**		
DM16897	*pdxJ736*::*Km* / pCV1	This study
DM16898	*pdxJ736*::*Km* / pDM1603	This study
DM16941	*pdxJ736*::*Km* / pDM1606	This study
DM16942	*pdxJ736*::*Km* / pDM1607	This study
Plasmids		
pCP20	Temperature-sensitive plasmid expressing Flp recombinase (Am^R, Cm^R)	(35)
pCV1	Modified pBAD24 (Am^R)	(37)
pDM1603	pCV1 expressing *S. enterica* PhoN (Am^R)	This study
pDM1604	pCV1 expressing *S. enterica* PhoP (Am^R)	This study
pDM1605	pCV1 expressing *S. enterica* PhoQ (Am^R)	This study
pDM1606	pCV1 expressing *S. enterica* Δ(1-20)PhoN (Am^R)	This study
pDM1607	pCV1 expressing *E. coli* TorA signal sequence fused to *S. enterica* Δ(1-20)PhoN (Am^R)	This study
pDM1620	pCV1 expressing *S. enterica* PhoP and PhoQ (Am^R)	This study
pDM1623	pTEV20 expressing *S. enterica* 6xHis-tagged PhoN (Am^R)	This study

*Phage P22 carrying donor DNA of *S. enterica* Typhimurium 14028s *pdxK*::*Km*, *phoN*::*Km*, *phoP*::*Km*, and *phoQ*::*Km* strains from the SGD-K collection (33) were kindly provided by Dr. Anna Karls at the University of Georgia (Athens, GA). *E. coli* BW25113 *pdxJ736*::*Km* mutant from the Keio collection (36) was a gift from Dr. Jorge C. Escalante-Semerena at the same institution.

Table 2.4 – Primers.

Primer	Sequence (5' to 3')	Description
PR1076	AACGCACAGTAAAAACGAAGAAAGATTAACGAGGATTGTCGTGTAGGGCTGGAGCTGCTTC	Inactivation of *S. enterica pdxJ*
PR1077	GGGCAATCTCTACAATATCCGTTCCCAGGCCGAGAATCGCCATATGAATATCCTCCTTAG	
PR1080	GTAACAGGGAGTGAGAAATCACTCCCTTATTTTTGATGTTGTGTAGGCTGGAGCTGCTTC	Inactivation of *S. enterica pdxY*
PR1081	GGGCAATCTCTACAATATCCGTTCCCAGGCCGAGAATCGCCATATGAATATCCTCCTTAG	
PR1374	TTGTCCGTTAACTCTCGTTCTCAAACAGGTACGACAGTCGTGTAGGCTGGAGCTGCTTC	Inactivation of *S. enterica pdxB*
PR1375	ACACCAAATGCGCCAGTCTTTTCAGCGTCGGTTGATCCAGCATATGAATATCCTCCTTAG	
PR1395	GCACAATAGCGCCACCCACTGATTATTTCTGATCAACGCCGTGTAGGCTGGAGCTGCTTC	Inactivation of *S. enterica pdxH*
PR1396	ATTCATCCGCACCAGTGCTTAAAACAAGATTTTTGCATCTCATATGAATATCCTCCTTAG	
PR1320	NNGCTCTTCNTTCATGAAAAGTCGTTATTTAGTATTTTTTCTACC	Construction of pDM1603
PR1321	NNGCTCTTCNTTATCAGTAATTAAGTTTGGGGTGATC	
PR1322	NNGCTCTTCNTTCATGATGCGCGTACTGG	Construction of pDM1604
PR1323	NNGCTCTTCNTTATAGCGCAATTCAAAAAGATATCCT	
PR1324	NNGCTCTTCNTTCATGAATAAATTTGCTCGCCATTTTC	Construction of pDM1605
PR1325	NNGCTCTTCNTTATTATTCCTCTTTCTGTGTGGGA	
PR1328	NNGCTCTTCNTTCATGGAAACAGTGCAACCCTTTC	Construction of pDM1606
PR1321	See above	
PR1329	NNGCTCTTCNTTCATGAACAATAACGATCTCTTTCAGGCATCACGT	Construction of pDM1607
PR1330	GCACTGTTTCTGCCGCAGTCGCACGTCG	
PR1331	CGACGTGCGACTGCGGCAGAAACAGTGCAACCCTTTCATTCTC	
PR1332	NNGCTCTTCNTTATCAGTAATTAAGTTTGGGGTGATCTTCTTTACTCAAT	
PR1322	See above	Construction of pDM1620
PR1325	See above	
PR1361	NNGCTCTTCNTACATGAAAAGTCGTTATTTAGTATTTTTTCTAC	Construction of pDM1623
PR1362	NNGCTCTTCATTCGTAATTAAGTTTGGGGTGATCTTC	

Primer	Sequence (5’ to 3’)	Description
Tn10R	ACCTTTGGTCACCAACGCTTTTCC	Transposon sequencing (40, 41)
Tn10L	TCCATTGCTGTTGACAAAGGGAAT	
Arb1	GGCCACGCGTCGACTAGTACNNNNNNNNNNGATAT	
Arb6	GGCCACGCGTCGACTAGTACNNNNNNNNNNACGCC	

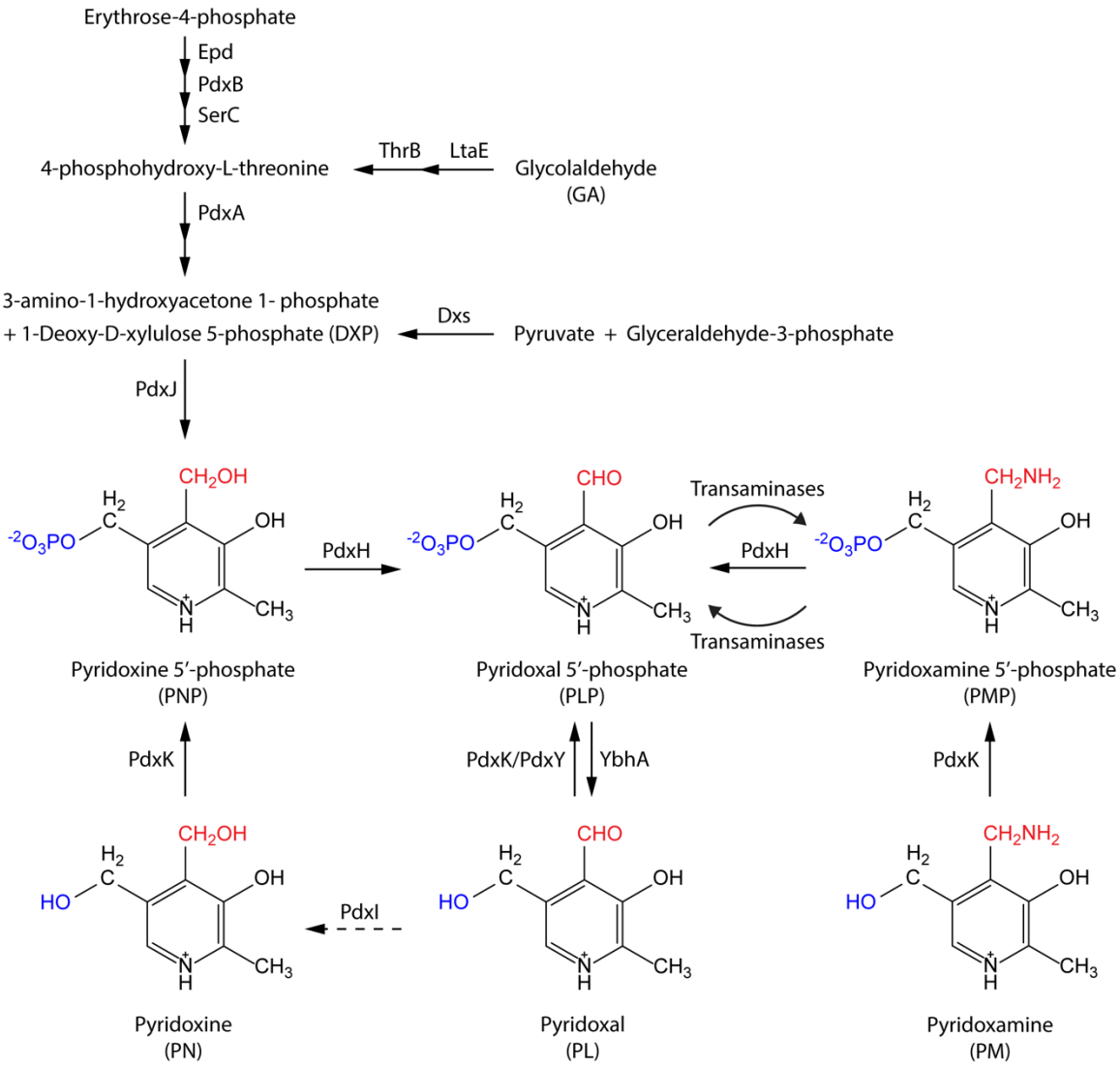

Figure 2.1 – Synthesis and salvage of pyridoxal 5′-phosphate (PLP). In *S. enterica* and *E. coli*, PLP is synthesized from erythrose-4-phosphate and 1-deoxy-D-xylulose 5-phosphate, or salvaged from other B_6 vitamers in the environment (1, 2). *E. coli* can convert glycolaldehyde (GA) to 4-phosphohydroxy-L-threonine and thus bypass the early steps in PLP synthesis (4). The relevant pathways are shown schematically and gene products that catalyze each step are indicated beside the arrows. The dashed arrow under PdxI reflects the absence of this enzyme in *S. enterica* (13).

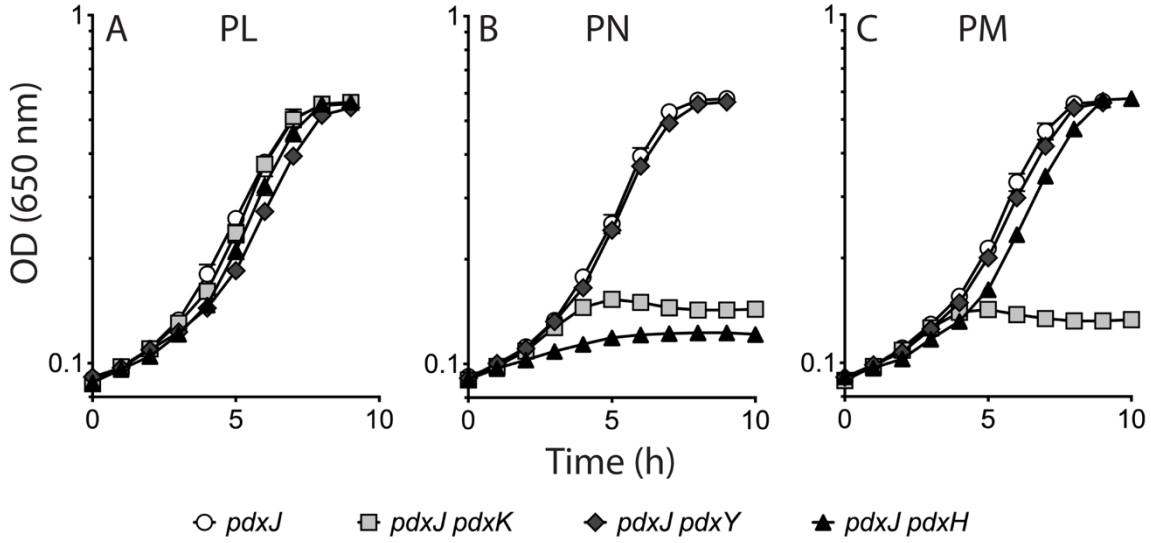

Figure 2.2 – *S. enterica* mutants lacking *pdxJ* can salvage B_6 vitamers. Strains lacking *pdxJ* and designated salvage genes were grown in minimal NCE glucose supplemented with a B_6 vitamer (1 μM) as indicated. Data were obtained from two independent experiments with three biological replicates each. Error bars show standard deviation from the mean. Abbreviations: PL, pyridoxal; PN, pyridoxine; PM, pyridoxamine.

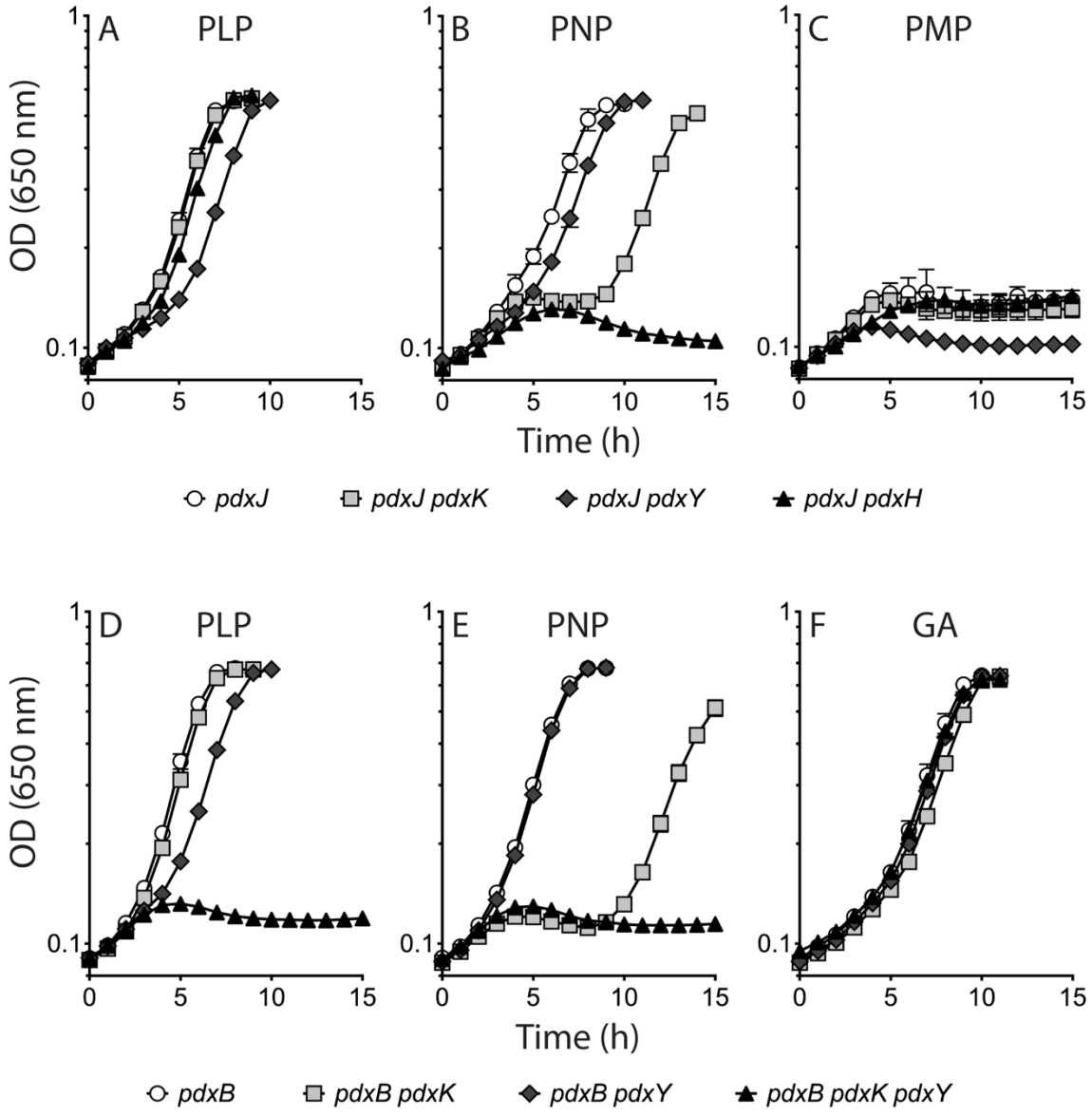

Figure 2.3 – PLP and PNP support growth of *pdxJ* and *pdxB* mutants. *S. enterica* strains lacking *pdxJ* and different salvage enzymes (A-C) and those lacking *pdxB* and salvage enzymes (D-F) were grown in minimal NCE glucose supplemented with a phosphorylated B_6 vitamer (1 μM) or glycolaldehyde (1 mM) as indicated. Data were obtained from three biological replicates and error bars represent standard deviation from the mean. Abbreviations: PLP, pyridoxal 5′-phosphate; PNP, pyridoxine 5′-phosphate; PMP, pyridoxamine 5′-phosphate; GA, glycolaldehyde.

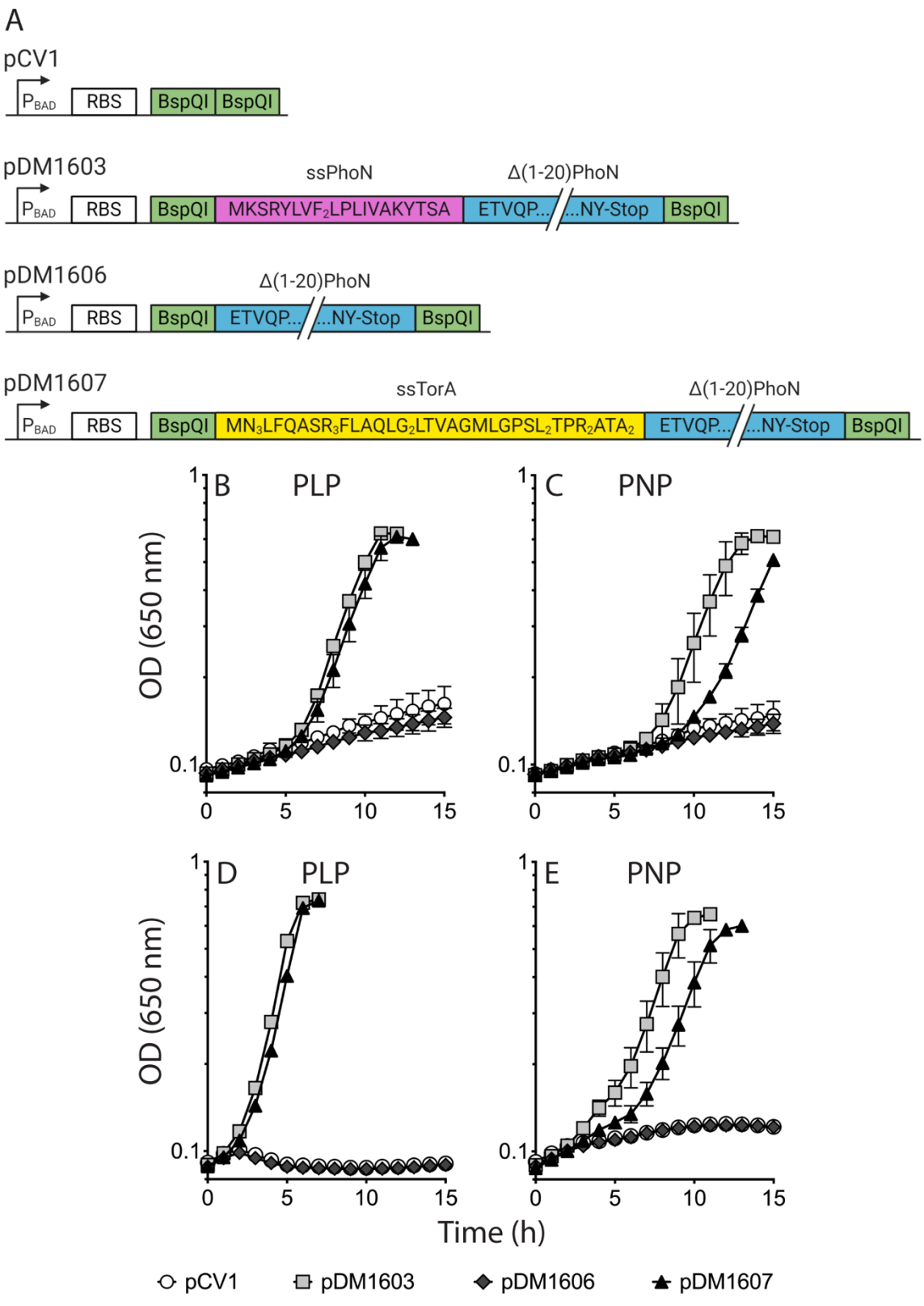
A
pCV1
P BAD
RBS
BspQI
BspQI
pDM1603
ssPhoN
Δ(1-20)PhoN
MKSRYLVF2LPLIVAKYTSA
ETVQP...
...NY-Stop
pDM1606
pDM1607
ssTorA
MN3LFQASR3FLAQLG2LTVAGMLGPSL2TPR2ATA2
B PLP
C PNP
D PLP
E PNP
OD (650 nm)
Time (h)
pCV1
pDM1603
pDM1606
pDM1607

Figure 2.4 – Periplasmic location is required for the *in vivo* role of PhoN in PLP and PNP salvage. (A) Relevant PhoN constructs and their general structure are depicted. Each was cloned into pCV1 at the BspQI sites. (B-C) *E. coli pdxJ* and (D-E) *S. enterica pdxJ phoN* strains carrying the designated vectors were grown in minimal NCE glucose supplemented with 1 μM PLP or PNP and 0.02% arabinose to induce expression. Abbreviations: P_{BAD}, arabinose-inducible promoter; RBS, ribosomal binding site; ssPhoN, signal sequence of *S. enterica* PhoN; ssTorA, signal sequence of *E. coli* TorA; Δ(1-20)PhoN, mature *S. enterica* PhoN; PLP, pyridoxal 5′-phosphate; PNP, pyridoxine 5′-phosphate.

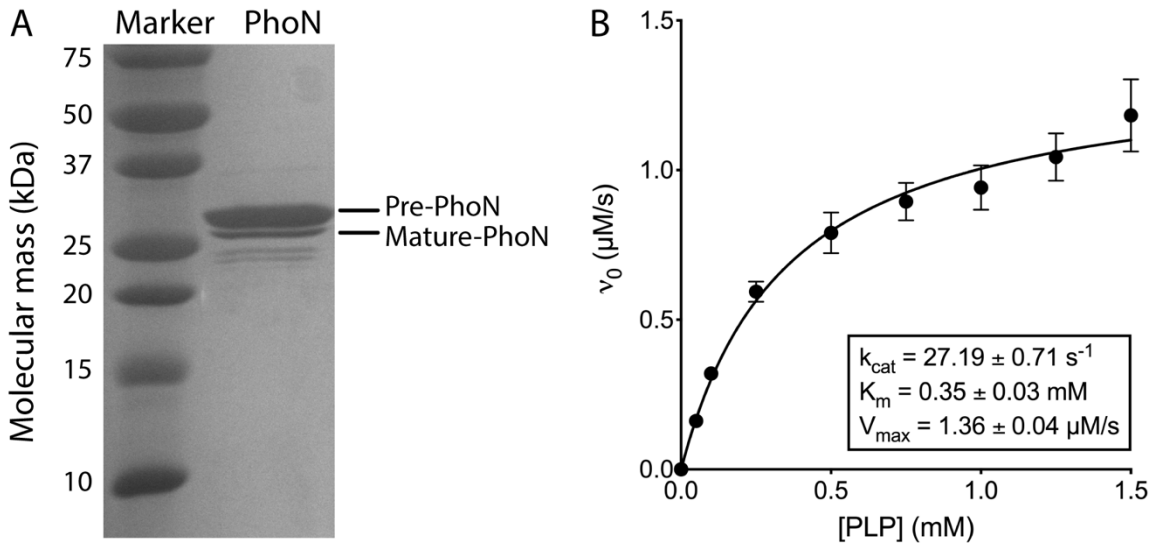

Figure 2.5 – PhoN has phosphatase activity on PLP. (A) After purification, PhoN protein was separated on a 14% SDS-PAGE gel and stained with Coomassie blue. Two major bands were visible at ~30 kDa, corresponding to the molecular mass of pre-PhoN and mature-PhoN. (B) Michaelis-Menten kinetics of PhoN were determined by plotting the initial velocity of PL formation at 37°C against varying PLP concentrations. Reactions contained 50 mM triethanolamine-HCl (pH 7.4) and 50 nM PhoN in addition to PLP. Data were obtained from two independent experiments with at least three technical replicates, and error bars are shown. Abbreviations: PLP, pyridoxal 5′-phosphate; PL, pyridoxal.

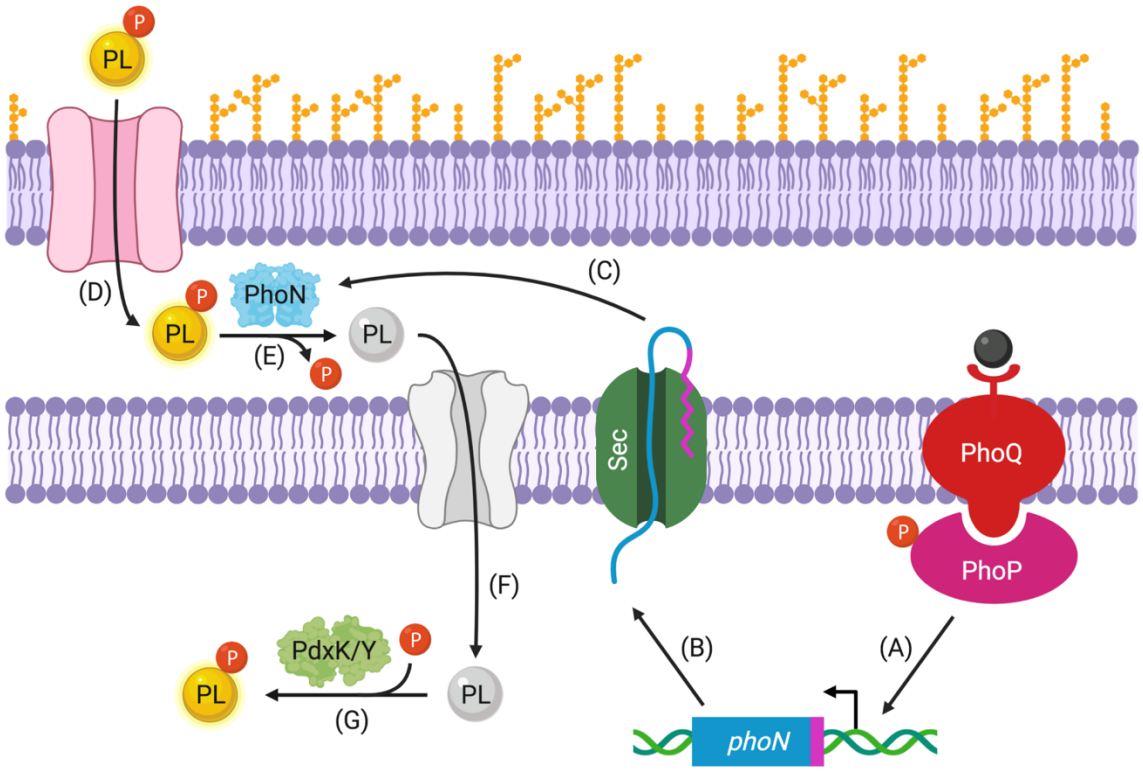

Figure 2.6 – Working model of PhoN-dependent PLP/PNP salvage pathway in *S. enterica*. (A) Expression of *phoN* requires the PhoQ sensor kinase phosphorylates the PhoP response regulator. (B) The PhoN peptide is translocated to the periplasm via the Sec-dependent system, (C) where it is processed to the mature form. (D) PLP enters the periplasm, possibly through a generic porin(s), and (E) PhoN dephosphorylates PLP to PL. (F) Via an unidentified mechanism, PL is transported into the cytoplasm, (G) where PdxK/PdxY phosphorylates PL back to PLP. PNP salvage mirrors that of PLP, but requires an additional step in which PNP is oxidized to PLP by PdxH (Figure 2.1). Abbreviations: PLP, pyridoxal 5′-phosphate; PNP, pyridoxine 5′-phosphate; PL: pyridoxal. Image was created with BioRender (Toronto, ON, Canada).

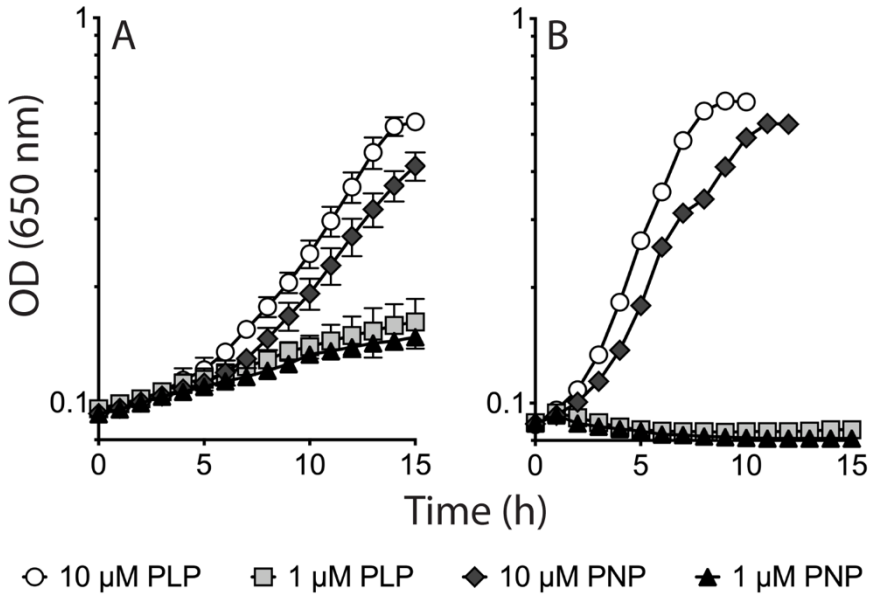

Figure 2.7 – At high concentration, PLP and PNP are utilized independent of PhoN. (A) *E. coli pdxJ* and (B) *S. enterica pdxJ phoN* strains carrying an empty pCV1 vector control were grown in minimal NCE glucose supplemented with 1 µM-10 µM PLP or PNP and induced with 0.02% arabinose. Data were obtained from two independent experiments with three biological replicates each. Error bars show standard deviation from the mean. Abbreviations: PLP, pyridoxal 5′-phosphate; PNP, pyridoxine 5′-phosphate.

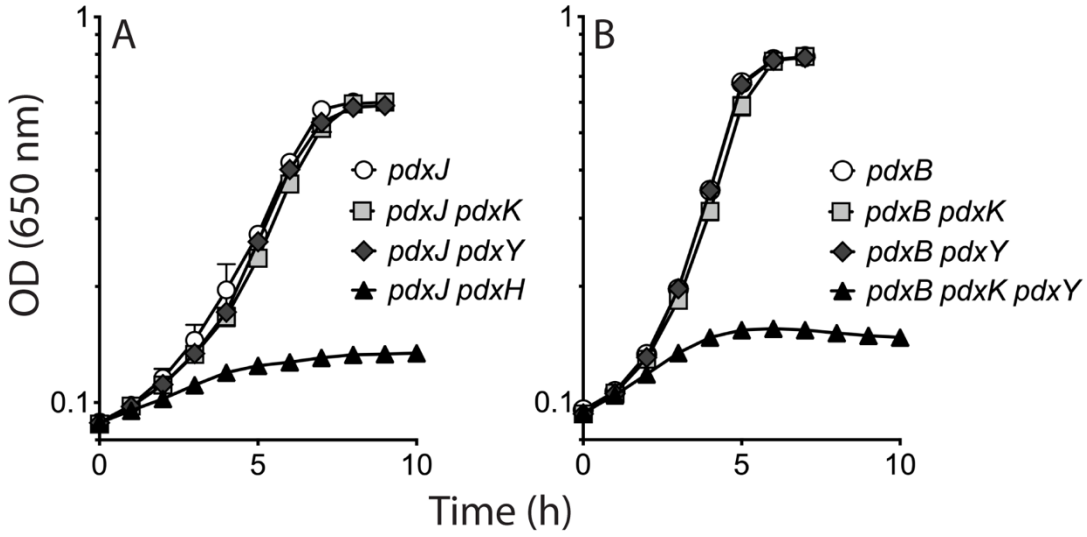

Figure 2.8 – At high concentration of PN, activity of PdxY allows growth of *S. enterica* strains blocked in *de novo* PLP synthesis. *S. enterica* (A) *pdxJ* and (B) *pdxB* strains were grown in minimal NCE glucose supplemented with 10 μM PN. Data were obtained from two independent experiments with three biological replicates each. Error bars represent standard deviation from the mean. Abbreviation: PN, pyridoxine.

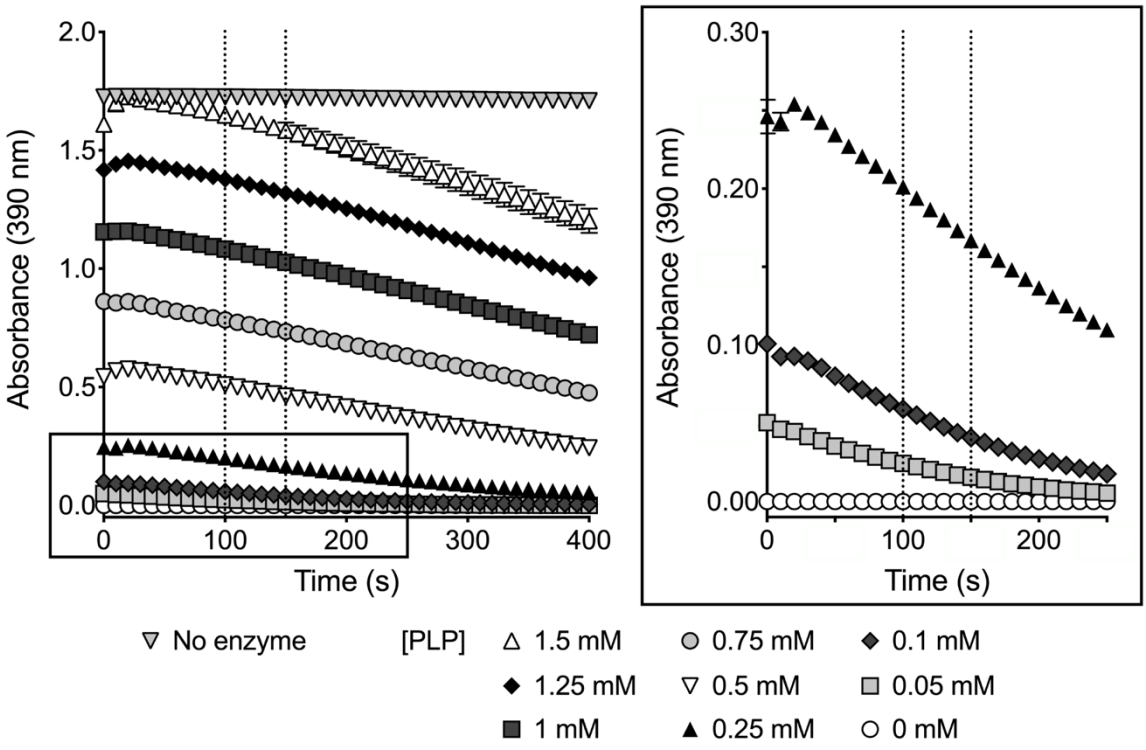

Figure 2.S1 – Continous assay of recombinant PhoN with PLP as substrate. Activity was measured in 50 mM triethanolamine-HCl (pH 7.4) containing 50 nM PhoN and 0-1.5 mM PLP at 37ºC. The right inset shows a magnified view of PhoN activity with 0-0.25 mM PLP. No enzyme control contained 1.5 mM PLP in assay buffer lacking PhoN. Data were obtained from two independent experiment with at least three technical replicates each. Representative results from one experiment are shown. Dashed lines indicate the time points at which initial velocity was determined for each concentration of PLP. Abbreviation: PLP, pyridoxal 5′-phosphate.

CHAPTER 3

GENETIC ANALYSIS USING VITAMIN B_6 ANTAGONIST 4-DEOXYPYRIDOXINE DEFINES A CONNECTION BETWEEN PYRIDOXAL 5′-PHOSPHATE AND COENZYME A METABOLISM IN *SALMONELLA ENTERICA* [2]

[2] Vu HN, Downs DM. 2021. To be submitted to *Journal of Bacteriology.*

3.1 ABSTRACT

Pyridoxal 5′-phosphate (PLP) is an essential cofactor for organisms in all three domains of life. Despite the central role of PLP, many aspects of vitamin B_6 metabolism, including its integration with other biological pathways, are not fully understood. In this study, we examined the metabolic perturbations caused by the vitamin B_6 antagonist 4-deoxypyridoxine (dPN) in a *ptsJ* mutant of *Salmonella enterica* serovar Typhimurium LT2. Our data suggest that PdxK (PL/PN/PM kinase, EC 2.7.1.35) phosphorylates dPN to 4-deoxypyridoxine 5′-phosphate (dPNP), which in turn can compromise the *de novo* biosynthesis of PLP. In addition, accumulated dPNP is proposed to inhibit GlyA (serine hydroxymethyltransferase, EC 2.1.2.1) and/or GcvP (glycine decarboxylase, EC 1.4.4.2), two PLP-dependent enzymes involved in the generation of one-carbon units, leading to reduced flux to coenzyme A precursors and subsequently lower CoA and thiamine synthesis. This study uncovers a hidden link between vitamin B_6 metabolism and biosynthesis of CoA and thiamine, highlighting the complexity and interconnection among metabolic nodes in microbes.

IMPORTANCE

PLP is a ubiquitous cofactor required by enzymes in diverse metabolic networks. The data herein expand our understanding of the toxic effects of dPN, a vitamin B_6 antagonist often used to mimic vitamin B_6 deficiency and to study PLP-dependent enzyme kinetics. In addition to *de novo* PLP biosynthesis, we define a metabolic connection between vitamin B_6 metabolism and synthesis of thiamine and CoA. This work provides a foundation for the use of dPN to study vitamin B_6 metabolism in other organisms.

3.2 INTRODUCTION

Pyridoxal 5′-phosphate (PLP) is the biologically active form of vitamin B_6 and a required cofactor in the metabolism of all organisms. Due to its unique chemical properties, PLP can facilitate diverse enzymatic reactions, including transamination, elimination, decarboxylation, and racemization (1). PLP-dependent enzymes, which are classified into seven fold types based on structural similarities (2), account for ~4% of all described activities by the Enzyme Commission (3). Except glycogen phosphorylases, most PLP-dependent enzymes are associated with metabolic pathways involving amino substrates (3).

In nature, PLP is synthesized *de novo* via one of the two biosynthetic routes (Figure 3.1). The deoxyxylulose 5-phosphate (DXP)-dependent pathway is found primarily in γ-proteobacteria such as *Salmonella enterica* and *Escherichia coli*, while the DXP-independent pathway is more widespread among other bacteria, fungi, and archaea (4, 5). Alternatively, PLP can be acquired from other B_6 vitamers using the salvage pathway as found in humans and animals (4, 5) (Figure 3.1). Due to the reactivity of this cofactor and the prevalence of PLP-dependent enzymes in metabolic networks, perturbations in PLP pools can have adverse consequences by inhibiting both PLP-independent and -dependent enzymes (6-10). Despite the importance of this cofactor, the mechanism(s) used by cells to control PLP homeostasis is not fully understood.

One approach to study vitamin B_6 metabolism is the use of analogs, compounds that are structurally similar to B_6 vitamers but lack the biochemical properties to aid enzyme catalysis. In particular, 4-deoxypyridoxine (dPN) (Figure 3.1) and its phosphorylated derivative 4-deoxypyridoxine 5′-phosphate (dPNP) have been used as potent vitamin B_6 antagonists in research for decades. Early studies in bacteria, fungi, plants, and animals focused on the inhibitory effects of dPN on growth, morphology, and the metabolism of other vitamins (11). Later work showed

that dPN and dPNP could competitively inhibit the *in vitro* activity of the human pyridoxal (PL)/pyridoxine (PN)/pyridoxamine (PM) kinase (PdxK, EC 2.7.1.35) (12) and pyridoxine 5′-phosphate (PNP)/pyridoxamine 5′-phosphate (PMP) oxidase (PdxH, EC 1.4.3.5) (13) respectively, which are two conserved enzymes essential for the salvage of B_6 vitamers (Figure 3.1). This study was initiated to understand the mechanism of dPN toxicity in *S. enterica* serovar Typhimurium LT2 (referred hereafter as *S. enterica*) using phenotypic and metabolite analyses. Our results uncover a link between vitamin B_6 metabolism and the biosynthesis of thiamine and coenzyme A, highlighting metabolic network complexity and the overarching consequences of perturbed pools of B_6 vitamers.

3.3 RESULTS AND DISCUSSION

Sensitivity of a *ptsJ* mutant to dPN is dependent on PdxK. Growth of an *S. enterica* wild-type strain was not affected by 10 μM dPN in minimal NCE glycerol (Figure 3.S1). However, if *pdxK* was overexpressed *in trans*, growth was inhibited by the presence of dPN (Figure 3.S1). Consistently, strain lacking PtsJ, a MocR-type transcriptional repressor that regulates expression of *pdxK* (14), was sensitive to dPN in minimal NCE glucose in a dose-dependent manner (Figure 3.2a). A null mutation in *pdxK* (Figure 3.2a) or expression of *ptsJ in trans* (Figure 3.2b) overcame the growth defect of the *ptsJ* mutant caused by dPN. The data demonstrate the importance of these two gene products in dPN sensitivity.

Unphosphorylated B_6 vitamers are thought to enter cells via facilitated diffusion and subsequently be trapped by phosphorylation (15-17). In addition, the human homolog of PdxK could use dPN as a substrate *in vitro* (18). Taken together, the data suggest that to be toxic, dPN was phosphorylated to dPNP by PdxK. Consistent with this hypothesis, HPLC analysis showed

that a *ptsJ* strain grown in minimal glucose medium supplemented with dPN (0.5 μM) accumulated intracellular dPNP (~257 ± 4 pmol/OD_{650}). No dPNP was detected in cells grown in the absence of dPN (Figure 3.2c). When a mutation in *pdxK* was introduced in the *pstJ* background, the profiles of intracellular B_6 vitamers in the absence and presence of dPN were indistinguishable. In total, these data support the conclusion that dPNP is the molecule that exerts toxic effects on *S. enterica*, and by extension other organisms that possess homologs of PdxK.

DXP-dependent biosynthesis of PLP is compromised in the presence of dPNP. dPNP inhibited both the *E. coli* and the human homolog of PdxH by competing with the native substrates PNP and PMP *in vitro* (13, 19). If such an inhibition were to occur in *S. enterica in vivo,* the growth defect of the *ptsJ* mutant in the presence of dPN could be due to PLP limitation caused by decreased PdxH activity. Growth of the *ptsJ* mutant in the presence of dPN was restored to different degrees with supplementation of 1 μM PL, PN, or PM (Figure 3.3a). However, it was unclear if these vitamers rescued growth by competing with dPN for transport, for PdxK as substrates, or by increasing intracellular PLP content.

To help distinguish between these possibilities, the native DXP-dependent PLP biosynthesis was eliminated in the *ptsJ* mutant by deleting *pdxJ* (encoding a PNP synthase, EC 2.6.99.2) and *pdxH.* As a replacement for the synthetic route, *Saccharomyces cerevisiae SNZ3* (encoding a PLP synthase, EC 4.3.3.6) was expressed *in trans.* The resulting strain synthesizes PLP from endogenous glyceraldehyde-3-phosphate, ribose-5-phosphate, and exogenous ammonium in the medium using Snz3p (20) (Figure 3.1). Growth of *ptsJ* strains carrying different PLP biosynthetic pathways in the presence of dPN was examined in minimal NCE glycerol (Figure 3.3b). Strains lacking *ptsJ* and utilizing either the native (DXP-dependent) or heterologous (Snz3p-

dependent) pathway for PLP synthesis grew similarly in the absence of dPN. When dPN was added, growth inhibition of the *ptsJ* strain synthesizing PLP with Snz3p was significantly less severe than that of the *ptsJ* strain using the native pathway. These data are consistent with the hypothesis that dPNP compromises the DXP-dependent PLP synthesis, while the remaining growth defect suggests that PdxH is not the only target of dPNP toxicity.

dPNP impacts ThiC-dependent thiamine synthesis. Probing the mechanism of dPNP toxicity beyond the presumed inhibition of PdxH required the concentration of dPN to be reduced to allow growth. Nutritional experiments showed that in the presence of low dPN (0.5 μM), the *ptsJ* strain was sensitive to adenosine, which was rescued by thiamine addition (Figure 3.4). The ability of thiamine to abolish the synergistic effect of adenosine and dPN was reminiscent of previous studies, in which adenosine sensitivity indicated compromised synthesis of the pyrimidine moiety of thiamine (HMP). In these scenarios, adenosine reduced flux toward 5-aminoimidazole ribotide (AIR) formation, which lowered HMP synthesis only if the efficiency of the AIR→HMP-P (4-amino-5-hydroxymethyl-2-methylpyrimidine phosphate) reaction was diminished (21-24) (Figure 3.5a). We hypothesized that the AIR→HMP-P conversion, catalyzed by ThiC (25, 26), was lowered in the presence of dPNP. In this scenario, the synergetic effect of adenosine and dPN would be due to reduced flux to AIR and reduced conversion of AIR to HMP-P, respectively. The effect of dPN on the efficiency of the AIR→HMP-P conversion was tested using a biosensor strain (DM7060) carrying a *ptsJ* mutation. The genotype of this strain allows the efficiency of the ThiC-dependent step to be assessed using 5-aminoimidazole riboside (AIRs) as a proxy (27, 28). This strain carries null alleles of *purG* and *purE*, which prevent flux to and from AIR in *de novo* purine synthesis, respectively. In addition to a purine auxotrophy, these mutations cause a thiamine

requirement that can be rescued by supplementation of HMP or AIRs (Figure 3.5a). A mutation in *stm4068* enables efficient utilization of exogenous AIRs by derepressing the kinase responsible for converting AIRs to AIR (29). Thus, the amount of AIRs that allows growth in this background is a measure of the efficiency of the AIR→HMP-P conversion by ThiC.

The AIRs requirement of the *purGE stm4068 ptsJ* strain was assessed with soft agar overlay on minimal NCE glucose medium supplemented with adenine (Figure 3.5bc). In the absence of dPN, the mutant grew with addition of AIRs, HMP, or thiamine (Figure 3.5b) as expected. When dPN (0.1 μM) was added to the medium, overall growth was not as robust. Nonetheless, it was still clear that growth was not supported by the amount of AIRs used in the absence of dPN (Figure 3.5c). These results demonstrate that the *ptsJ* mutant required more AIRs to grow with dPN, supporting the conclusion that the efficiency of AIR→HMP-P conversion by ThiC was compromised by dPNP.

dPNP inhibits the pantoate branch of coenzyme A biosynthesis. Defects in several metabolic processes affect ThiC activity *in vivo*, including iron-sulfur cluster metabolism (28), synthesis of S-adenosylmethionine (AdoMet) from methionine (30), and intracellular CoA levels (31) (Figure 3.6a). If dPNP caused a defect in iron-sulfur cluster synthesis/repair, it was expected to compromise both the HMP and thiazole (THZ) branches of thiamine synthesis (28, 32-35) (Figure 3.5a). However, our data showed that only HMP-P synthesis was affected by dPNP (Figure 3.5c). To determine if dPNP affected ThiC activity by compromising the synthesis of AdoMet and/or CoA, the AIRs requirement of the *purGE stm4068 ptsJ* strain was determined in dPN medium with exogenous methionine or pantothenate (a precursor to CoA) (Figure 3.6b). Methionine had no effect on the AIRs requirement in the presence of dPN, making it unlikely the effect was via

compromised AdoMet synthesis. In contrast, pantothenate and pantoate significantly lowered the amount of AIRs required for growth. These data implicated CoA biosynthesis, specifically the pantoate branch as a target for the effect of dPNP. The weak stimulation by β-alanine was thought to be by increasing flux through PanC when the pantoate substrate was lowered. Consistent with our hypothesis, a *ptsJ* mutant had a significant ~2-fold decrease in the total CoA pool when grown in medium supplemented with dPN (0.5 μM) (Figure 3.6c).

Addition of α-ketoisovalerate (KIV), serine, or glycine lowered the AIRs requirement for growth in dPN, albeit to a lesser extent than pantothenate and pantoate (Figure 3.6b). Serine and glycine are substrates in the generation of one-carbon units by GlyA (serine hydroxymethyltransferase, EC 2.1.2.1) and glycine-cleavage (GCV) system, respectively (Figure 3.6a). Both reactions produce 5,10-methylenetetrahydrofolate (mTHF) (36, 37), which is a co-substrate for PanB (ketopantoate hydroxymethyltransferase, EC 2.1.2.11) to convert KIV to ketopantoate (Figure 3.6a). The PanB-dependent reaction was suggested to be the rate-limiting step for CoA synthesis (38). Notably, GlyA and GcvP (glycine decarboxylase, EC 1.4.4.2) of the GCV system are PLP-dependent enzymes, which could be targeted by dPNP. There is precedent for damaged GlyA causing a decrease in CoA levels in *S. enterica* (39). In addition, mitogen-induced GlyA activity measured in crude extracts was lowered when human leukocytes and T-cells were cultured with dPN supplementation, and the activity was rescued by addition of vitamin B_6 (40). Although the effect of dPNP on GcvP has not been reported, PNP, a B_6 vitamer with similar structure to dPNP (Figure 3.1), could inhibit *in vitro* activity of *E. coli* and *Bacillus subtilis* GCV system (41). In total, the data are consistent with a model in which dPNP inhibits GlyA and/or the GCV system by competing with PLP. Such inhibition would lead to a reduction in mTHF level and lower flux to CoA synthesis.

Working model for growth limitation by dPN. The cumulative effects of dPN toxicity, exacerbated by a *ptsJ* mutation, are depicted in Figure 3.7. The working model suggests that exogenous dPN is phosphorylated to dPNP by PdxK (Figure 3.2, Figure 3.S1). Intracellular dPNP then competes with PNP as a substrate for PdxH and thus compromises the DXP-dependent synthesis of PLP (Figure 3.3). Additionally, dPNP inhibits activity of the GlyA and/or GcvP PLP-dependent enzymes, which reduces the level of mTHF. Finally, lower than optimal mTHF compromises the activity of PanB, reducing formation of pantothenate and lowering flux to CoA (Figure 3.6). Reduced CoA levels then indirectly affects the synthesis of the pyrimidine moiety of thiamine, resulting in overall lower thiamine formation (Figure 3.4, Figure 3.5).

The conclusions made from phenotypic analyses are bolstered by considering the kinetic parameters of PdxH. Based on our HPLC data, it was estimated that the intracellular concentration of dPNP was ~1.7- and 250-fold higher than PMP and PNP, respectively (data not shown) under conditions that growth was significantly impaired (Figure 3.2). The binding affinity of dPNP to *E. coli* PdxH is similar to that of PMP and ~50-fold lower than PNP (19). Together, these considerations support the ability of dPNP to compete with PNP and/or PMP for PdxH and reduce its ability to generate PLP. Similar kinetic parameters with GlyA and GcvP have not been reported, and additional *in vitro* experiments are required to further support the genetic analyses with biochemical data.

It was surprising that our data did not support a role for PdxY in the mechanism of dPNP toxicity. PdxY is another PL kinase (EC 2.7.1.35) able to salvage PL (42). PdxK and PdxY have promiscuous kinase activity with pyrimidine and pyridine derivatives, including the HMP moiety of thiamine and unphosphorylated B_6 vitamers (42-45). A potential explanation for the lack of a role for PdxY is that *S. enterica* evolved differential regulation of *pdxK* and *pdxY*. Strains lacking

PtsJ, like those used herein, led to an ~80-fold increase in expression of *pdxK*, while only a 2/3-fold increase was observed with *pdxY* (14). Alternatively, PdxY may not phosphorylate dPN with the efficiency that would make it relevant under the conditions tested.

In addition, this work did not address whether dPN/dPNP could be metabolized or detoxified in *S. enterica*. Rapid excretion and modification of dPN was proposed to be a detoxifying mechanism in higher organisms (46). Precedent exists for metabolic detoxification in humans and rats, in which dPN appeared to be converted to 4-deoxy-5-pyridoxic acid and deoxypyridoxine-3-(hydrogen sulfate), respectively (46). Isolation and characterization of *S. enterica* mutants that are more or less sensitive to dPN may address this question in the future.

Concluding remarks. In summary, this study contributes to our understanding of the mechanism by which exogenous dPN inhibits growth in *S. enterica.* In addition to characterizing the *in vivo* impact of the putative inhibition of PdxH, the data herein provide a template for probing the metabolic network structure involving vitamin B_6 in other organisms. Further, the use of dPN provides another approach to disrupt PLP metabolism, which can be coupled with mutations that impact PLP-dependent enzymes and PLP homeostasis such as *ridA* and *yggS* respectively, to better understand all metabolic aspects of this critical cofactor.

3.4 MATERIALS AND METHODS

Strains, plasmids, and primers. Strains and plasmids are presented in Table 3.1. Primers used for strain and plasmid construction are listed in Table 3.2. Strains are derivatives of *S. enterica* serovar Typhimurium LT2. *Escherichia coli* DH5α and BL21AI (Invitrogen, Carlsbad, CA) were used to propagate plasmids and purify recombinant protein, respectively. Phage λ Red

recombineering method (47) was adapted for *S. enterica* to generate gene deletions. Initial deletions were transduced into appropriate strain backgrounds using phage P22 *HT105/1 int-201* (48) following published protocol (49) and confirmed by colony PCR.

Plasmid pDM1643 and pDM1647 were constructed by cloning *S. enterica pdxK* and *ptsJ*, respectively, into pCV1 (50) as described (51) and validated using Sanger sequencing (Eton Bioscience, San Diego, CA). Plasmid pBsPTA1 was generated by cloning *pta* (encoding a phosphotransacetylase, EC 2.3.1.8) from *B. subtilis* 168 into pTEV5 (52) and was a gift from Jorge C. Escalante-Semerena at the University of Georgia (Athens, GA). Plasmids were electroporated into *S. enterica* and *E. coli* using standard protocol.

Media and chemicals. Strains were grown at 37°C in nutrient broth (8 g/liter Difco mix, 5 g/liter NaCl) or minimal no-carbon E (NCE) medium supplemented with 1 mM $MgSO_4$, trace metals (53), and 11 mM glucose or 22 mM glycerol as a sole carbon source. Lysogeny broth (10 g/liter Bacto tryptone, 5 g/liter yeast extract, 5 g/liter NaCl) and super broth (32 g/liter Bacto tryptone, 20 g/liter yeast extract, 5 g/liter NaCl, 5 mM NaOH) were used to culture *E. coli* for protein purification. Agar was added to a final concentration of 1.5% wt/vol to obtain solid media. Additional supplements included 0.1-10 μM dPN, 1 μM PL, 1 μM PN, 1 μM PM, 1 mM adenosine, 0.4 mM adenine, 0.1 mM pantothenate, 0.1 mM pantoate, 0.1 mM β-alanine, 0.1 mM α-ketoisovalerate, 2.5 mM serine, 0.67 mM glycine, 0.3 mM methionine, or 0.1 μM thiamine as indicated in text. When needed, antibiotics were added as followed: ampicillin (Am, 150 μg/ml in rich medium and 15 μg/ml in minimal medium), chloramphenicol (Cm, 20 μg/ml in rich medium and 5 μg/ml in minimal medium), and kanamycin (Km, 50 μg/ml).

Unless otherwise stated, all chemicals were purchased from MilliporeSigma (formerly Sigma-Aldrich, St. Louis, MO). Crude dPNP was obtained from Cayman Chemical (Ann Arbor, MI). PNP was synthesized from PLP by reduction with $NaBH_4$ (45). PMP was synthesized by dissolving PLP in concentrated NH_4OH, which was subsequently reduced by addition of $NaBH_4$ (54). Restriction enzymes and *Taq* polymerase were purchased from New England BioLabs (Ipswich, MA). Primers were synthesized by Eton Bioscience (San Diego, CA).

Growth analysis. Strains were precultured in 2 ml nutrient broth at 37°C for 6-8 hours in an Innova 43 shaker (New Brunswick Scientific, Edison, NJ) at 250 rpm. Cells were washed with equal volume of 0.85% NaCl and inoculated (2.5% vol/vol) into minimal NCE medium containing appropriate carbon sources and supplements. Growth was monitored in a 96-well plate following the optical density at 650 nm (OD_{650}) over time using a BioTek Elx808 plate reader (BioTek Instruments, Winooski, VT). Data were visualized using GraphPad Prism 8.4.3 (GraphPad Software, La Jolla, CA).

HPLC analysis of B_6 vitamers. Intracellular vitamin B_6 profile of *ptsJ* (DM17239) and *ptsJ pdxk* (DM17168) strain grown in minimal NCE glucose without or with addition of 0.5 μM dPN was determined following described protocol (55), except dPN was replaced by 4-pyridoxic acid (PA) as an internal standard. The identity of dPNP peak was confirmed by co-injecting crude dPNP with the samples and by treatment with wheat germ acid phosphatase (55). Internal dPNP level was inferred by quantifying the concentration of dPN in phosphatase-treated samples.

Assessment of AIRs requirement. *S. enterica purGE stm4068 ptsJ* (DM17274) was precultured in 2 ml nutrient broth and washed as described for growth analysis. 3 ml of molten soft agar (0.7% wt/vol) seeded with 100 µl washed cells was overlaid onto minimal NCE glucose containing 0.4 mM adenine without or with addition of 0.1 µM dPN, 0.1 mM pantothenate, 0.1 mM pantoate, 0.1 mM β-alanine, 0.1 mM α-ketoisovalerate, 2.5 mM serine, 0.67 mM glycine, or 0.3 mM methionine. 1 µl of ~300 mM AIRs, 0.1 mM thiamine, 0.1 mM HMP, and 0.1 mM THZ was subsequently spotted on top of the solidified agar layer. After overnight incubation at 37°C, plates were photographed using a FOTO/Analyst FX workstation (Fotodyne, Hartland, WI).

Purification and activity assay of *B. subtilis* phosphotransacetylase (PTA). *E. coli* BL21AI strain carrying pBsPTA1 was precultured in 10 ml lysogeny broth in duplicates at 37°C in an Innova 43 shaker (New Brunswick Scientific, Edison, NJ) at 250 rpm. Overnight cultures were inoculated into two Fernbach flasks, each of which contained 1.5 liters of super broth. Growth resumed at 37°C in an Innova 44 shaker (New Brunswick Scientific, Edison, NJ) at 180 rpm until mid-log phase (OD_{650} ~0.6) as determined by a Spectronic 20D+ instrument (Thermo Fisher Scientific, Waltham, MA). After addition of arabinose (0.02% wt/vol) and isopropyl-β-D-thiogalactopyranoside (0.5 mM) to induce expression of *pta*, the temperature was shifted to 30°C. Cells were harvested (6,000 × g, 15 min, 4°C) after 20 hours and stored at -80°C until purification.

Protein purification and dialysis steps were performed at 4°C. Frozen cell pellet was resuspended (3 ml/g wet weight) in buffer A (50 mM HEPES, 500 mM NaCl, 20 mM imidazole, pH 7.5) containing lysozyme (1 mg/ml), DNase (0.14 mg/ml), and phenylmethylsulfonyl fluoride (1 mM) and lysed at 18,000 psi using a Constant Systems Limited One Shot cell disruptor (Northants, United Kingdom). Cell lysate was clarified (45,000 × g, 45 min, 4°C), filtered (0.45-

μm PVDF), and loaded onto a pre-equilibrated 5-ml HisTrap HP Ni-sepharose column (GE Healthcare, Chicago, IL) using an NGC Quest 10 Chromatography System (Bio-Rad, Hercules, CA). The loaded column was washed and eluted with 10 column volumes (CV) of buffer A, 6 CV of 4% buffer B (50 mM HEPES, 500 mM NaCl, 500 mM imidazole, pH 7.5), and 10-CV gradient of 4-100% buffer B at a flow rate of 2 ml/min. Fractions containing PTA was visualized on 14% SDS-PAGE gel and pooled. Protein was concentrated using an Amicon Ultra-15 30K centrifugal filter unit (MilliporeSigma, St. Louis, MO), dialyzed against buffer C (50 mM HEPES, 150 mM NaCl, 10% glycerol, pH 7.5) overnight, flash-frozen with liquid nitrogen, and stored at -80°C until assay. Protein concentration was determined spectrophotometrically using a NanoDrop 2000 (Thermo Fisher Scientific, Waltham, MA) from calculated molecular mass and extinction coefficient (ExPASy).

Enzyme activity was assayed using described protocol (56) adapted for 96-well plates. Briefly, 0-10 ng of PTA was added to a 300-μl reaction mixture containing 100 mM Tris-Cl (pH 7.4), 1.6 mM glutathione, 0.4 mM CoA, 7.2 mM acetyl phosphate, and 13.3 mM $(NH_4)_2SO_4$ to initiate the reaction. Acetyl-CoA formation is monitored at 233 nm (ε_{233} = 4.44 mM^{-1} cm^{-1}) in a 96-well quartz plate using a SpectraMax 398 Plus plate reader (Molecular Devices, Sunnyvale, CA) and normalized to 1-cm pathlength. 1 U of PTA converts 1 micromole of CoA to acetyl-CoA per minute at 25°C (pH 7.4) using acetyl phosphate as a substrate.

Coenzyme A quantification. Total CoA was determined as described (57, 58) with modifications. *S. enterica ptsJ* strain (DM17239) was precultured in 10 ml nutrient broth in triplicates overnight. Cells were washed with equal volume of 0.85% NaCl and inoculated (2% vol/vol) into Klett flasks containing 200 ml minimal NCE glucose without or with 0.5 μM dPN supplementation. After

reaching OD_{650} ~0.7, cells were harvested (8,000 × g, 15 min, 4°C), washed with 5 ml cold phosphate-buffered saline (PBS), and stored at -80°C until analysis.

Frozen cell pellets were resuspended in cold PBS and lysed by addition of formic acid to a final concentration of 0.32 N. After 30-min incubation on ice with occasional agitation, cell debris was pelleted (17,000 × g, 10 min, 4°C) and the lysate was neutralized with NH_4OH (pH ~6.5-7.5). Dithiothreitol (0.7% vol/vol) was added to aliquots of neutralized lysate to reductively cleave CoA thioesters. Assay mixture (120 µl) contained 250 mM Tris-Cl (pH 7.2), 50 mM KCl, 15 mM malate, 6 mM acetyl phosphate, 1 mM NAD^+, 0.4 U citrate synthase, 2 U porcine malate dehydrogenase, 40 µl treated extract, and 0.8 U *B. subtilis* PTA, which was added last to initiate the reaction. NADH formation was monitored at 340 nm in a 96-well quartz plate and normalized to 1-cm pathlength using a SpectraMax 398 Plus plate reader (Molecular Devices, Sunnyvale, CA). CoA level for each biological sample was measured with four technical replicates and normalized to dry cell weight. A 7-point standard curve was generated with addition of 0-1.2 nmol CoA and used as reference for CoA quantification.

ACKNOWLEDGEMENTS

We thank Jorge C. Escalante-Semerena for access to his laboratory strain collection and Rachel M. Burckhardt for constructing plasmid pBsPTA1. This work was supported by an award from the competitive grants program at the NIH (GM095837) to DMD.

3.5 REFERENCES

1. Di Salvo ML, Budisa N, Contestabile R. 2012. PLP-dependent enzymes: a powerful tool for metabolic synthesis of non-canonical amino acids. Proceedings of the Beilstein Bozen Symposium on Molecular Engineering and Control. 27-66.

2. Percudani R, Peracchi A. 2009. The B_6 database: a tool for the description and classification of vitamin B_6-dependent enzymatic activities and of the corresponding protein families. BMC Bioinformatics. 10:1-8.

3. Percudani R, Peracchi A. 2003. A genomic overview of pyridoxal-phosphate-dependent enzymes. EMBO Reports. 4:850-854.

4. Mittenhuber G. 2001. Phylogenetic analyses and comparative genomics of vitamin B_6 (pyridoxine) and pyridoxal phosphate biosynthesis pathways. Journal of Molecular Microbiology and Biotechnology. 3:1-20.

5. Tanaka T, Tateno Y, Gojobori T. 2004. Evolution of vitamin B_6 (pyridoxine) metabolism by gain and loss of genes. Molecular Biology and Evolution. 22:243-250.

6. Venegas A, Martial J, Valenzuela P. 1973. Active site-directed inhibition of *E. coli* DNA-dependent RNA polymerase by pyridoxal 5′-phosphate. Biochemical and Biophysical Research Communications. 55:1053-1059.

7. Bartzatt R, Beckmann JD. 1994. Inhibition of phenol sulfotransferase by pyridoxal phosphate. Biochemical Pharmacology. 47:2087-2095.

8. Vermeersch JJ, Christmann-Franck S, Karabashyan LV, Fermandjian S, Mirambeau G, Der Garabedian PA. 2004. Pyridoxal 5′-phosphate inactivates DNA topoisomerase IB by modifying the lysine general acid. Nucleic Acids Research. 32:5649-5657.

9. Whittaker MM, Penmatsa A, Whittaker JW. 2015. The Mtm1p carrier and pyridoxal 5′-phosphate cofactor trafficking in yeast mitochondria. Archives of Biochemistry and Biophysics. 568:64-70.

10. Boycheva S, Dominguez A, Rolcik J, Boller T, Fitzpatrick TB. 2015. Consequences of a deficit in vitamin B_6 biosynthesis de novo for hormone homeostasis and root development in *Arabidopsis*. Plant Physiology. 167:102-117.

11. Coburn SP. 2018. The chemistry and metabolism of 4′-deoxypyridoxine. CRC Press.

12. Hanna MC, Turner AJ, Kirkness EF. 1997. Human pyridoxal kinase: cDNA cloning, expression, and modulation by ligands of the benzodiazepine receptor. Journal of Biological Chemistry. 272:10756-10760.

13. Salamon N, Gurgui C, Leistner E, Drewke C. 2009. Influence of antivitamins ginkgotoxin 5′-phosphate and deoxypyridoxine 5′-phosphate on human pyridoxine 5′-phosphate oxidase. Planta Medica. 75:563-567.

14. Tramonti A, Milano T, Nardella C, di Salvo ML, Pascarella S, Contestabile R. 2017. *Salmonella typhimurium* PtsJ is a novel MocR-like transcriptional repressor involved in regulating the vitamin B_6 salvage pathway. The FEBS Journal. 284:466-484.

15. Mulligan JH, Snell E. 1976. Transport and metabolism of vitamin B_6 in *Salmonella typhimurium* LT2. Journal of Biological Chemistry. 251:1052-1056.

16. Yamada R, Tsuji T, Nose Y. 1977. Uptake and utilization of vitamin B_6 and its phosphate esters by *Escherichia coli*. Journal of Nutritional Science and Vitaminology. 23:7-17.

17. Yamada R, Furukawa Y. 1981. Role of pyridoxal kinase in vitamin B_6 uptake by *Escherichia coli*. Journal of Nutritional Science and Vitaminology. 27:177-191.

18. Kästner U, Hallmen C, Wiese M, Leistner E, Drewke C. 2007. The human pyridoxal kinase, a plausible target for ginkgotoxin from *Ginkgo biloba*. The FEBS Journal. 274:1036-1045.

19. Zhao G, Winkler ME. 1995. Kinetic limitation and cellular amount of pyridoxine (pyridoxamine) 5′-phosphate oxidase of *Escherichia coli* K-12. Journal of Bacteriology. 177:883-891.

20. Paxhia MD, Downs DM. 2019. *SNZ3* encodes a PLP synthase involved in thiamine synthesis in *Saccharomyces cerevisiae*. G3: Genes, Genomes, Genetics. 9:335-344

21. Moyed H. 1964. Inhibition of the biosynthesis of the pyrimidine portion of thiamine by adenosine. Journal of Bacteriology. 88:1024-1029.

22. Rolfes RJ, Zalkin H. 1988. *Escherichia coli* gene *purR* encoding a repressor protein for purine nucleotide synthesis. Cloning, nucleotide sequence, and interaction with the *purF* operator. Journal of Biological Chemistry. 263:19653-19661.

23. Zhou G, Smith J, Zalkin H. 1994. Binding of purine nucleotides to two regulatory sites results in synergistic feedback inhibition of glutamine 5-phosphoribosylpyrophosphate amidotransferase. Journal of Biological Chemistry. 269:6784-6789.

24. Petersen L, Enos-Berlage J, Downs DM. 1996. Genetic analysis of metabolic crosstalk and its impact on thiamine synthesis in *Salmonella typhimurium*. Genetics. 143:37-44.

25. Chatterjee A, Li Y, Zhang Y, Grove TL, Lee M, Krebs C, Booker SJ, Begley TP, Ealick SE. 2008. Reconstitution of ThiC in thiamine pyrimidine biosynthesis expands the radical SAM superfamily. Nature Chemical Biology. 4:758-765.

26. Martinez-Gomez NC, Downs DM. 2008. ThiC is an [Fe-S] cluster protein that requires AdoMet to generate the 4-amino-5-hydroxymethyl-2-methylpyrimidine moiety in thiamin synthesis. Biochemistry. 47:9054-9056.

27. Dougherty MJ, Downs DM. 2004. A mutant allele of *rpoD* results in increased conversion of aminoimidazole ribotide to hydroxymethyl pyrimidine in *Salmonella enterica*. Journal of Bacteriology. 186:4034-4037.

28. Dougherty MJ, Downs DM. 2006. A connection between iron–sulfur cluster metabolism and the biosynthesis of 4-amino-5-hydroxymethyl-2-methylpyrimidine pyrophosphate in *Salmonella enterica*. Microbiology. 152:2345-2353.

29. Dougherty M, Downs DM. 2003. The *stm4066* gene product of *Salmonella enterica* serovar Typhimurium has aminoimidazole riboside (AIRs) kinase activity and allows AIRs to satisfy the thiamine requirement of *pur* mutant strains. Journal of Bacteriology. 185:332-339.

30. Palmer LD, Dougherty MJ, Downs DM. 2012. Analysis of ThiC variants in the context of the metabolic network of *Salmonella enterica*. Journal of Bacteriology. 194:6088-6095.

31. Frodyma M, Rubio A, Downs D. 2000. Reduced flux through the purine biosynthetic pathway results in an increased requirement for coenzyme A in thiamine synthesis in *Salmonella enterica* serovar Typhimurium. Journal of Bacteriology. 182:236-240.

32. Skovran E, Downs DM. 2000. Metabolic defects caused by mutations in the *isc* gene cluster in *Salmonella enterica* serovar Typhimurium: implications for thiamine synthesis. Journal of Bacteriology. 182:3896-3903.

33. Leonardi R, Fairhurst SA, Kriek M, Lowe DJ, Roach PL. 2003. Thiamine biosynthesis in *Escherichia coli*: isolation and initial characterisation of the ThiGH complex. FEBS Letters. 539:95-99.

34. Martinez-Gomez NC, Robers M, Downs DM. 2004. Mutational analysis of ThiH, a member of the radical S-adenosylmethionine (AdoMet) protein superfamily. Journal of Biological Chemistry. 279:40505-40510.

35. Leonardi R, Roach PL. 2004. Thiamine biosynthesis in *Escherichia coli*: *in vitro* reconstitution of the thiazole synthase activity. Journal of Biological Chemistry. 279:17054-17062.

36. Florio R, di Salvo ML, Vivoli M, Contestabile R. 2011. Serine hydroxymethyltransferase: a model enzyme for mechanistic, structural, and evolutionary studies. Biochimica et Biophysica Acta (BBA)-Proteins and Proteomics. 1814:1489-1496.

37. Kikuchi G, Motokawa Y, Yoshida T, Hiraga K. 2008. Glycine cleavage system: reaction mechanism, physiological significance, and hyperglycinemia. Proceedings of the Japan Academy, Series B. 84:246-263.

38. Rubio A, Downs D. 2002. Elevated levels of ketopantoate hydroxymethyltransferase (PanB) lead to a physiologically significant coenzyme A elevation in *Salmonella enterica* serovar Typhimurium. Journal of Bacteriology. 184:2827-2832.

39. Flynn JM, Christopherson MR, Downs DM. 2013. Decreased coenzyme A levels in *ridA* mutant strains of *Salmonella enterica* result from inactivated serine hydroxymethyltransferase. Molecular Microbiology. 89:751-759.

40. Trakatellis A, Dimitriadou A, Exindari M, Scountzou J, Koliakos G, Christodoulou D, Malissiovas N, Antoniadis A, Polyzoni T. 1992. Effect of pyridoxine deficiency on immunological phenomena. Postgraduate Medical Journal. 68:S70-77.

41. Ito T, Hori R, Hemmi H, Downs DM, Yoshimura T. 2020. Inhibition of glycine cleavage system by pyridoxine 5′-phosphate causes synthetic lethality in *glyA yggS* and *serA yggS* in *Escherichia coli*. Molecular Microbiology. 113:270-284.

42. Yang Y, Tsui H-CT, Man T-K, Winkler ME. 1998. Identification and function of the *pdxY* gene, which encodes a novel pyridoxal kinase involved in the salvage pathway of pyridoxal 5′-phosphate biosynthesis in *Escherichia coli* K-12. Journal of Bacteriology. 180:1814-1821.

43. Reddick JJ, Kinsland C, Nicewonger R, Christian T, Downs DM, Winkler ME, Begley TP. 1998. Overexpression, purification and characterization of two pyrimidine kinases involved in the biosynthesis of thiamin: 4-amino-5-hydroxymethyl-2-methylpyrimidine kinase and 4-amino-5-hydroxymethyl-2-methylpyrimidine phosphate kinase. Tetrahedron. 54:15983-15991.

44. di Salvo ML, Hunt S, Schirch V. 2004. Expression, purification, and kinetic constants for human and *Escherichia coli* pyridoxal kinases. Protein Expression and Purification. 36:300-306.

45. Vu HN, Downs DM. 2021. An unexpected role for the periplasmic phosphatase PhoN in the salvage of B_6 vitamers in *Salmonella enterica*. Applied and Environmental Microbiology. 87:e02300-02320.

46. Coburn S, Mahuren J. 1976. *In vivo* metabolism of 4′-deoxypyridoxine in rat and man. Journal of Biological Chemistry. 251:1646-1652.

47. Datsenko KA, Wanner BL. 2000. One-step inactivation of chromosomal genes in *Escherichia coli* K-12 using PCR products. Proceedings of the National Academy of Sciences. 97:6640-6645.

48. Schmieger H. 1971. A method for detection of phage mutants with altered transducing ability. Molecular and General Genetics MGG. 110:378-381.

49. Chan RK, Botstein D, Watanabe T, Ogata Y. 1972. Specialized transduction of tetracycline resistance by phage P22 in *Salmonella typhimurium*: II. Properties of a high-frequency-transducing lysate. Virology. 50:883-898.

50. VanDrisse C, Escalante-Semerena J. 2016. New high-cloning-efficiency vectors for complementation studies and recombinant protein overproduction in *Escherichia coli* and *Salmonella enterica*. Plasmid. 86:1-6.

51. Galloway NR, Toutkoushian H, Nune M, Bose N, Momany C. 2013. Rapid cloning for protein crystallography using type IIS restriction enzymes. Crystal Growth and Design. 13:2833-2839.

52. Rocco C, Dennison K, Klenchin VA, Rayment I, Escalante-Semerena J. 2008. Construction and use of new cloning vectors for the rapid isolation of recombinant proteins from *Escherichia coli*. Plasmid. 59:231-237.

53. Davis R, Botstein D, Roth J. 1980. Advanced bacterial genetics. Cold Spring Harbor Laboratory. New York.

54. Yang ES, Schirch V. 2000. Tight binding of pyridoxal 5′-phosphate to recombinant *Escherichia coli* pyridoxine 5′-phosphate oxidase. Archives of Biochemistry and Biophysics. 377:109-114.

55. Vu HN, Ito T, Downs DM. 2020. The role of YggS in vitamin B_6 homeostasis in *Salmonella enterica* is informed by heterologous expression of yeast *SNZ3*. Journal of Bacteriology. 202:e00383-20.

56. Klotzsch HR. 1969. Phosphotransacetylase from *Clostridium kluyveri*. Elsevier. Methods in Enzymology. 13:381-386.

57. Allred JB, Guy DG. 1969. Determination of coenzyme A and acetyl CoA in tissue extracts. Analytical Biochemistry. 29:293-299.

58. Ernst DC, Borchert AJ, Downs DM. 2018. Perturbation of the metabolic network in *Salmonella enterica* reveals cross-talk between coenzyme A and thiamine pathways. PloS One. 13:e0197703.

Table 3.1 – Strains and plasmids used in this study.

Strain/plasmid	Description	Source
S. enterica		
DM17239	*ptsJ617*::*Km*	This study
DM17238	*pdxK682*::*Cm*	This study
DM17168	*ptsJ617*::*Km pdxK682*::*Cm*	This study
DM17274	*purG3111 purE3043 stm4068-6*::Tn*10*(d)Tc *ptsJ617*::*Km*	This study
DM16666	Wild type / pCV1	This study
DM17210	Wild type / pDM1643	This study
DM17242	*ptsJ617*::*Km* / pCV1	This study
DM17243	*ptsJ617*::*Km* / pDM1647	This study
DM17253	*ptsJ617*::*Km pdxK682*::*Cm* / pCV1	This study
DM17244	*ptsJ617*::*Km* / pBAD33-SD1	This study
DM17246	*pdxJ664 pdxH673 ptsJ617*::*Km* / pDM1594	This study
Plasmid		
pBAD33-SD1	Modified pBAD33 (Cm^R)	(55)
pCV1	Modified pBAD24 (Am^R)	(50)
pDM1594	pBAD33-SD1 expressing *S. cerevisiae SNZ3* (Cm^R)	(55)
pDM1643	pCV1 expressing *S. enterica pdxK* (Am^R)	This study
pDM1647	pCV1 expressing *S. enterica ptsJ* (Am^R)	This study
pBsPTA1	pTEV5 expressing *B. subtilis* 6xHis-tagged PTA (Am^R)	Escalante*

*Provided by Jorge C. Escalante-Semerena at the University of Georgia (Athens, GA).

Table 3.2 – Primers used in this study.

Primer	Sequence (5' to 3')	Description
PR1383	GGAAAATTTTATGGGACAAGAGAGTGATATTCAGTCAGTGGTGTAGGCTGGAGCTGCTTC	Inactivation of *pdxK*
PR1384	CGATAACTCTTCATCGCGCCTCCCCTGCCGGCGGCAGAATCATATGAATATCCTCCTTAGTTCCTATTCC	
PR1461	ATTAAAGGCAGTCCGTCTCCCGTAGCGCTGGAAGGCGGCGTGTAGGCTGGAGCTGCTTC	Inactivation of *ptsJ*
PR1462	TCCCTCACGTACCAGCCAGCCGGATTTTGCCAACGTAAACATATGAATATCCTCCTTAGTTCCTATTCC	
PR1318	NNGCTCTTCNTTCATGGGACAAGAGAGTGATATTCAGTCAGTG	Construction of pDM1643
PR1319	NNGCTCTTCNTTATCATCGCGCCTCCCCTG	
PR1449	NNGCTCTTCNTTCATGATCGACGGAAAAACCGCTAACGAAATTTTTGACAG	Construction of pDM1647
PR1450	NNGCTCTTCNTTATTAGCGATTTAGCGCCTGATGGATATCAGCC	

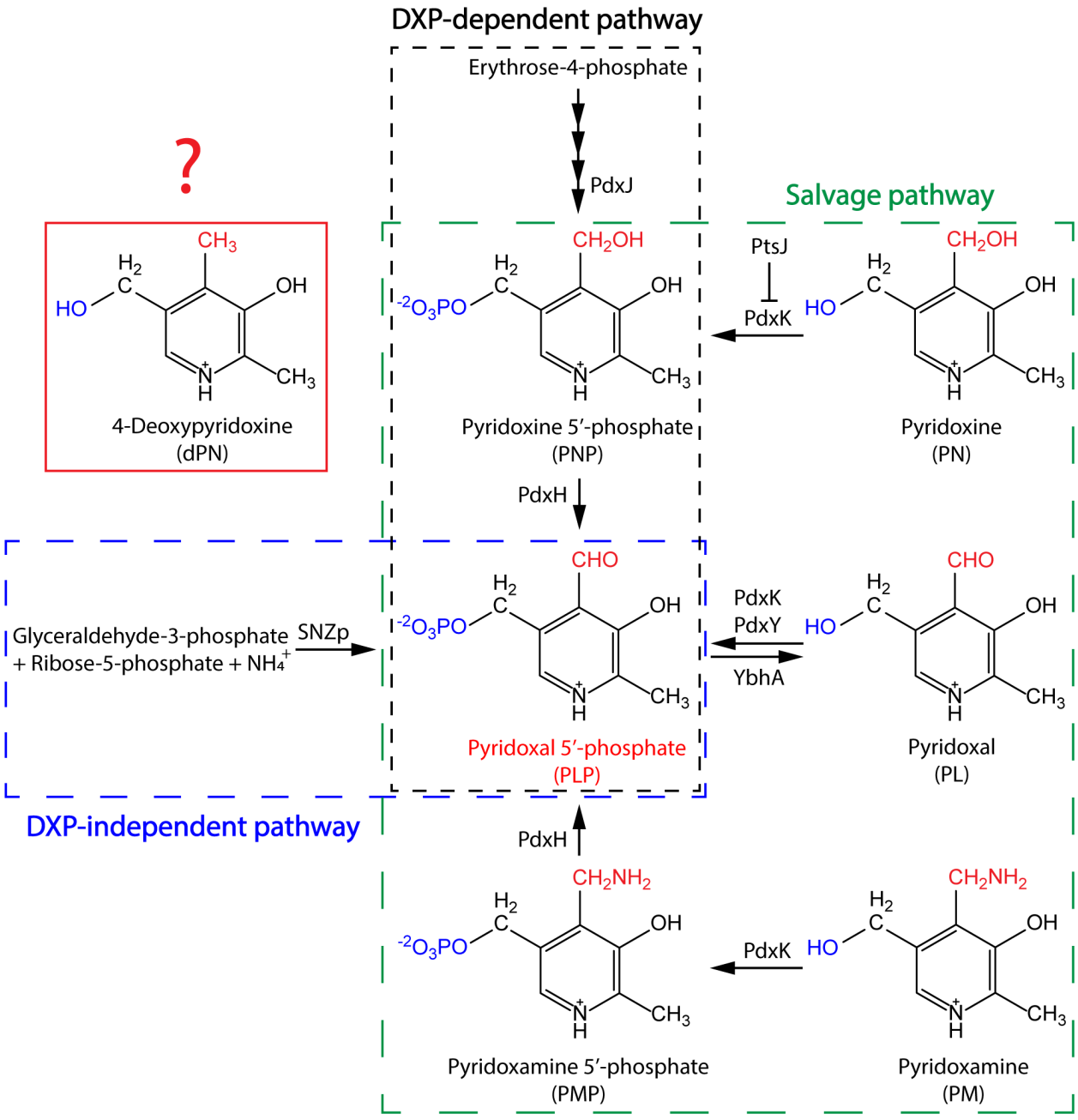

Figure 3.1 – PLP biosynthesis and salvage. In *S. enterica*, PLP can be synthesized *de novo* via the DXP-dependent pathway (black box), or salvaged from other B_6 vitamers (green box). Other organisms, such as *Saccharomyces cerevisiae*, use the DXP-independent pathway (blue box) to synthesize PLP in addition to salvaging. Animals, including humans, lack the biosynthetic pathway and rely exclusively on salvage to acquire this cofactor. Relevant enzymes involved in biosynthesis

and salvage of PLP are shown next to the arrows, each of which represents a biochemical reaction catalyzed by the corresponding enzyme. Abbreviation: DXP, deoxyxylulose 5-phosphate.

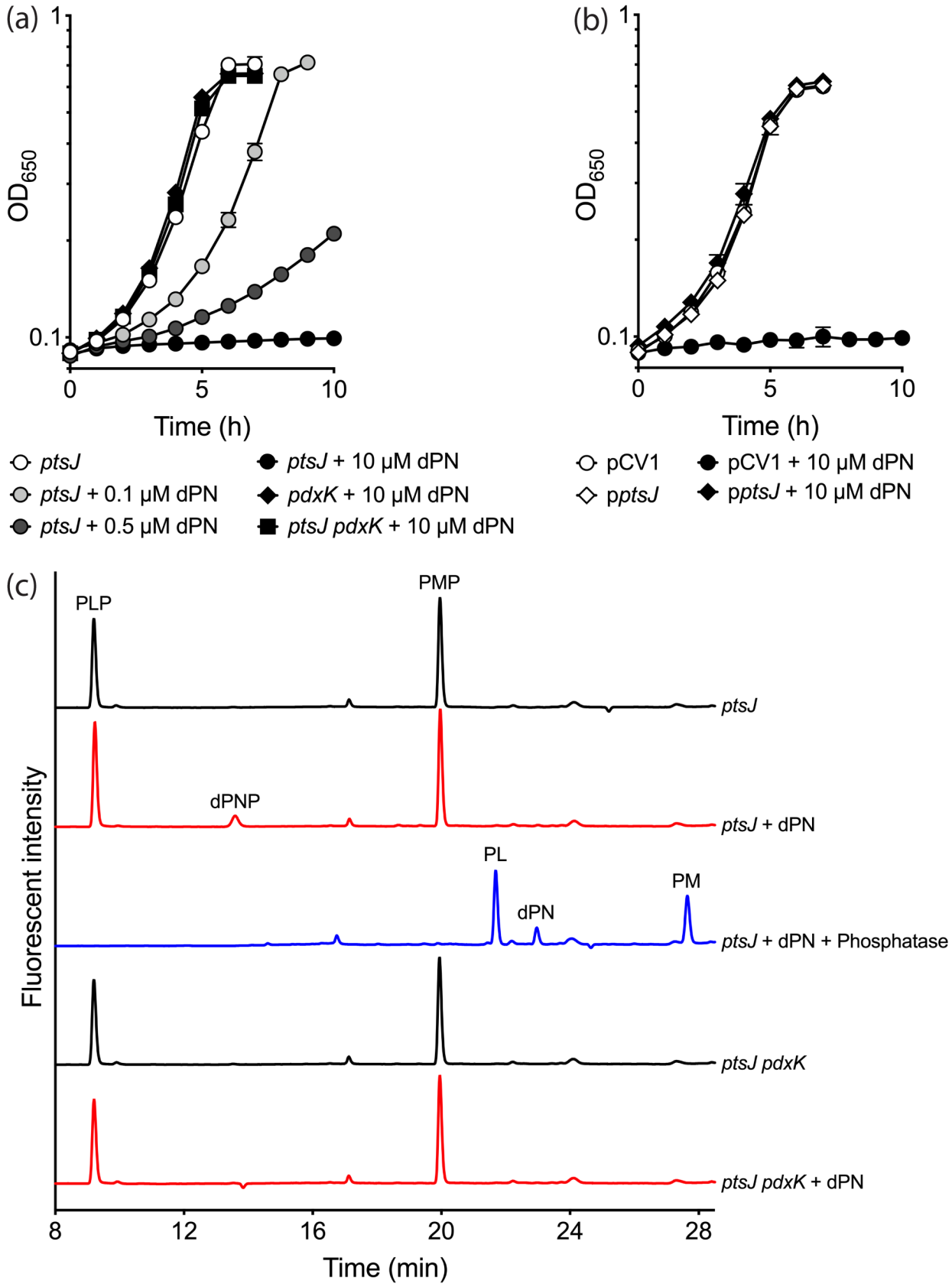
(a)
1
0.1
OD650
0
5
10
Time (h)
ptsJ
ptsJ + 0.1 μM dPN
ptsJ + 0.5 μM dPN
ptsJ + 10 μM dPN
pdxK + 10 μM dPN
ptsJ pdxK + 10 μM dPN
(b)
1
0.1
OD650
0
5
10
Time (h)
pCV1
pptsJ
pCV1 + 10 μM dPN
pptsJ + 10 μM dPN
(c)
PLP
PMP
dPNP
PL
dPN
PM
ptsJ
ptsJ + dPN
ptsJ + dPN + Phosphatase
ptsJ pdxK
ptsJ pdxK + dPN
Fluorescent intensity
8
12
16
20
24
28
Time (min)

Figure 3.2 – dPN sensitivity of a *ptsJ* mutant is PdxK-dependent. (a) *S. enterica ptsJ* (DM17239), *pdxK* (DM17238), and *ptsJ pdxK* (DM17168) were grown in minimal NCE glucose without (white symbols) or with addition of 0.1 μM (light gray symbols), 0.5 μM (dark gray symbols), or 10 μM (black symbols) dPN. (b) *ptsJ* strains carrying an empty vector control (pCV1, DM17242) or vector expressing *ptsJ in trans* (p*ptsJ*, DM17243) were grown in minimal NCE glucose supplemented with 0.02% arabinose in the absence (white symbols) or presence (black symbols) of 10 μM dPN. (c) HPLC chromatogram of intracellular vitamin B_6 content of *ptsJ* (DM17239) and *ptsJ pdxK* (DM17168) strain grown in minimal NCE glucose with or without addition of 0.5 μM dPN. Representative data from at least two independent experiments with three biological replicates are shown. Error bars depict standard deviation from the mean value. Abbreviation: PLP, pyridoxal 5′-phosphate; PL, pyridoxal; PMP, pyridoxamine 5′-phosphate; PM, pyridoxamine; dPNP, 4-deoxypyridoxine 5′-phosphate; dPN, 4-deoxypyridoxine.

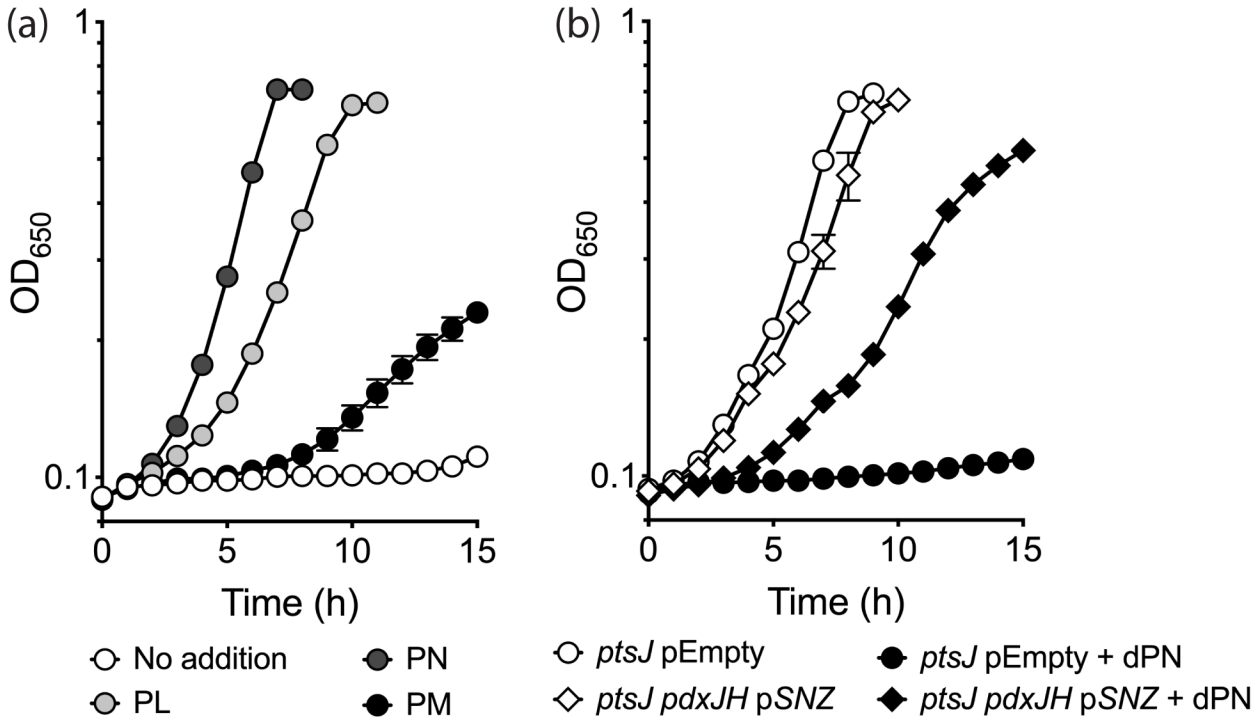

Figure 3.3 – dPNP affects PLP synthesis via the DXP-dependent pathway. (a) *S. enterica ptsJ* strain (DM17239) was grown in minimal NCE glucose supplemented with 10 μM dPN in the absence (white symbols) or presence of 1 μM PL (light gray symbols), PN (dark gray symbols), or PM (black symbols). (b) *S. enterica ptsJ* strains with the native DXP-dependent pathway intact (*ptsJ* pEmpty, DM17244) or replaced with *S. cerevisiae* DXP-independent pathway (*ptsJ pdxJH* p*SNZ*, DM17246) were grown in minimal NCE glycerol supplemented with 0.02% arabinose in the absence (white symbols) or presence (black symbols) of 10 μM dPN. Representative data from at least two independent experiments with three biological replicates are shown. Error bars depict standard deviation from the mean value. Abbreviations: DXP, deoxyxylulose 5-phosphate; dPN, 4-deoxypyridoxine; PL, pyridoxal; PN, pyridoxine; PM, pyridoxamine.

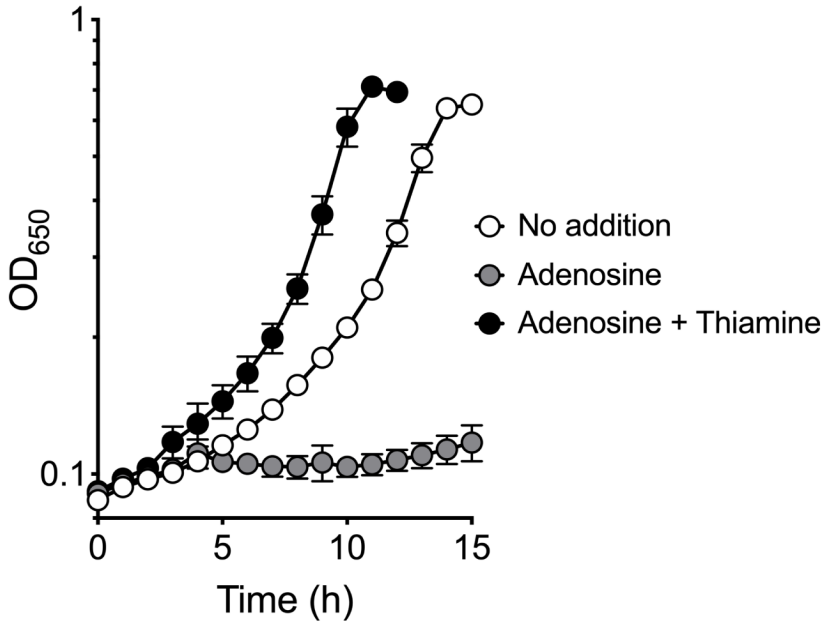

Figure 3.4 – Adenosine exacerbates dPN sensitivity. *S. enterica ptsJ* strain (DM17239) was grown in minimal NCE glucose supplemented with 0.5 μM dPN in the absence (white symbols) or presence of 1 mM adenosine (gray symbols) and 0.1μM thiamine (black symbols). Representative data from two independent experiments with three biological replicates are shown. Error bars depict standard deviation from the mean. Abbreviation: dPN, 4-deoxypyridoxine.

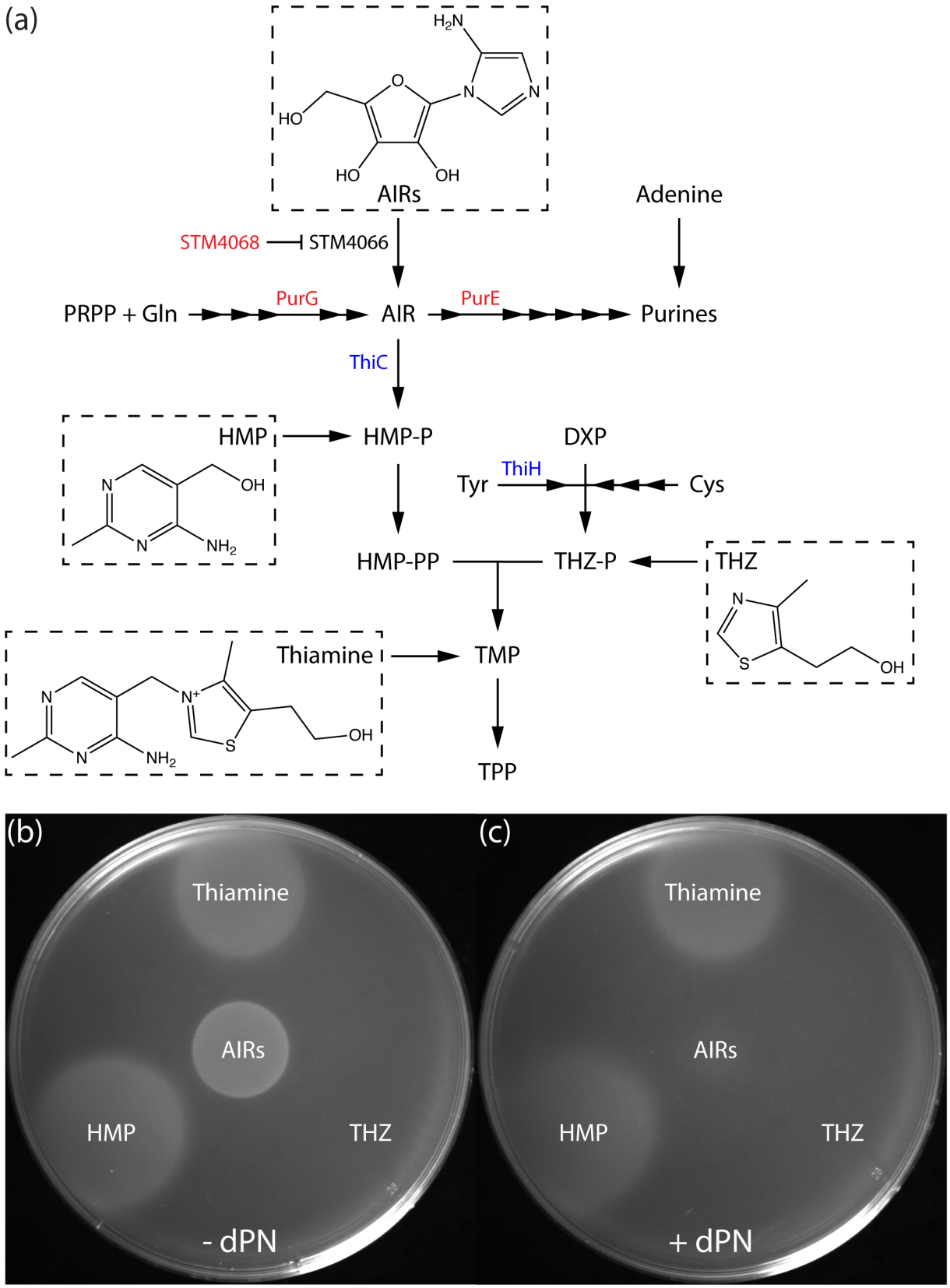
(a)
AIRs
Adenine
STM4068
STM4066
PRPP + Gln
PurG
AIR
PurE
Purines
ThiC
HMP
HMP-P
DXP
Tyr
ThiH
Cys
HMP-PP
THZ-P
THZ
Thiamine
TMP
TPP
(b)
Thiamine
AIRs
HMP
THZ
- dPN
(c)
Thiamine
AIRs
HMP
THZ
+ dPN

Figure 3.5 – dPN increases AIRs requirement for ThiC-dependent thiamine synthesis. (a) Thiamine and purine biosynthesis and salvage in *S. enterica.* Each arrow represents a biochemical reaction, and relevant catalyzing enzymes are indicated next to the arrows. DM7060 background carries lesions in genes that encode proteins in red. Blue highlight indicates radical *S*-adenosylmethionine enzymes that utilize iron-sulfur clusters. Compounds accompanied by chemical structures were used in subsequent feeding experiments. Molten soft agar (0.7% wt/vol) inoculated with *purGE stm4068 ptsJ* culture (DM17274) was overlaid onto minimal NCE glucose containing 0.4 mM adenine in the (b) absence or (c) presence of 0.1 μM dPN. Other supplementation was added by spotting 1 μl of ~300 mM AIRs, 0.1 mM thiamine, 0.1 mM HMP, and 0.1 mM THZ on top of the solidified soft agar layer. Representative growth from three independent experiments is shown. Abbreviations: AIRs, 5-aminoimidazole riboside; AIR, 5-aminoimidazole ribotide; PRPP, phosphoribosyl pyrophosphate; HMP, 4-amino-5-hydroxymethyl-2-methylpyrimidine; HMP-P, 4-amino-5-hydroxymethyl-2-methylpyrimidine phosphate; HMP-PP, 4-amino-5-hydroxymethyl-2-methylpyrimidine diphosphate; THZ, 4-methyl-5-(2-hydroxyethyl)-thiazole; THZ-P, 4-methyl-5-(2-hydroxyethyl)-thiazole phosphate; TMP, thiamine monophosphate; TPP, thiamine pyrophosphate; Gln, L-glutamine; Tyr, L-tyrosine; Cys, L-cysteine; DXP, deoxyxylulose 5-phosphate; dPN, 4-deoxypyridoxine.

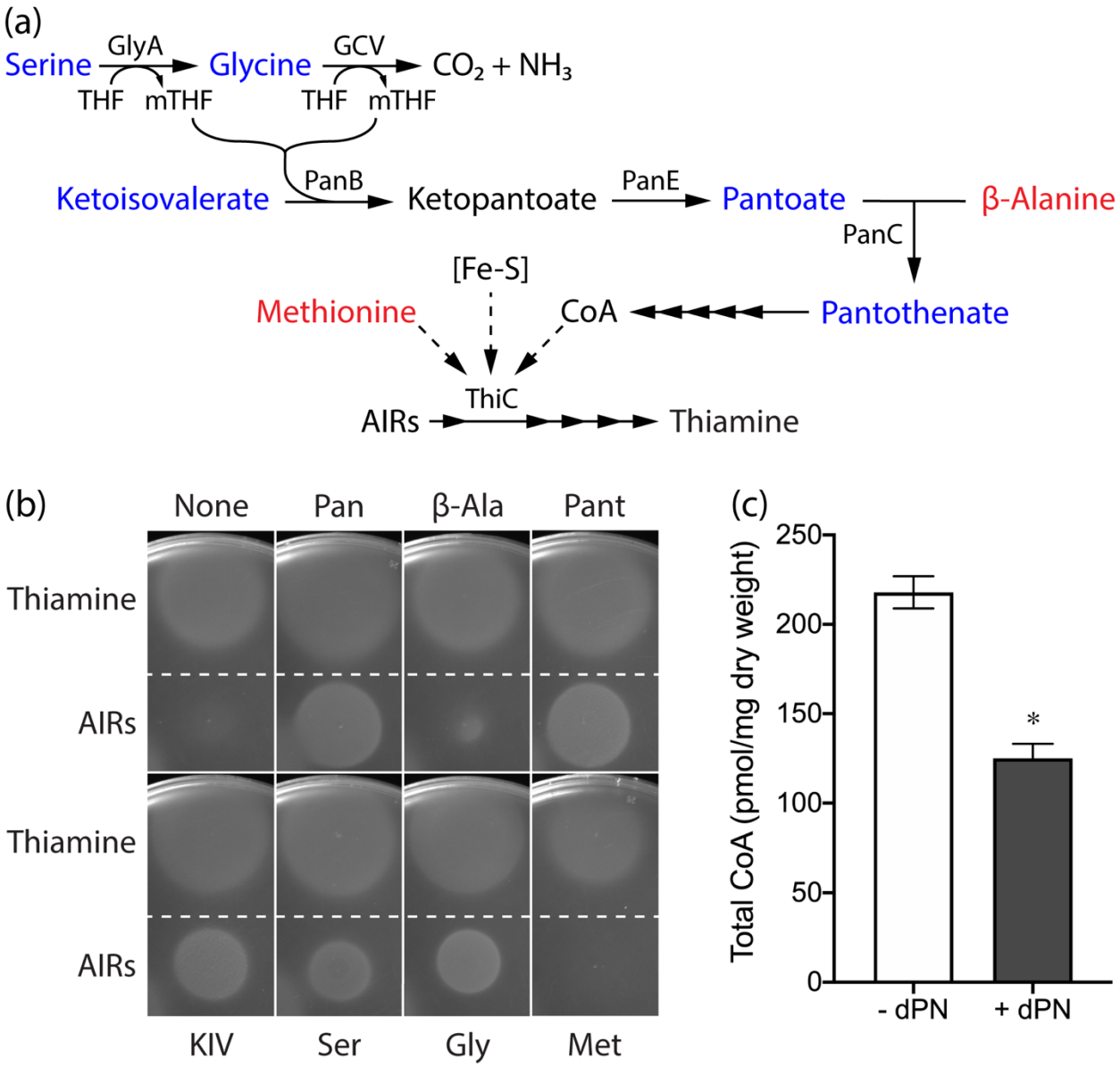

Figure 3.6 – Precursors for coenzyme A synthesis rescue dPN sensitivity of a *ptsJ* mutant. (a) The integrated serine-glycine metabolic node, CoA, and thiamine synthesis in *S. enterica.* Blue highlight indicates metabolites that mitigate the inhibition of dPN on ThiC-dependent thiamine synthesis, while those in red have little to no effect. Solid arrows indicate biochemical reactions in the pathways. Dash arrows depict metabolic processes that affect ThiC activity. (b) *purGE stm4068 ptsJ* strain (DM17274) was mixed with soft agar and overlaid onto minimal NCE glucose containing 0.4 mM adenine and 0.1 μM dPN without or with one of the following

supplementations: 0.1 mM pantothenate, 0.1 mM pantoate, 0.1 mM β-alanine, 0.1 mM α-ketoisovalerate, 2.5 mM serine, 0.67 mM glycine, or 0.3 mM methionine. AIRs requirement was assessed by spotting 1 μl of ~300 mM AIRs and 0.1 mM thiamine as a control. (c) Total intracellular CoA level of a *ptsJ* mutant (DM17239) grown in minimal NCE glucose in the absence or presence of 0.5 μM dPN. An asterisk indicates $P < 0.0001$ as determined by two-tailed unpaired Student's *t* test. Representative data from two experiments, each with three biological replicates, are shown. Error bars depict standard deviation from the mean. Abbreviations: GCV, glycine cleavage; THF, tetrahydrofolate; mTHF, 5,10-methylenetetrahydrofolate; [Fe-S], iron-sulfur cluster; AIRs, 5-aminoimidazole riboside; Pan, pantothenate; β-Ala, β-alanine; Pant, pantoate; KIV, α-ketoisovalerate; Ser, L-serine; Gly, L-glycine; Met, L-methionine; dPN, 4-deoxypyridoxine.

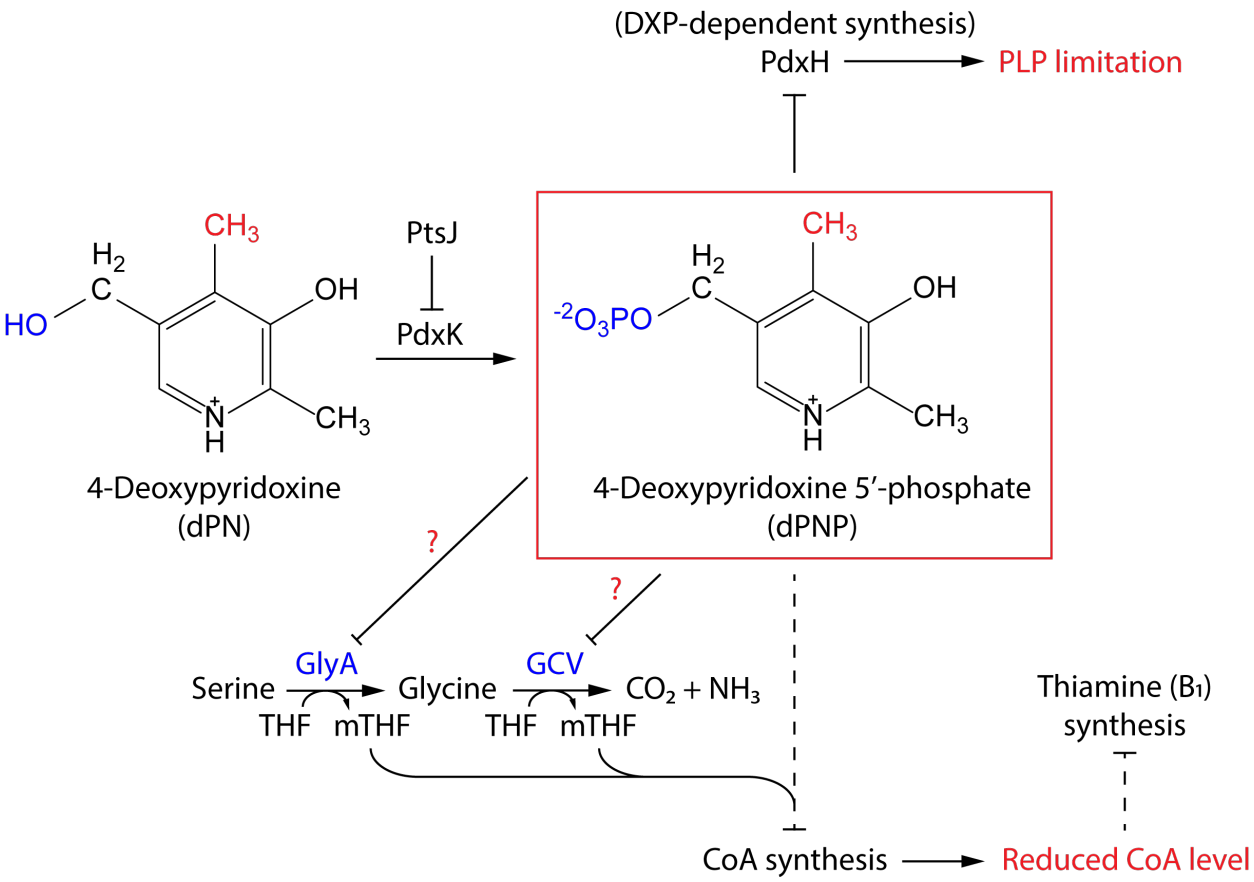

Figure 3.7 – Working model on how dPN affects *S. enterica* metabolism. PdxK converts exogenous dPN to dPNP, which inhibits PLP biosynthesis via PdxH leading to PLP limitation. In addition, dPNP inhibits PLP-dependent enzyme GlyA and/or GcvP, lowering flux through the pantoate branch of CoA synthesis. Reduced CoA level indirectly dampens ThiC-dependent thiamine synthesis. Abbreviations: dPN, 4-deoxypyridoxine; dPNP, 4-deoxypyridoxine 5′-phosphate; PLP, pyridoxal 5′-phosphate; DXP, deoxyxylulose 5-phosphate; THF, tetrahydrofolate; mTHF, 5,10-methylenetetrahydrofolate.

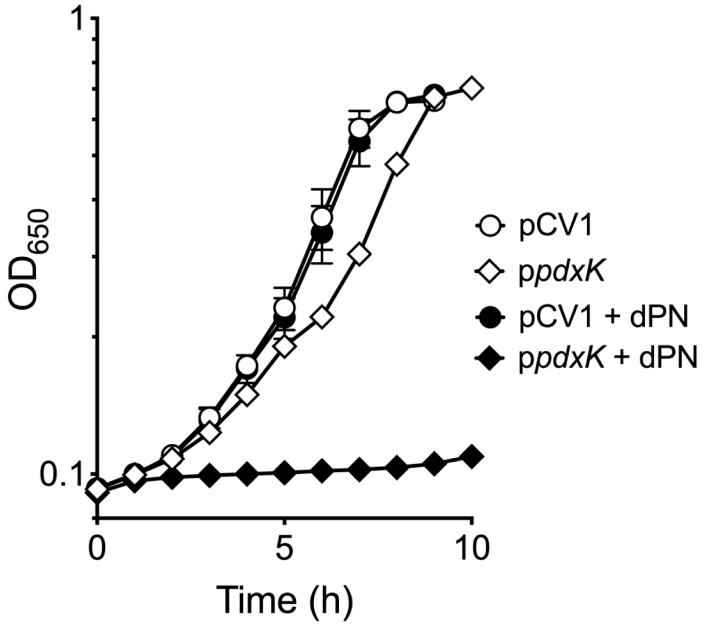

Figure 3.S1 – Overexpression of *pdxK* phenocopies a *ptsJ* mutation. Wild-type strains carrying an empty vector control (pCV1, DM16666) or vector expressing *pdxK* (p*pdxK*, DM17210) were grown in minimal NCE glycerol supplemented with 0.02% arabinose in the absence (white symbols) or presence (black symbols) of 10 μM dPN. Representative data from at least two independent experiments with three biological replicates are shown. Error bars depict standard deviation from the mean value. Abbreviation: dPN, 4-deoxypyridoxine.

CHAPTER 4

THE ROLE OF YGGS IN VITAMIN B_6 HOMEOSTASIS IN *SALMONELLA ENTERICA* IS INFORMED BY HETEROLOGOUS EXPRESSION OF YEAST *SNZ3* [3]

[3] Vu HN, Ito T, Downs DM. 2020. *Journal of Bacteriology*. 202(22):e00383-20.
Reprinted here with permission of the publisher.

4.1 ABSTRACT

YggS (COG0325) is a pyridoxal 5′-phosphate (PLP)-binding protein proposed to be involved in homeostasis of B_6 vitamers. In *Salmonella enterica*, lack of *yggS* resulted in phenotypes that were distinct, and others that were similar, to those of a *yggS* mutant of *Escherichia coli.* Like other organisms, *yggS* mutants of *S. enterica* accumulate endogenous pyridoxine 5′-phosphate (PNP). Data herein show that strains lacking YggS accumulated ~10-fold more PLP in growth medium than a parental strain. The deoxyxylulose 5-phosphate-dependent biosynthetic pathway for PLP and the pyridoxine 5′-phosphate (PNP)/pyridoxamine 5′-phosphate (PMP) oxidase credited with interconverting B_6 vitamers were replaced with a single PLP synthase from *Saccharomyces cerevisiae*. The impact of a *yggS* deletion on the intracellular and extracellular levels of B_6 vitamers in this restructured strain supported a role for PdxH in PLP homeostasis and led to a general model for YggS function in PLP-PMP cycling. Our findings uncovered broader consequences of a *yggS* mutation than previously reported and suggest the accumulation of PNP is not a direct effect of lacking YggS, but rather a downstream consequence.

IMPORTANCE

Pyridoxal 5′-phosphate (PLP) is an essential cofactor for enzymes in all domains of life. Perturbations in PLP or B_6 vitamer content can be detrimental, notably causing B_6-dependent epilepsy in humans. YggS homologs are broadly conserved and have been implicated in altered levels of B_6 vitamers in multiple organisms. The biochemical activity of YggS, expected to be conserved across domains, is not yet known. Herein, a simplified heterologous pathway minimized metabolic variables and allowed the dissection of this system to generate new metabolic knowledge that will be relevant to understanding YggS.

4.2 INTRODUCTION

In *Salmonella enterica* serovar Typhimurium LT2 (referred to hereafter as *S. enterica*), YggS is a member of the pyridoxal 5′-phosphate (PLP)-binding protein family (COG0325), which is highly conserved and distributed in all domains of life. Members of this family bind PLP, and residues crucial for this binding are required for *in vivo* function, as defined by phenotypic manifestation (1-4). Correlations between the status of *yggS* and the pool sizes of various B_6 vitamers led to several reports suggesting a role for this protein in maintaining the homeostasis of PLP (4-8). Other than a presumed role for the bound PLP, no biochemical activity for YggS has been described.

YggS from *Escherichia coli* covalently binds PLP via a Schiff base linkage with residue Lys36, and loss of PLP binding leads to pleiotropic phenotypes in *E. coli*, which include an imbalance in intracellular levels of amino acids, α-keto acids and coenzyme A (1, 5, 7-9), along with sensitivity to pyridoxine (PN) (5, 7). YggS proteins from multiple organisms complement the sensitivity of an *E. coli yggS* mutant to PN (5, 6), consistent with the expectation that members of this conserved protein family have the same molecular function. Some phenotypes in *E. coli* were strain- and condition-dependent, which complicates efforts to define the precise role of YggS *in vivo*. A homolog of *yggS*, designated *pipY*, was identified and studied in the context of nitrogen regulation in *Synechococcus elongatus* (2, 10). Compared to wild type, the *pipY* mutant exhibited increased sensitivity to PN, 3-chloro-D-alanine, and D-cycloserine, the latter two of which are antibiotics that target some PLP-dependent enzymes (10). In humans, various mutations in the *PLPBP* gene (formerly known as *PROSC*), a homolog of *yggS*, are biomarkers for vitamin-B_6-dependent epilepsy. Analyses performed on cerebrospinal fluid and plasma of these patients showed perturbations in amino acid and vitamin B_6 profiles (3, 4, 6, 11), mirroring the global

effects reported in an *E. coli yggS* mutant. Recently, these results were extended to a HEK293 cell line and zebrafish larvae lacking functional *PLPBP* (4).

PLP is an essential cofactor in numerous enzymes including racemases, decarboxylases, and transaminases across all domains of life (12). All free-living organisms possess PLP-dependent enzymes, which account for ~4% of all activities classified by the Enzyme Commission (EC) (13), making this cofactor essential for cellular function. Organisms must synthesize PLP or obtain it by salvaging other B_6 vitamers from the environment. PLP can be synthesized *de novo* via the deoxyxylulose 5-phosphate (DXP)-dependent pathway (Figure 4.1A), which is found primarily in γ-proteobacteria, including *S. enterica* and *E. coli*, or the DXP-independent pathway, which is found in other bacteria, archaea, and eukaryotes (Figure 4.1B) (14, 15). PLP can also generated by acquiring pyridoxal (PL), pyridoxine (PN), or pyridoxamine (PM) from the environment using enzymes of the PLP salvage pathway (Figure 4.1C). Components of the salvage pathway are at least partially conserved in organisms that do not synthesize PLP *de novo*, including humans and most animals (14, 15). PLP has a reactive aldehyde moiety, which has been proposed to generate cellular stress by forming covalent adducts with PLP-independent enzymes that then impact their activity (16-18). The requirement for PLP, coupled with its reactivity, suggests that the cellular pools of this molecule would be tightly regulated.

Phenotypic analyses have been the starting point for functional elucidation of gene products for decades and remain one of the most powerful approaches available to understand complex systems. This study was initiated to use the properties of *yggS* mutants in *S. enterica* under different metabolic configurations to gain insights into the function of the conserved YggS protein family. The data show that while PLP levels are maintained inside a *yggS* mutant, significant accumulation is found in the growth medium. Metabolic complexity was minimized by

expressing the PLP synthase SNZ3p from *Saccharomyces cerevisiae* in an *S. enterica* strain lacking the DXP-dependent pathway for PLP synthesis and the pyridoxine 5′-phosphate (PNP)/pyridoxamine 5′-phosphate (PMP) oxidase (PdxH; EC 1.4.3.5). Metabolic analyses of this strain supported a role for PdxH in PLP homeostasis and led to a general model placing the role of YggS in the cycling of PLP→PMP→PLP.

4.3 RESULTS AND DISCUSSION

Phenotypic consequences of lacking *yggS* in *S. enterica*. An in-frame deletion of *yggS* was constructed in *S. enterica* and subjected to a range of simple growth analyses. When growth was assessed on minimal NCE medium with sole carbon sources that included glucose, gluconate, sorbitol, trehalose, galactose, mannose, fructose, xylose, ribose, arabinose, succinate, rhamnose, glycerol, citrate, malate, pyruvate, fumarate, and acetate, lack of *yggS* had no detectable effect (representative growth in Figure 4.S1A). These results paralleled those reported for *E. coli* on M9 glucose medium (1, 5) and *S. elongatus* on BG11 nitrate/ammonium medium (10). A double mutant of *S. enterica* with lesions in *yggS* and *glyA* (encoding a serine hydroxymethyltransferase, EC 2.1.2.1) grew in LB (data not shown) and minimal NCE glucose medium if glycine or 0.4% casamino acids was added (glycine, $T_{D\text{-}glyA} = 2.3 \pm 0.1$ h, $T_{D\text{-}yggS\ glyA} = 2.8 \pm 0.1$ h; casamino acids, $T_{D\text{-}glyA} = 1.4 \pm 0.1$ h, $T_{D\text{-}yggS\ glyA} = 2.9 \pm 0.1$ h) (Figure 4.S1B). This result contrasted with an *E. coli* mutant of the same genotype, which was not viable on LB and had a severe growth defect in M9 glucose medium supplemented with glycine or 0.4% casamino acids (5). Further, growth of a *cysK* (encoding a cysteine synthase A, EC 2.5.1.47) mutant of *S. enterica* and *yggS cysK* double mutant were indistinguishable on minimal medium ($T_{D\text{-}cysK} = 1.7 \pm 0.1$ h, $T_{D\text{-}yggS\ cysK} = 1.6 \pm 0.1$h) (Figure 4.S1A). In *S. elongatus,* lesions in these two loci were synthetically lethal (10). Growth of *E. coli*

strains lacking *yggS* was perturbed by exogenous PN and PL, while an *S. enterica yggS* mutant was not affected by either (Figure 4.S2). The phenotype of an *E. coli yggS* mutant in response to PN was attributed to an impact on two valine-sensitive acetohydroxy acid synthases (AHAS) I and III (EC 2.2.1.6) encoded by *ilvBN* and *ilvIH* (7). *S. enterica* possesses a valine-insensitive AHAS II encoded by *ilvGM* in addition to AHAS I. The additional sensitivity of *E. coli yggS* mutant to PL could be explained by a recently discovered PL reductase (PdxI, EC 1.1.1.65), which is capable of converting PL to PN (19).

A *yggS* mutant of *E. coli* accumulates intracellular PNP, a result that was critical for the conclusion that YggS was involved in PLP homeostasis (5, 7, 8). Wild-type and *yggS* mutant strains of *S. enterica* were grown to mid-log phase in minimal NCE glucose medium and the intracellular concentration of B_6 vitamers was determined using HPLC. *E coli* strains were included as controls. The data (Figure 4.2A and Table 4.S1) showed that the *S. enterica yggS* mutant had an elevated pool of intracellular PNP (146 ± 6 pmol/OD_{650}) compared to the wild-type strain (9.0 ± 0.7 pmol/OD_{650}). Importantly, when *yggS* was expressed *in trans* in the *S. enterica yggS* mutant, internal PNP was reduced to near wild-type level (17.2 ± 0.4 pmol/OD_{650}). Intracellular levels of PLP and PMP were not significantly altered by the *yggS* mutation. As expected, an *E. coli yggS* mutant also accumulated PNP (192 ± 6 pmol/OD_{650}), while none was detectable in the parental strain.

Strains lacking *yggS* accumulate a B_6 vitamer(s) in the growth medium. In the course of other experiments, colonies of *S. enterica yggS* mutants appeared to cross-feed a mutant lacking *pdxJ* (encoding a PNP synthase, EC 2.6.99.2) on solid medium. Spent medium of a *yggS* mutant was tested for presence of B_6 vitamer(s) with a bioassay by exploiting the nutritional requirement of a

pdxJ mutant. Spent media from relevant strains grown in minimal glucose medium were filter-sterilized, supplemented with carbon source and trace elements, and used as growth medium for a *pdxJ* mutant (Figure 4.S3). Spent growth medium from *yggS* mutants, but not the wild-type parental strains, allowed full growth of a *pdxJ* mutant. When *yggS* was expressed *in trans*, the spent medium no longer supported growth. The *pdxJ* mutant could grow in the spent media from all strains with the addition of 1 μM PL (data not shown). These data showed that one or more B_6 vitamers accumulated in the growth medium of strains lacking *yggS* and described a phenotype of a *yggS* mutant not previously reported in bacteria.

Analysis by HPLC showed that PLP and PMP were present in the spent medium of an *S. enterica yggS* mutant (Figure 4.2B and Table 4.S1). Lack of *yggS* increased the concentration of PLP in the growth medium by ~10-fold over wild type, to near micromolar levels (829 ± 16 nM/OD_{650}, 81 ± 2 nM/OD_{650}, respectively). Importantly, the vitamer accumulation was restored to the pattern of a wild-type strain if *yggS* was provided *in trans*. Similar to *S. enterica*, the culture supernatant of an *E. coli yggS* mutant accumulated ~7-fold more PLP externally than the wild-type strain (data not shown). Other vitamers accumulated to a lesser extent (PMP, 41 ± 1 nM/OD_{650}; PL, 63 ± 1 nM/OD_{650}; PN, 36 ± 1 nM/OD_{650}) in the medium of an *S. enterica yggS* mutant, and were undetectable (<10 nM) in the growth medium of wild type. Due to their physiological relevance, further characterization focused only on the phosphorylated vitamers PLP, PNP and PMP.

Effect of *yggS* mutation is not mediated by DXP-dependent PLP biosynthesis. In *S. enterica*, dissecting control of vitamin B_6 homeostasis, and any role YggS may have in it, is complicated by the presence of PNP as an obligatory intermediate in the synthesis of PLP via the DXP-dependent

pathway (Figure 4.1). The PLP synthase from *S. cerevisiae* (SNZ3p) was used to bypass a need for the native DXP-dependent pathway (Figure 4.1). *S. enterica* strains expressing *SNZ3 in trans* synthesize PLP in a single step using endogenous glyceraldehyde-3-phosphate (G3P), ribose-5-phosphate (R5P), and ammonium from the medium (20). A heterologous system expressing *SNZ3* has the advantage that *de novo* PLP synthesis is intact, which removes the need to supplement the medium and can eliminate transport and/or salvage of B_6 vitamers as variables in metabolic studies.

SNZ3p was provided in several genetic backgrounds to generate strains that synthesized PLP in different ways. The resulting strains were grown in minimal NCE glycerol medium, and endogenous and exogenous levels of PLP, PNP and PMP were quantified with HPLC (Figure 4.3 and Table 4.S2). The data showed that in an otherwise wild-type *S. enterica* strain, lack of *yggS* disrupted the pool size of multiple B_6 vitamers on glycerol, with the dominant effect being increased PLP in the growth medium as it was on glucose (Figure 4.3(1)). The remaining strains lacked one or more of the *pdx* genes and required SNZ3p to generate PLP. The relevant strains consisted of three pairs isogenic at the *yggS* locus, and each pair was considered in turn (Figure 4.3).

The first pair of strains lacked *pdxH* (encoding PNP/PMP oxidase, EC 1.4.3.5) and expressed *SNZ3* in addition to the native DXP-dependent pathway to PNP (Figure 4.1). The *pdxH* mutation led to an endogenous accumulation of PNP as might be expected (Figure 4.3(2) and Table 4.S2). Introduction of a *yggS* mutation (*pdxH yggS* p*SNZ*) disrupted all measured B_6 pools, with the exception of endogenous PLP. This strain, which possessed both the DXP-dependent and independent pathways, accumulated ~4-fold more PNP than the isogenic *pdxH* p*SNZ* strain. These data suggested that lack of YggS resulted in increased flux through the DXP-dependent pathway,

which was the only defined way to generate PNP in this strain. Interpretation of these results was complicated by input from two pathways, but nonetheless these data hinted at a link between PdxH and YggS that was supported below.

PdxH and YggS modulate PLP/PMP homeostasis. Unlike PNP, both PMP and PLP are physiologically relevant and involved in key enzymatic reactions. To focus on these vitamers, two pairs of strains that lacked the DXP-dependent pathway, and thus the ability to generate PNP (Figure 4.1), were considered. When SNZ3p was the sole source of PLP (i.e., in a *pdxJ* mutant), the status of both PdxH and YggS impacted the pool sizes of PLP and PMP (Figure 4.3(3), 4.3(4)). Considering strains *pdxJ* p*SNZ* and *pdxJH* p*SNZ*, lack of *pdxH* increased the internal and external PMP concentration by ~2 and 4-fold respectively, while decreasing external PLP by ~half. These results were consistent with a general role for PdxH in converting PMP to PLP (Figure 4.1), utilizing a catalytic activity it is known to have (21). The data in Figure 4.3(3) showed that a lack of YggS in a *pdxJ* background did little to pool sizes, causing only a small but significant decrease in internal PMP levels. In contrast, in strains lacking *pdxJ* and *pdxH* (Figure 4.3(4)), a *yggS* mutation increased external PLP concentration by ~3-fold, and decreased the amount of internal and external PMP by ~2-fold. Notably, regardless of the source of PLP biosynthesis or background mutations, endogenous PLP level remained similar to the levels in wild-type *S. enterica*. These data suggest a mechanism to maintain internal PLP levels, perhaps by regulating the release of excess PLP to the medium. Such a mechanism appears to be independent of YggS and PdxH.

Considering the data in Figure 4.3 from different perspectives, a general trend emerged. The status of YggS and the status of PdxH had opposing effects on the ratio of PLP to PMP. Specifically, lack of PdxH increased accumulated PMP and slightly decreased exogenous PLP

levels, while additional loss of YggS minimized the extent of these changes. In contrast, lack of YggS decreased PMP and increased exogenous PLP levels in the absence of PdxH, suggesting an epistatic interaction between these gene products. In total, the data suggested a model in which both PdxH and YggS are involved in modulating PLP/PMP homeostasis (Figure 4.4). It is formally possible that SNZ3p levels are different among the strains, and this impacts B_6 vitamer pools. We consider this unlikely since the expression vector is engineered and utilizes the same components in each strain.

Working model for PdxH and YggS in PLP-PMP recycling. Data obtained with the heterologous strains that lacked the ability to synthesize PNP led to a working model for the interconversion of PLP/PMP that implicates both YggS and PdxH. The model recognizes that the primary destination of PLP is the active site of PLP-dependent enzymes (Figure 4.4A), which includes at least 14 aminotransferases encoded in the *S. enterica* genome. Importantly, the catalytic cycle of this latter class of enzymes involves the generation of PMP followed by the regeneration of PLP. Initially, an α-amino acid substrate donates an amino group to enzyme-bound PLP to generate the corresponding α-keto acid and PMP (Figure 4.4B). The PMP, if retained in the active site of the enzyme, can then donate an amino group to an α-keto acid, leading to regeneration of PLP and a restored balance of keto- and amino- acids (Figure 4.4C). Unlike PLP, the PMP molecule is not covalently bound to the enzyme: *in vitro* data showed that PMP binds ~100-fold less tightly than PLP to apo-aminotransferases, and 70% of intracellular PMP is free (8, 22). Our model invokes an equilibrium between two pools of PMP, one enzyme-bound and one free (Figure 4.4D). The latter pool of PMP is oxidized by PdxH to PLP (Figure 4.4E), and the PLP is reloaded into an apoenzyme (Figure 4.4A) or released from the cell. In this scenario, blocking PdxH would

result in the accumulation of PMP and decrease of PLP, consistent with the data herein (*yggS*$^{+}$, Figure 4.3(3), 4.3(4)). We suggest that YggS has a negative effect on some, if not all, reactions that convert keto acids to amino acids, many of which are critical for metabolic homeostasis and involve α-ketoglutarate (Figure 4.4C). In this scenario, the absence of YggS would result in an increased regeneration of PLP-holoenzyme and potentially lead to an overflow of newly synthesized PLP, which is released into the medium (Figure 4.2B). A *pdxH* mutation would have little impact in the absence of YggS (*yggS*$^{-}$, Figure 4.3(3), 4.3(4)), since the pool of free PMP would be reduced by elevated levels of transamination acting on the PMP-bound enzyme before the vitamer was lost from the active site. It is formally possible that YggS stimulates transamination reactions that convert PLP to PMP, though it is more difficult to envision a general mechanism for this effect. This model does not propose mechanistic details for the metabolic regulation involved, though we favor an indirect effect via altering metabolite pools and/or catalyzing an unknown reaction.

Conclusions. The data herein showed that in an otherwise wild-type strain, a *yggS* mutation results in a greater than 10-fold increase in PLP accumulation in growth medium. This result, in combination with the stability of the endogenous PLP pools in numerous strain backgrounds used here, suggests that internal PLP pools are capped, and excess PLP is released to the extracellular milieu. Notably, elevated levels of PLP were reported in the plasma of patients carrying variants of the human YggS homolog, PLPHP (11). Cellular excretion has been described for other key metabolites such as acetate, amino acids, and heme (reviewed in (23-25)) and may be part of a strategy to maintain stable levels of metabolites that can interfere with metabolic homeostasis.

The use of a heterologous strain background with a single PLP synthase enzyme as the only source of generating PLP (20) provided a novel means to probe the role of PdxH and YggS in the homeostasis of PLP and PMP. Importantly, this strain had no defined mechanism to generate PNP, a vitamer that is non-physiological, but nonetheless has figured prominently in multiple studies on the role of YggS (5, 7, 8, 10). In total, the data showed that the status of PdxH and YggS impact the levels of PMP and exogenous PLP, which led to a working model to explain these effects. Future studies, both genetic and biochemical, can build on these findings to ultimately identify the biochemical function of the YggS protein family.

4.4 MATERIALS AND METHODS

Strains, media, and chemicals. Plasmids and strains used in this study are listed in Table 4.S3. Strains are derivatives of *S. enterica* serovar Typhimurium LT2 and *E. coli* strain BW25113 as indicated. Bacterial strains were incubated at 37°C. *S. enterica* was cultured in Difco nutrient broth (NB, 8 g/l) with NaCl (5 g/l). Lysogeny broth (LB) was used as a rich medium for *E. coli*. Minimal medium for *S. enterica* and *E. coli* was no-carbon E (NCE) supplemented with 1 mM $MgSO_4$, trace elements (26) and one of the following as sole carbon source: glucose (11 mM), gluconate (11 mM), sorbitol (11 mM), trehalose (5.5 mM), galactose (11 mM), mannose (11 mM), fructose (11 mM), xylose (13.2 mM), ribose (13.2 mM), arabinose (13.2 mM), succinate (20 mM), rhamnose (22 mM), glycerol (22 mM), citrate (22 mM), malate (40 mM), pyruvate (50 mM), fumarate (50 mM), or acetate (50 mM). Media supplements were vitamin-free casamino acids (0.4%), glycine (0.67 mM), and PL (1 μM) when appropriate. For solid media, agar was added to a final concentration of 1.5% (w/v). Antibiotics were used as needed: kanamycin (Km; 50 μg/ml), ampicillin (Am; 150 μg/ml), and chloramphenicol (Cm; 20 μg/ml in rich and 5 μg/ml in minimal

media). Chemicals were purchased from MilliporeSigma (formerly Sigma-Aldrich, St. Louis, MO) unless otherwise stated. Restriction enzymes and *Taq* DNA polymerase were purchased from New England BioLabs (Ipswich, MA).

Plasmid and strain construction. Primers used for plasmid and strain construction are listed in Table 4.S4. Plasmid pBAD33-SD1 was generated by inserting the Shine-Delgarno sequence (AGGAGG) in front of *Nhe*I site on pBAD33 (27) and was a gift from Jorge C. Escalante-Semerena (University of Georgia, Athens, GA). Plasmids pDM1601 and pDM1594 were constructed by cloning *yggS* from *S. enterica* and *SNZ3* from *S. cerevisiae* YJF153, respectively, at the *Sac*I and *Xba*I sites downstream of an arabinose-inducible promoter in pBAD33-SD1. Gene insertions were confirmed by Sanger sequencing at Eton Bioscience (San Diego, CA). Plasmids were propagated in *E. coli* DH5α.

In-frame deletions of *yggS*, *pdxJ*, and *pdxH* were generated by one-step gene inactivation using phage λ Red recombinase (28) that has been adapted for *S. enterica*. The initial mutations were introduced into a wild-type strain (DM15847) via phage P22 *HT105/1 int-201* transduction (29). Transductants were purified and made phage-free as described (30). Insertion-deletion mutations of *cysK* and *glyA* were present in the laboratory collection and were transduced into appropriate backgrounds. Antibiotic markers were resolved using pCP20 as needed (31). Gene deletions were confirmed by colony PCR. The heterologous *S. enterica* strains were constructed by inactivating the native *pdxJ* (DM16710) or *pdxH* (DM16844) alone or a combination of both (DM16627) and transforming pDM1594 for *in-trans* expression of the yeast *SNZ3*. The *E. coli yggS* mutant was obtained from the Keio collection (32). Plasmids were transformed into *S. enterica* and *E. coli* strains via electroporation.

Growth analysis. *S. enterica* strains were grown in 2 ml NB overnight. Cells were then pelleted and resuspended in 0.85% NaCl prior to inoculation (2.5%) into minimal NCE medium containing carbon sources and supplements as described. Growth was monitored in a 96-well plate by measuring the optical density at 650 nm (OD_{650}) using a BioTek Elx808 plate reader (BioTek Instruments, Winooski, VT). Graphs and doubling time (T_D) were generated from GraphPad Prism 7.0c (GraphPad Software, La Jolla, CA).

Inhibitory effect of B_6 vitamers. Wild-type and *yggS* strains of *S. enterica* and *E. coli* were cultured in rich media overnight. An aliquot of 100 µl of washed cells was inoculated into molten agar (0.7%) and overlaid onto minimal NCE glucose containing 2,3,5-triphenyltetrazolium chloride (0.5 mM). 5 µl of 1 mM PL, PN, and PM were spotted on solidified top agar. After overnight incubation, plates were photographed by a 13 MP rear camera on Samsung Galaxy J7 Prime (San Jose, CA).

Vitamin B_6 bioassay. Overnight cultures of *S. enterica* and *E. coli* in rich media were washed with 0.85% NaCl and 200 µl was sub-cultured into 5 ml minimal NCE medium containing glucose as a sole carbon source. After reaching mid-log phase (OD_{650} = 0.7 – 0.8) as determined by a Spectronic 20D+ instrument (Thermo Fisher Scientific, Waltham, MA), cells were pelleted (7,000 × g, 10 min, 4ºC), and spent medium was filter-sterilized. Glucose (11 mM), $MgSO_4$ (1 mM), and trace elements were added to the spent medium. Growth analysis of *S. enterica pdxJ* strain in spent medium was monitored in a 96-well plate as described. The formal possibility that vitamer accumulation was due to cell lysis was eliminated by screening spent medium for released proteins. Aliquots (5 µl) of cell-free spent medium from relevant strains (DM16018, DM16020, DM16021)

were run on 14% SDS-PAGE and visualized by Coomassie blue staining. No protein bands were visible in any of the spent medium.

Analysis of B_6 vitamers by high performance liquid chromatography (HPLC). Minimal NCE medium containing glucose (11 mM) or glycerol (22 mM) as a sole carbon source and 0.02% arabinose was used to cultivate *S. enterica* and *E. coli* strains. Cells were harvested during mid-log phase (OD_{650} = 0.7 – 0.8) and subjected to analysis using Shimadzu Prominence HPLC system (Shimadzu Scientific Instruments Inc., Columbia, MD). Intracellular content of B_6 was adapted from protocol described elsewhere, and did not distinguish free and enzyme-bound pools of the vitamers (7). Briefly, cell pellets were treated with 5 volumes (v/w) of 0.7 M $HClO_4$ containing 5 µM 4-deoxypyridoxine (dPN) as internal standard (50 µl for 10 mg cells), resuspended, and incubated on ice for 15 min with occasional agitation. Then 2.5 volumes of chilled 0.7 M K_2CO_3 were added, followed by another 15-min ice incubation. The mixture was centrifuged (17,000 × g, 15 min, 4°C), and the supernatant was diluted 3-fold before 25 µl was injected to a 250 x 4.6 mm Cosmosil AR-II ODS column (5 µm particle size, Nacalai USA Inc., San Diego, CA). Mobile phase A contained phosphoric acid (33 mM) and 1-octanesulfonic acid (8 mM) at pH 2.2 (adjusted with KOH). Mobile phase B contained 80% (v/v) acetonitrile. Vitamin B_6 content was analyzed at 27°C (excitation at 328 nm and emission at 393 nm) using a linear gradient program as followed: 0% B to 1% B for 5 min; 1% B to 19% B for 5 min; 19% B to 28% B for 10 min; 28% B to 63% B for 5 min; 63% B for 5 min; 63% to 0% B for 5 min; and column equilibration with 100% A for 15 min. Total flow rate was 0.8 ml/min and running time was 50 min. Fluorescence was enhanced using 1 M potassium phosphate buffer (pH 7.5) containing sodium bisulfite (1 g/l) at a flow rate of 0.3 ml/min. Extraction of extracellular B_6 vitamers was similar to that of intracellular B_6 analysis

with slight modifications: 10 µl of $HClO_4$ (7 M) containing dPN (15 µM) was added to 90 µl cell-free culture supernatant (obtained as described in the bioassay), 50 µl of chilled K_2CO_3 (0.7 M) was added after a 15-min ice incubation, and extracted content was used for HPLC analysis. Data were analyzed using Shimadzu Labsolutions 5.42 SP2 software, with a detection range of 10 nM-10 µM for each vitamer. Concentrations of intracellular and extracellular B_6 vitamers were calculated as area under the curve normalized to final OD_{650} at which cells were harvested. Peak identity was assigned based on retention time obtained from vitamin B_6 standards and by co-injecting 1 µM of each vitamer with the samples. In addition, phosphorylated B_6 vitamers were confirmed by phosphatase treatment (100 mM sodium citrate at pH 5.0, 1 unit of wheat germ acid phosphatase, and 50 µl of cell extract or culture supernatant in a total volume of 150 µl). Following overnight incubation at 37ºC, the reactions were stopped by heat-inactivation at 95ºC for 5 minutes, and the content was extracted with $HClO_4$ and analyzed as described. The disappearance of PLP/PNP/PMP peaks and concomitant appearance of corresponding PL/PN/PM peaks confirmed the identity of the phosphorylated B_6 vitamers. Statistical analyses were performed on data obtained with three biological replicates in each of two independent experiments using GraphPad Prism 7.0c (GraphPad Software, La Jolla, CA).

ACKNOWLEDGEMENTS

The authors thank Dr. Jorge C. Escalante-Semerena for access to his laboratory strain collection. We acknowledge Michael D. Paxhia for helpful discussions and for the construction of the original *pdxH* mutant strain in *S. enterica* in addition to plasmids pDM1594 and pDM1601. This work was supported by an award from the competitive grants program at the NIH (GM095837) to DMD and from the JSPS KAKENHI (16K18686 and 17KK0153) to TI.

4.5 REFERENCES

1. Ito T, Iimori J, Takayama S, Moriyama A, Yamauchi A, Hemmi H, Yoshimura T. 2013. Conserved pyridoxal protein that regulates Ile and Val metabolism. J Bacteriol 195:5439-5449.

2. Tremiño L, Forcada-Nadal A, Contreras A, Rubio V. 2017. Studies on cyanobacterial protein PipY shed light on structure, potential functions, and vitamin B_6-dependent epilepsy. FEBS Lett 591:3431-3442.

3. Tremiño L, Forcada-Nadal A, Rubio V. 2018. Insight into vitamin B_6-dependent epilepsy due to *PLPBP* (previously *PROSC*) missense mutations. Human Mutat 39:1002-1013.

4. Johnstone DL, Al-Shekaili HH, Tarailo-Graovac M, Wolf NI, Ivy AS, Demarest S, Roussel Y, Ciapaite J, van Roermund CW, Kernohan KD. 2019. PLPHP deficiency: clinical, genetic, biochemical, and mechanistic insights. Brain 142:542-559.

5. Prunetti L, El Yacoubi B, Schiavon CR, Kirkpatrick E, Huang L, Bailly M, ElBadawi-Sidhu M, Harrison K, Gregory JF, Fiehn O, Hanson AD, de Crecy-Lagard V. 2016. Evidence that COG0325 proteins are involved in PLP homeostasis. Microbiology 162:694-706.

6. Darin N, Reid E, Prunetti L, Samuelsson L, Husain RA, Wilson M, El Yacoubi B, Footitt E, Chong WK, Wilson LC, Prunty H, Pope S, Heales S, Lascelles K, Champion M, Wassmer E, Veggiotti P, de Crécy-Lagard V, Mills PB, Clayton PT. 2016. Mutations in *PROSC* disrupt cellular pyridoxal phosphate homeostasis and cause vitamin-B_6-dependent epilepsy. Am J Hum Genet 99:1325-1337.

7. Ito T, Yamamoto K, Hori R, Yamauchi A, Downs DM, Hemmi H, Yoshimura T. 2019. Conserved pyridoxal 5′-phosphate-binding protein YggS impacts amino acid metabolism through pyridoxine 5′-phosphate in *Escherichia coli*. Appl Environ Microbiol 85:e00430-19.

8. Ito T, Hori R, Hemmi H, Downs DM, Yoshimura T. 2020. Inhibition of glycine cleavage system by pyridoxine 5′-phosphate causes synthetic lethality in *glyA yggS* and *serA yggS* in *Escherichia coli*. Mol Microbiol 113:270-284.

9. Ito T, Yamauchi A, Hemmi H, Yoshimura T. 2016. Ophthalmic acid accumulation in an *Escherichia coli* mutant lacking the conserved pyridoxal 5′-phosphate-binding protein YggS. J Biosci Bioeng 122:689-693.

10. Labella JI, Cantos R, Espinosa J, Forcada-Nadal A, Rubio V, Contreras A. 2017. PipY, a member of the conserved COG0325 Family of PLP-binding proteins, expands the cyanobacterial nitrogen regulatory network. Front Microbiol 8:1244.

11. Plecko B, Zweier M, Begemann A, Mathis D, Schmitt B, Striano P, Baethmann M, Vari MS, Beccaria F, Zara F. 2017. Confirmation of mutations in *PROSC* as a novel cause of vitamin B_6-dependent epilepsy. J Med Genet 54:809-814.

12. Rosenberg J, Ischebeck T, Commichau FM. 2017. Vitamin B_6 metabolism in microbes and approaches for fermentative production. Biotechnol Adv 35:31-40.

13. Percudani R, Peracchi A. 2003. A genomic overview of pyridoxal-phosphate-dependent enzymes. EMBO Rep 4:850-854.

14. Mittenhuber G. 2001. Phylogenetic analyses and comparative genomics of vitamin B_6 (pyridoxine) and pyridoxal phosphate biosynthesis pathways. J Mol Microbiol Biotechnol 3:1-20.

15. Tanaka T, Tateno Y, Gojobori T. 2004. Evolution of vitamin B_6 (pyridoxine) metabolism by gain and loss of genes. Mol Biol Evol 22:243-250.

16. Venegas A, Martial J, Valenzuela P. 1973. Active site-directed inhibition of *E. coli* DNA-dependent RNA polymerase by pyridoxal 5′-phosphate. Biochem Biophys Res Commun 55:1053-1059.

17. Bartzatt R, Beckmann JD. 1994. Inhibition of phenol sulfotransferase by pyridoxal phosphate. Biochem Pharmacol 47:2087-2095.

18. Vermeersch JJ, Christmann-Franck S, Karabashyan LV, Fermandjian S, Mirambeau G, Der Garabedian PA. 2004. Pyridoxal 5′-phosphate inactivates DNA topoisomerase IB by modifying the lysine general acid. Nucleic Acids Res 32:5649-5657.

19. Ito T, Downs DM. 2020. Pyridoxal reductase, PdxI, is critical for salvage of pyridoxal in *Escherichia coli*. J Bacteriol 202:e00056-20.

20. Paxhia MD, Downs DM. 2019. *SNZ3* Encodes a PLP synthase involved in thiamine synthesis in *Saccharomyces cerevisiae*. G3 (Bethesda) 9:335-344.

21. Zhao G, Winkler ME. 1995. Kinetic limitation and cellular amount of pyridoxine (pyridoxamine) 5′-phosphate oxidase of *Escherichia coli* K-12. J Bacteriol 177:883-891.

22. Jenkins W. 1985. Kinetics, equilibria, and affinity for coenzymes and substrates. Transaminases:216-234.

23. Wolfe AJ. 2005. The acetate switch. Microbiol Mol Biol Rev 69:12-50.

24. Eggeling L, Sahm H. 2003. New ubiquitous translocators: amino acid export by *Corynebacterium glutamicum* and *Escherichia coli*. Arch Microbiol 180:155-160.

25. Choby JE, Skaar EP. 2016. Heme synthesis and acquisition in bacterial pathogens. J Mol Biol 428:3408-3428.

26. Davis R, Botstein D, Roth J. 1980. Advanced bacterial genetics. Cold Spring Harbor Laboratory Press, Cold Spring Harbor, NY.

27. Guzman LM, Belin D, Carson MJ, Beckwith J. 1995. Tight regulation, modulation, and high-level expression by vectors containing the arabinose P_{BAD} promoter. J Bacteriol 177:4121-4130.

28. Datsenko KA, Wanner BL. 2000. One-step inactivation of chromosomal genes in *Escherichia coli* K-12 using PCR products. Proc Natl Acad Sci USA 97:6640-6645.

29. Schmieger H. 1971. A method for detection of phage mutants with altered transducing ability. Mol Gen Genet MGG 110:378-381.

30. Chan RK, Botstein D, Watanabe T, Ogata Y. 1972. Specialized transduction of tetracycline resistance by phage P22 in *Salmonella* Typhimurium: II. Properties of a high-frequency-transducing lysate. Virology 50:883-898.

31. Cherepanov PP, Wackernagel W. 1995. Gene disruption in *Escherichia coli*: Tc^R and Km^R cassettes with the option of Flp-catalyzed excision of the antibiotic-resistance determinant. Gene 158:9-14.

32. Baba T, Ara T, Hasegawa M, Takai Y, Okumura Y, Baba M, Datsenko KA, Tomita M, Wanner BL, Mori H. 2006. Construction of *Escherichia coli* K-12 in-frame, single-gene knockout mutants: the Keio collection. Mol Syst Biol 2:2006.0008.

Table 4.S1 – Vitamin B_6 profiles of *E. coli* and *S. enterica*.

Source	Organism	Strain[a]	PLP	PMP	PNP
Intracellular ($pmol/OD_{650}$)	*E. coli*	WT	1066 ± 33	563 ± 24	N.D.[b]
		yggS	1154 ± 17	580 ± 17	192 ± 6
	S. enterica	WT	701 ± 38	582 ± 66	9.0 ± 0.7
		yggS	763 ± 47	598 ± 29	146 ± 6
		p*yggS*	767 ± 29	627 ± 8	17.2 ± 0.4
Extracellular (nM/OD_{650})	*S. enterica*	WT	81 ± 2	N.D.	N.D.
		yggS	829 ± 16	41 ± 1	N.D.
		p*yggS*	124 ± 1	N.D.	N.D.

[a]Wild-type and *yggS* strains of *E. coli* and *S. enterica* carried a pBAD33-SD1 empty vector control (WT, DM16787 and DM16018; *yggS*, DM16788 and DM16020) or with *yggS* expressed *in trans* (p*yggS*, DM16021). Strains were grown in minimal NCE glucose medium with 0.02% arabinose. Data represent the average of three biological replicates and standard deviation is shown.

[b]N.D. not detected.

Table 4.S2 – Vitamin B_6 profiles of heterologous *S. enterica* strains.

Source	Strain[a]	PLP	PMP	PNP
Intracelullar (pmol/OD_{650})	WT	649 ± 55	704 ± 19	N.D.[b]
	yggS	758 ± 14	817 ± 46	115 ± 11
	pdxH / p*SNZ*	605 ± 4	830 ± 14	142 ± 16
	pdxH yggS / p*SNZ*	627 ± 33	239 ± 37	585 ± 107
	pdxJ / p*SNZ*	603 ± 18	591 ± 67	N.D.
	pdxJ yggS / p*SNZ*	489 ± 24	436 ± 20	13 ± 5
	pdxJH / p*SNZ*	559 ± 34	915 ± 28	N.D.
	pdxJH yggS / p*SNZ*	488 ± 49	538 ± 56	N.D.
Extracellular (nM/OD_{650})	WT	79 ± 5	N.D.	N.D.
	yggS	930 ± 4	44 ± 3	N.D.
	pdxH / p*SNZ*	272 ± 23	165 ± 5	N.D.
	pdxH yggS / p*SNZ*	851 ± 154	69 ± 8	81 ± 23
	pdxJ / p*SNZ*	546 ± 124	37 ± 6	N.D.
	pdxJ yggS / p*SNZ*	678 ± 150	35 ± 4	N.D.
	pdxJH / p*SNZ*	239 ± 17	164 ± 1	N.D.
	pdxJH yggS / p*SNZ*	670 ± 182	87 ± 13	N.D.

[a]*S. enterica* wild-type and *yggS* strains harbored a pBAD33-SD1 empty vector control (WT, DM16018; *yggS*, DM16020), had the native DXP-dependent PLP biosynthetic pathway replaced by expressing *S. cerevisiae* SNZ3p *in trans* (*pdxJ* / p*SNZ*, DM16710; *pdxJ yggS* / p*SNZ*, DM16712; *pdxJH* / p*SNZ*, DM16627; *pdxJH yggS* / p*SNZ*, DM16629), or expressed both pathways (*pdxH* / p*SNZ*, DM16844; *pdxH yggS* / p*SNZ*, DM16846). Strains were grown in minimal NCE glycerol medium with 0.02% arabinose. HPLC data were from three biological replicates and normalized to final cell optical density at 650 nm.

[b]N.D. not detected.

Table 4.S3 – List of strains and plasmids used in this study.

Strain or plasmid	Description	Source
***S. enterica* LT2**		
DM15847	Wild type	This study
DM15948	*yggS651*	This study
DM16018	Wild type / pBAD33-SD1	This study
DM16020	*yggS651* / pBAD33-SD1	This study
DM16021	*yggS651* / pDM1601	This study
DM16108	*pdxJ666::Cm*	This study
DM16523	*glyA1112::Cm*	This study
DM16524	*yggS651 glyA1112::Cm*	This study
DM16527	*cysK::Cm*	This study
DM16528	*yggS651 cysK::Cm*	This study
DM16627	*pdxJ664 pdxH673* / pDM1594	This study
DM16629	*pdxJ664 pdxH673 yggS648::Km* / pDM1594	This study
DM16710	*pdxJ664* / pDM1594	This study
DM16712	*pdxJ664 yggS648::Km* / pDM1594	This study
DM16844	*pdxH667* / pDM1594	This study
DM16846	*pdxH667 yggS648::Km* / pDM1594	This study
***E. coli* BW25113**		
JE6653	Wild type	Escalante[a]
DM15634	*yggS725::Km*	(32)[a]
DM16787	Wild type / pBAD33-SD1	This study
DM16788	*yggS725::Km* / pBAD33-SD1	This study
Plasmids		
pCP20	$Temp^S$ plasmid expressing *S. cerevisiae* Flp recombinase (Cm^R, Am^R)	(31)
pBAD33-SD1	Modified pBAD33 (Cm^R)	Escalante[a]
pDM1594	pBAD33-SD1 expressing *S. cerevisiae* SNZ3p (Cm^R)	This study
pDM1601	pBAD33-SD1 expressing *S. enterica* YggS (Cm^R)	This study

[a]Provided by Dr. Jorge C. Escalante-Semerena at the University of Georgia (Athens, GA).

Table 4.S4 – List of primers used in this study.

Primer	Sequence (5' to 3')	Description
PR1137	TAGGGAGCTCAGGAGGACAGCTATGTCAGAATTCAAGGTTAAAACTG	Construction of pDM1594
PR1138	TAGGTCTAGACTACCATCCGATTTCAGAAAGTC	
PR1140	TAGGGAGCTCATGAACGATATCGCGCATAACC	Construction of pDM1601
PR1141	TAGGTCTAGATTAATTTTTTGTGTAATCACGAGCAC	
PR1052	ATAACCTGGCATACATCCGGGACAAAATCTCCGCCGCGGCGTGTAGGCTGGAGCTGCTTC	Inactivation of *S. enterica yggS*
PR1053	ACAGCTCAATTACCGTTGAGAGCAGGAAGGTCAACGTATTCATATGAATATCCTCCTTAG	
PR1076	AACGCACAGTAAAAACGAAGAAAGATTAACGAGGATTGTCGTGTAGGGCTGGAGCTGCTTC	Inactivation of *S. enterica pdxJ*
PR1077	GGGCAATCTCTACAATATCCGTTCCCAGGCCGAGAATCGCCATATGAATATCCTCCTTAG	
PR1395	GCACAATAGCGCCACCCACTGATTATTTCTGATCAACGCCGTGTAGGCTGGAGCTGCTTC	Inactivation of *S. enterica pdxH*
PR1396	ATTCATCCGCACCAGTGCTTAAAACAAGATTTTTGCATCTCATATGAATATCCTCCTTAG	

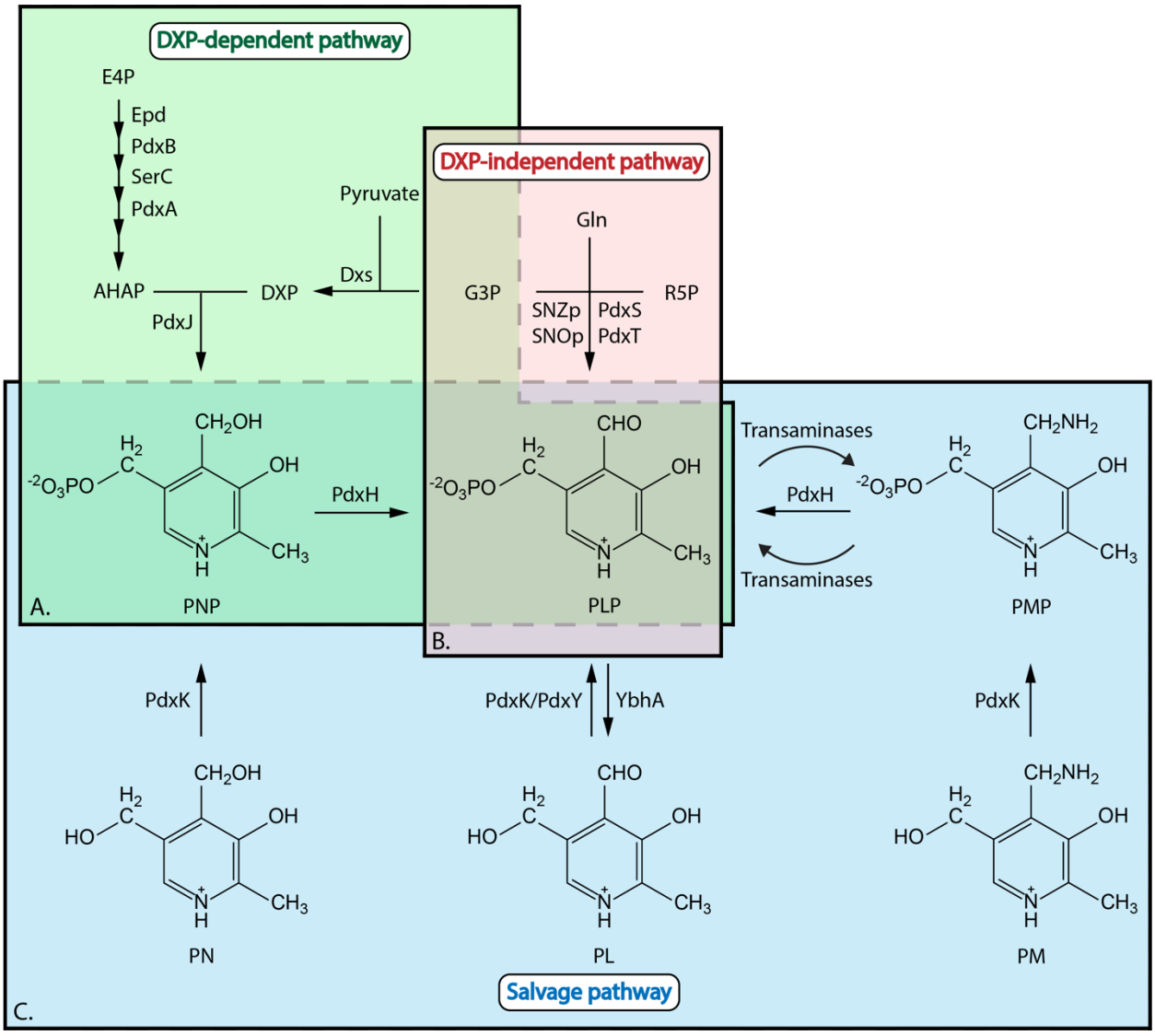

Figure 4.1 – PLP biosynthesis and salvage. Organisms can synthesize PLP *de novo* using either (A) the DXP-dependent pathway (green, representative pathway in *S. enterica* and *E. coli*) or (B) the DXP-independent pathway (pink, representative pathway in *S. cerevisiae* and *B. subtilis*). Synthesis of PLP via the DXP-independent pathway involves a PLP synthase/glutaminase complex, designated as SNZp/SNOp in yeast and PdxS/PdxT in *B. subtilis* respectively. (C) Some organisms have all or part of a salvage pathway (blue, representative pathway in *S. enterica* and *E. coli*) to obtain PLP from the environment. Abbreviations: DXP, deoxyxylulose 5-phosphate; E4P, erythrose-4-phosphate; AHAP, 3-amino-1-hydroxyacetone 1-phosphate; Gln, glutamine;

G3P, glyceraldehyde-3-phosphate; R5P, ribose-5-phosphate; PL, pyridoxal; PN, pyridoxine; PM, pyridoxamine; PLP, pyridoxal 5′-phosphate; PNP, pyridoxine 5′-phosphate; PMP, pyridoxamine 5′-phosphate.

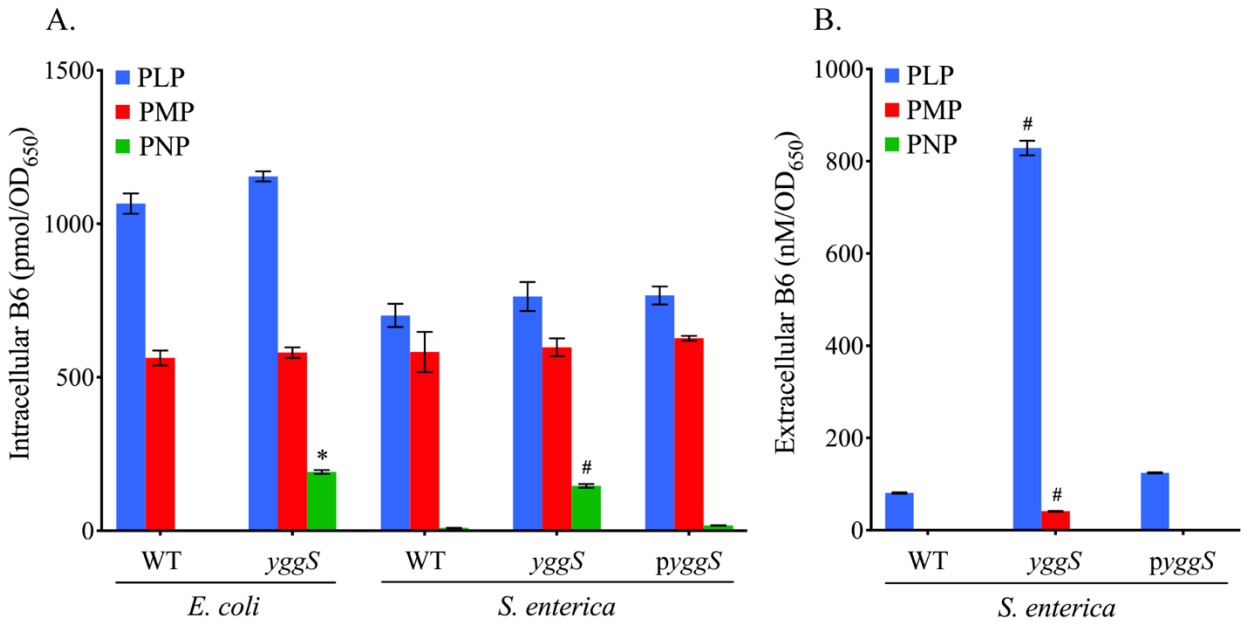

Figure 4.2 – Levels of phosphorylated B_6 vitamers. HPLC analysis of (A) intracellular phosphorylated B_6 vitamers of *E. coli* and *S. enterica* wild-type (DM16787 and DM16018, respectively) and *yggS* strains carrying a pBAD33-SD1 empty vector control (DM16788 and DM16020) or with *yggS* expressed *in trans* (p*yggS*, DM16021) and (B) phosphorylated B_6 vitamers of relevant *S. enterica* strains that accumulated in the medium after growth to mid-log phase in minimal NCE glucose with 0.02% arabinose. Data were obtained from three biological replicates and normalized to final cell optical density at 650 nm. Limit of detection is 10 nM – 10 µM for each vitamer. Error bars represent standard deviation from the mean. An asterisk (*) denotes $P < 0.0001$ between *E. coli* wild type and *yggS* mutant as determined by two-tailed unpaired Student's *t*-test. A pound (#) denotes adjusted $P < 0.0001$ with respect to *S. enterica* wild type as determined by one-way ANOVA followed by Dunnett's *post hoc* test.

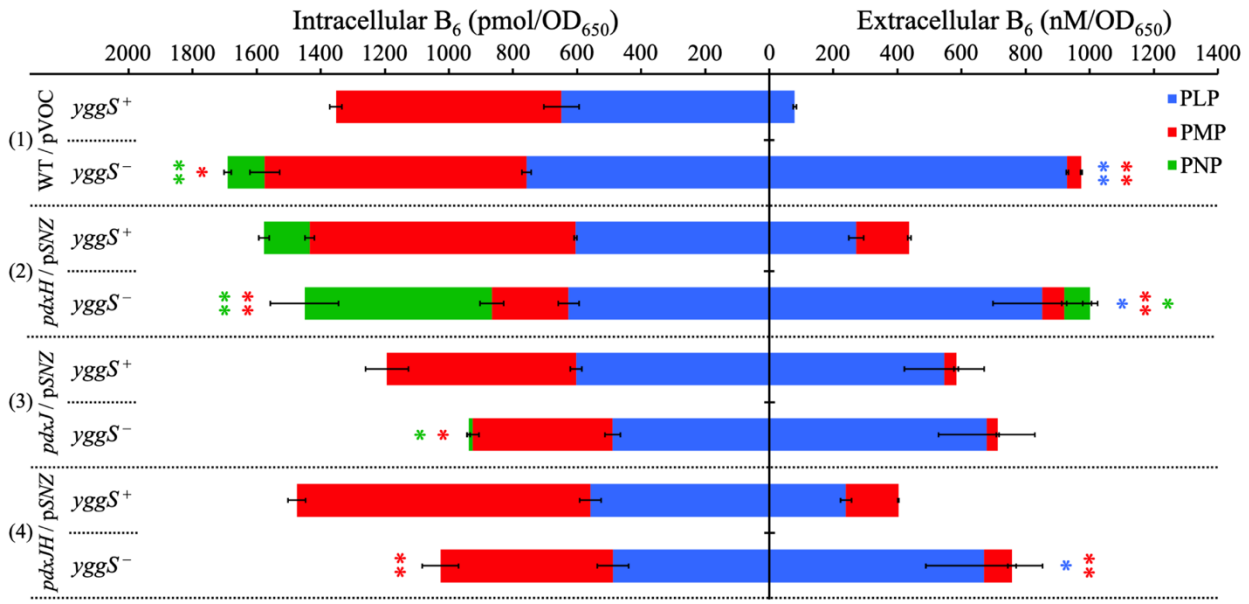

Figure 4.3 – Status of YggS and PdxH impacts vitamin B_6 pools. Intracellular and extracellular vitamin B_6 profiles are shown. Each panel (1-4) shows a pair of strains differing only at the *yggS* locus. Strains of the indicated genotype carry a pBAD33-SD1 empty vector control (pVOC) or one expressing *S. cerevisiae SNZ3* (p*SNZ*). Strains were grown in minimal NCE glycerol supplemented with 0.02% arabinose. HPLC data were obtained from three biological replicates and normalized to final cell optical density at 650 nm. Error bars depict standard deviation from the mean. In each panel, an asterisk (*) denotes $P < 0.02$ and a double asterisk denotes $P < 0.002$ (determined by two-tailed unpaired Student's *t*-test), when the *yggS*$^+$ strain and its isogenic *yggS* derivative are compared. Significance as indicated was obtained in at least two independent experiments.

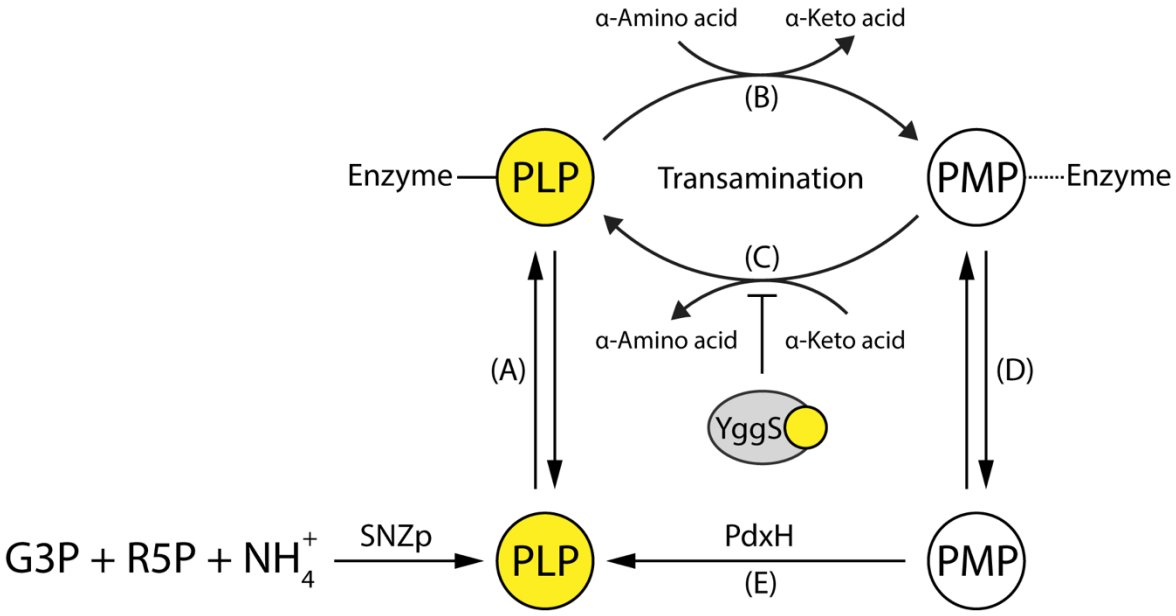

Figure 4.4 – Working model for YggS placement in vitamin B_6 homeostasis. (A) Newly synthesized PLP is incorporated into PLP-dependent enzymes via an unknown mechanism. (B) During transamination catalyzed by aminotransferases, enzyme-bound PLP is converted to PMP in the first half-reaction. (C) PMP can be retained in the active site to regenerate PLP in the second half-reaction, or (D) released from the active site and (E) converted back to PLP by PdxH. The status of YggS and PdxH affects PLP-PMP recycling. YggS function is proposed to have a negative impact on the recycling of PMP to PLP. Thus, loss of YggS would lead to increased total PLP and decreased total PMP pools. Intracellular PLP is maintained via loss of excess PLP to the environment. This model does not consider internal accumulation of PNP, which has been examined in other studies (5, 7, 8). Abbreviations: PLP, pyridoxal 5′-phosphate; PMP, pyridoxamine 5′-phosphate; PNP, pyridoxine 5′-phosphate; G3P, glyceraldehyde-3-phosphate; R5P, ribose-5-phosphate.

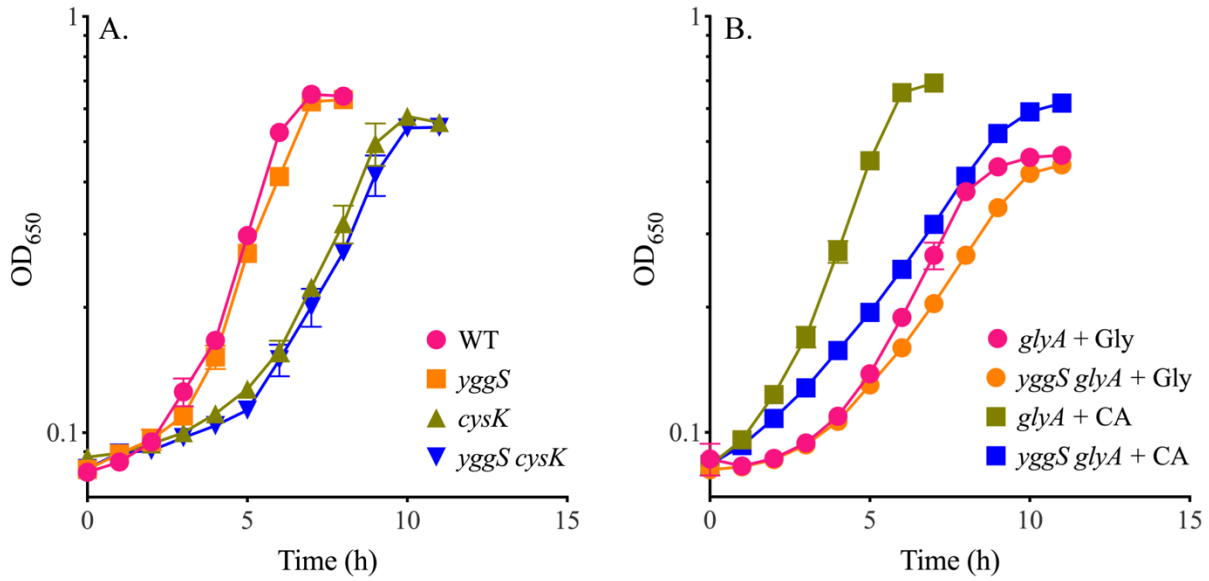

Figure 4.S1 – Synthetic phenotypes of *yggS*$^{+}$ and *yggS*$^{-}$ strains. Growth of *S. enterica* (A) wild-type (DM15847), *yggS* (DM15948), *cysK* (DM16527), and *yggS cysK* (DM16528) strains in minimal NCE glucose and (B) *glyA* (DM16523) and *yggS glyA* (DM16524) strains in minimal NCE glucose supplemented either with 0.67 mM glycine (Gly) or 0.4% vitamin-free casamino acid (CA). Data were obtained from three biological replicates. Error bars show standard deviation from the mean

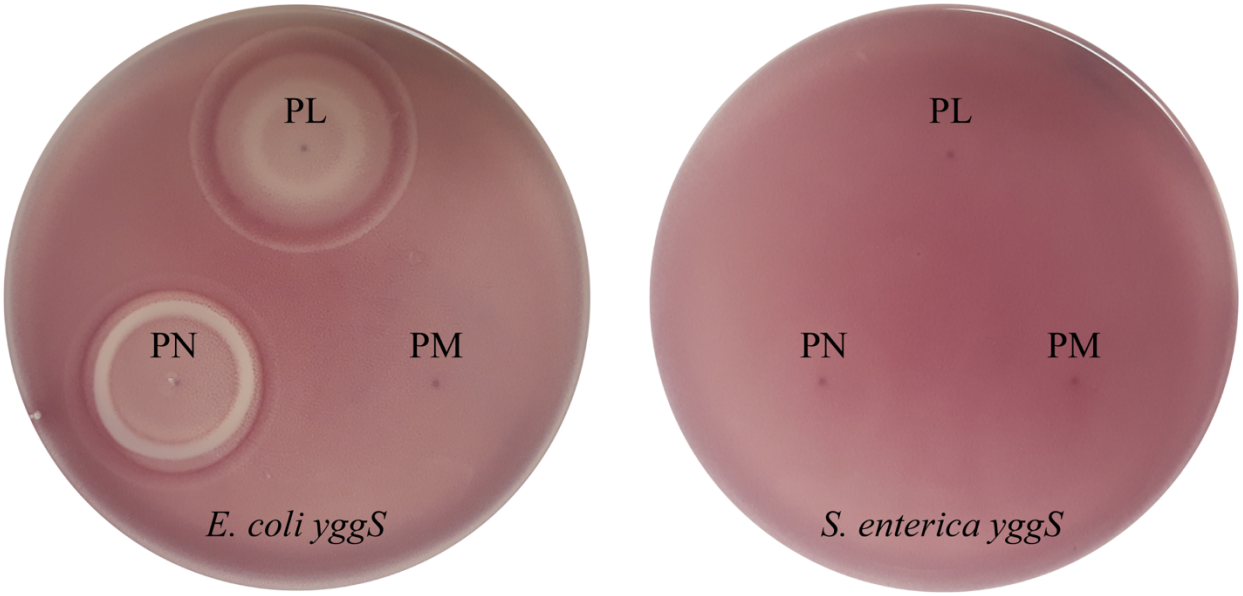

Figure 4.S2 – Exogenous PL, PN, and PM affect a *yggS* mutant of *E. coli,* but not *S. enterica.*

Cells were plated as described in Materials and Methods. 5 nmol of PL, PN, and PM were spotted onto soft agar overlay inoculated with a *yggS* strain of either *E. coli* (DM15634) or *S. enterica* (DM15948). 2,3,5-triphenyltetrazolium chloride was embedded in the agar to facilitate visualization of bacterial growth. The presence of a clear zone around a spotted B_6 vitamer indicated inhibition of growth. Isogenic strains of wild-type *E. coli* and *S. enterica* showed no growth inhibition under the same conditions (data not shown). Representative growth of three replicates is presented.

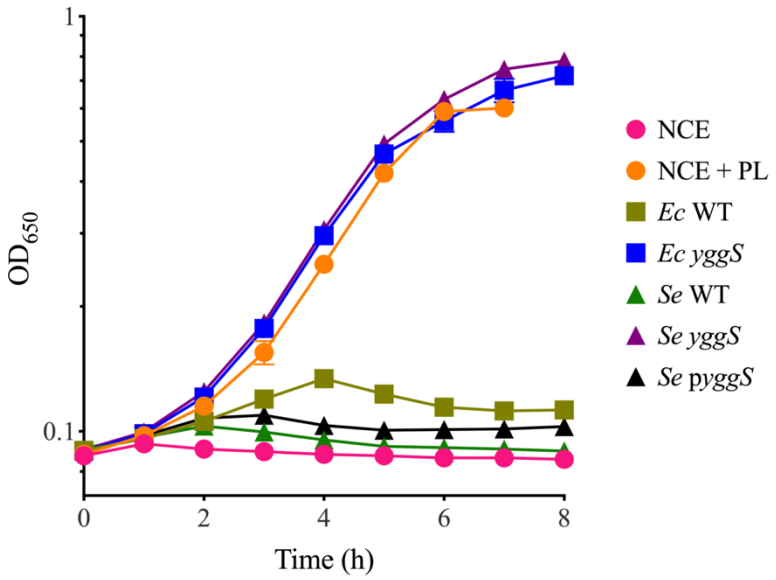

Figure 4.S3 – Vitamin B_6 bioassay of spent media. The presence of vitamin B_6 was determined based on the growth phenotype of the *S. enterica pdxJ* mutant strain (DM16108) in minimal NCE glucose (without or with supplementation of 1 µM PL) or in cell-free culture supernatant of *E. coli* (*Ec*) and *S. enterica* (*Se*) wild type carrying a pBAD33-SD1 empty vector control (DM16787 and DM16018, respectively), *yggS* carrying a pBAD33-SD1 empty vector control (DM16788 and DM16020, respectively), and *S. enterica yggS* carrying a pBAD33-SD1 vector expressing *yggS* (DM16021). The bioassay was conducted using three biological replicates of *pdxJ* growth. Spent media were collected in three independent experiments (representative growth using spent media from one experiment is shown). Error bars depict standard deviation from the mean.

CHAPTER 5

LOSS OF YGGS (COG0325) IMPACTS ASPARTATE METABOLISM IN *SALMONELLA ENTERICA* [4]

[4] Vu HN, Downs DM. 2021. *Molecular Microbiology*. 116(4): 1232-1240.
Reprinted here with permission of the publisher.

5.1 ABSTRACT

YggS is a pyridoxal 5′-phosphate (PLP)-binding protein of the conserved COG0325 family. Despite a connection with vitamin B_6 homeostasis in many species, neither a precise biochemical activity nor molecular mechanism of how YggS contributes to cellular function has been described. In a transposon mutagenesis screen, we found that insertions in *aspC* (encoding a PLP-dependent aspartate aminotransferase, EC 2.6.1.1) in a *Salmonella enterica* strain lacking *yggS* caused a synthetic growth defect, which could be rescued by addition of exogenous aspartate. Characterization of spontaneous suppressors which improved growth of the *yggS aspC* double mutant suggested that this synthetic aspartate limitation was dependent on TyrB, a PLP-dependent aromatic-amino-acid aminotransferase (EC 2.6.1.57). Genetic and biochemical data were consistent with the hypothesis that TyrB activity was inhibited by accumulated pyridoxine 5′-phosphate and α-keto acids caused by a *yggS* mutation. This study provides data consistent with a working model implicating YggS in modulating concentrations of B_6 vitamers via transamination.

ABBREVIATED SUMMARY

In *Salmonella enterica*, AspC and TyrB are pyridoxal 5′-phosphate (PLP)-dependent aminotransferases capable of catalyzing glutamate-aspartate transamination. Herein we show that loss of YggS, an uncharacterized PLP-binding protein implicated in vitamin B_6 homeostasis, impacts TyrB-dependent aspartate synthesis. Our data suggest this effect is mediated by accumulation of pyridoxine 5′-phosphate (PNP) and perturbations of α-keto acids pool, such as α-ketobutyrate (αKB) and α-ketoglutarate (αKG), which are consequences of a *yggS* mutation.

5.2 INTRODUCTION

Pyridoxal 5′-phosphate (PLP), the active form of vitamin B_6, is a required cofactor for many enzymes in all three domains of life. To survive and thrive, organisms must synthesize PLP *de novo* via the deoxyxylulose 5-phosphate (DXP)-dependent or -independent pathway, or obtain PLP by salvaging B_6 vitamers from the environment (1, 2). PLP carries a reactive aldehyde group (Figure 5.1) and has been shown to inhibit several PLP-independent enzymes *in vitro* (3-5), suggesting a need to maintain a balanced level of this cofactor. Despite the essential role of PLP in cellular functions, the mechanism(s) that maintains PLP homeostasis is not fully understood.

YggS, a PLP-binding protein of unknown function from the conserved COG0325 family, has emerged as a potential player in the regulation of PLP homeostasis. Mutations in *yggS* and its homologs have been linked to pleiotropic effects in different organisms. Notably in *Escherichia coli* and *Salmonella enterica* serovar Typhimurium (referred hereafter as *S. enterica*), strains lacking a functional YggS exhibited perturbed intracellular and extracellular levels of phosphorylated B_6 vitamers (6-9), α-keto acids, and amino acids (6-8, 10, 11). Additionally, mutations in *PLPBP* (a human homolog of *yggS*) were identified as genetic markers for vitamin B_6-dependent epilepsy in humans, and similar metabolic pool perturbations were present in these patients (12-17). Finally, a link between PipY (a cyanobacterial homolog of YggS) and nitrogen regulation was studied in *Synechococcus elongatus* (18, 19).

Among various reactions catalyzed by PLP-dependent enzymes, transamination reactions are of particular interest because they connect YggS, PLP, α-keto acids, amino acids, and central metabolism. Our previous work implicated YggS in modulating activity (directly or indirectly) of transaminases *in vivo* (9). A canonical transamination reaction consists of two half-reactions and the cycling of PLP→pyridoxamine 5′-phosphate (PMP)→PLP. In the first half-reaction, an α-

amino acid donates an amino group to PLP to produce a corresponding α-keto acid and PMP. The subsequent half-reaction involves a transfer of the amino group from PMP to an α-keto acid, generating a corresponding α-amino acid and converting PMP back to PLP. In addition to synthesizing amino acids needed for growth, transamination reactions indirectly impact carbon and nitrogen metabolism due to the involvement of glutamate and α-ketoglutarate (αKG) (20).

Relevant to this work is the glutamate-aspartate transamination reaction catalyzed by AspC and TyrB enzymes in *S. enterica* (Figure 5.1). AspC is a PLP-dependent aspartate aminotransferase/transaminase (AspAT, EC 2.6.1.1) that catalyzes the reversible conversion of oxaloacetate (OAA) to aspartate. An *S. enterica aspC* mutant grows in the absence of exogenous aspartate because TyrB, a PLP-dependent aromatic-amino-acid aminotransferase (EC 2.6.1.57), has weak AspAT activity (21, 22). In this study, we determined that a lesion in *yggS* generated a requirement for aspartate in an *aspC* mutant background. Our data supported a model in which two metabolic consequences of a *yggS* mutation compromised the AspAT activity of TyrB, resulting in the noted requirement for exogenous aspartate in the *yggS aspC* double mutant.

5.3 RESULTS

Lack of *yggS* generates a conditional aspartate requirement in an *S. enterica aspC* mutant. In a transposon mutagenesis experiment, Tn*10*(d)Tc insertions that prevented growth of a *yggS* mutant on minimal NCE glucose medium were identified. Significantly, two independent insertions caused a growth defect in strain lacking *yggS*, while they had less impact on growth of a wild-type strain (data not shown). Sequence analysis determined that these insertions were in different positions in the *aspC* gene. A deletion of *aspC* was constructed in both wild-type and *yggS* backgrounds, and growth of these strains on various carbon sources was assessed (Table

5.S1). As expected, the wildtype and *yggS* parental strains grew similarly in all tested carbon sources (representative data in gluconate and pyruvate are shown in Figure 5.2) (9). However, growth of the *aspC* mutant varied depending on the carbon source provided. In general, the *aspC* mutant grew less well than wild type, and growth was restored by exogenous aspartate (Figure 5.2) or by expressing *aspC in trans* (data not shown). A lesion in *yggS* nearly abolished growth of the *aspC* strain on minimal gluconate medium (Figure 5.2a) and compromised growth to different degrees on other carbon sources (Figure 5.2b, Table 5.S1). The carbon sources that best supported growth of the *yggS aspC* double mutant enter metabolism downstream of phosphoenolpyruvate (PEP) and are either intermediates of, or feed directly into, the TCA cycle and potentially increase flux toward aspartate synthesis. Regardless of the carbon source, i) lack of *yggS* reduced growth of the *aspC* mutant (Table 5.S1), and ii) addition of aspartate fully restored growth to both the *aspC* and the *yggS aspC* strains (Figure 5.2). In total, these data suggested that an aspartate limitation in the *aspC* mutant was exacerbated by a *yggS* lesion.

The cellular aspartate requirement is not increased by loss of *yggS*. The data above suggested that a *yggS* mutation causes a higher cellular requirement for aspartate, and/or compromised aspartate synthesis. To address the former possibility, growth of an *aspC tyrB* and a *yggS aspC tyrB* mutant was assessed in minimal NCE gluconate with increasing concentrations of exogenous aspartate. A null mutation in *tyrB* was present to eliminate endogenous synthesis and ensure that growth of these two strains was solely dependent on exogenous aspartate. Both *aspC tyrB* and *yggS aspC tyrB* mutants reached a similar final optical density when aspartate was added to the medium (Table 5.1). The *yggS* derivative had a slight growth defect even in the presence of aspartate. For instance, the doubling time for the *aspC tyrB* strain was 1.4 ± <0.1 h, while for the

yggS aspC tyrB mutant it was 1.8 ± 0.1 h at 0.6 mM aspartate. Increasing aspartate concentration only improved growth yield (Table 5.1) but not growth rate of these two strains (data not shown). These results suggested that i) loss of *yggS* does not increase the requirement for aspartate, and ii) lack of YggS slightly impacted growth independent of aspartate metabolism.

Increased TyrB-dependent aspartate synthesis restores growth of a *yggS aspC* mutant. Spontaneous revertants of the *yggS aspC* strain were isolated on minimal glucose and minimal gluconate medium. Colonies arose on these media at a frequency of ~4 x 10^{-6} cells. Ten independent mutants that were isolated on glucose and sixteen isolated on gluconate were confirmed phenotypically. A single mutant was reconstructed and used as a guide for characterizing the additional strains (Table 5.S2). Standard genetic techniques utilizing a pool of random Tn*10*(d)Cm insertions found that the causative mutation in this strain was genetically linked to *tyrB*. Using a combination of *alr*::*Cm* and *qor*::Tn*10*(d)Cm insertions located ~0.2 kb and ~ 2.8 kb upstream of *tyrB* respectively, the causative mutation in each of twenty suppressor isolates (#1-20) was mapped to the *tyrB* region (Table 5.S2). Sequence analysis of nineteen suppressor strains showed that each had a single base substitution with the potential to affect the level of TyrB (Figure 5.3a). Six distinct substitutions identified in twelve independent isolates were in the promoter region of *tyrB* (*tyrB948p*-*tyrB953p*). Two of these substitutions (*tyrB948p* and *tyrB949p*) changed the promoter sequence closer to the consensus (23, 24) and thus would be expected to increase *tyrB* expression (25). The role of the remaining four mutations in *tyrB* promoter is unclear, but growth data (Figure 5.3b, Table 5.S2) and activity assays (Table 5.2) predict they also increase expression of *tyrB*. Another suppressor (*tyrB954p*) had a base substitution located in one of the two operators of *tyrB* (Figure 5.3a) (26), which may weaken the

binding of the TyrR repressor and result in increased expression. Six of the twenty isolates (#12-17) had a substitution changing the start codon of TyrB from GTG to ATG (*tyrB955*). There is precedent for this substitution in improving translation efficiency (27).

Tn*10*(d)Cm insertions in *tyrR* and *nadR* independently allowed growth of a *yggS aspC* double mutant on gluconate (data not shown). TyrR is a repressor of *tyrB* transcription, and its absence results in ~1.3-fold increase in expression of *tyrB* (25). Further, two suppressors isolated on gluconate (*tyrR956*, *tyrR957*) carried a single nucleotide substitution located in *tyrR* coding sequence, one generating a frameshift and one a single base substitution (Table 5.S2). Thus, with the exception of the insertion in *nadR*, all identified suppressor mutations supported a hypothesis that increasing TyrB level restored growth of a *yggS aspC* double mutant. Expression of *tyrB in trans* allowed a *yggS aspC* mutant to grow (Figure 5.3c), further strengthening this hypothesis. The mechanism of NadR-dependent suppression was not pursued further.

Suppressor mutations result in increased AspAT activity. The aspartate titration (Table 5.1) indicated that a *yggS* mutation did not impact the cellular aspartate requirement. This result, in combination with the suppressors isolated (Table 5.S2), suggested a lack of *yggS* might decrease expression and/or activity of TyrB, leading to an aspartate limitation in a *yggS aspC* strain. The identity of the suppressor mutations supported a model in which an increased cellular level of TyrB resulted in higher AspAT activity, thus relieving the limitation. To address this interpretation, AspAT activity was measured in cell-free extracts of multiple strains in minimal NCE glucose medium (Table 5.2). The presence or absence of aspartate in the growth medium did not significantly affect AspAT activity in a wild-type strain (data not shown). Therefore, cells to be assayed were grown in medium supplemented with aspartate to ensure equal growth. Loss of *yggS*

did not significantly impact AspAT activity of a wild-type or *aspC* background (Table 5.2). These data eliminated a role for the *yggS* lesion in transcription or translation of TyrB, and suggested that a metabolic perturbation resulting from a *yggS* mutation impacted TyrB, perhaps via metabolic or allosteric regulation.

To confirm the effect ascribed to the mutations isolated, AspAT activity was determined in three representative suppressor strains in minimal NCE glucose supplemented with aspartate (Table 5.2). Several points could be taken from the data in Table 5.2. In strains carrying a suppressor mutation, AspAT activity increased by 1.5 to 4.4-fold compared to that in the parental *yggS aspC* strain, with the *tyrB948p* mutation generating the most significant increase. This was the only mutation that restored TyrB level to those found in the wild type and *yggS* mutant, presumably completely overcoming the need for AspC activity. Despite the fairly mundane increase in TyrB activity in many suppressor strains, the mutant alleles restored near full growth to the *aspC yggS* strain (Figure 5.3b). These data suggest that TyrB can provide the aspartate needed for growth, despite AspAT being a minor activity of this enzyme (22). This balance may explain the distribution of growth rates for an *aspC* mutant (and the *yggS* derivative) on different carbon sources, possibly due to the specific need for aspartate and/or the availability of the substrate OAA. In total, the data suggest that increasing TyrB-dependent AspAT activity is the primary strategy available to overcome aspartate limitation in a *yggS aspC* mutant.

TyrB activity is inhibited by pyridoxine 5′-phosphate (PNP) *in vitro*. Since AspAT activity was not decreased in a *yggS* mutant, we hypothesized that the metabolic environment could dampen TyrB activity, perhaps by allosteric inhibition. Prior studies showed that a *yggS* mutation significantly increased intracellular levels of PNP, a B_6 vitamer, in both *S. enterica* (9) and *E. coli*

(6-9). To determine if PNP could directly inhibit AspAT, *S. enterica* TyrB-5xHis and AspC-5xHis were purified (Figure 5.4a) and AspAT activity of each enzyme was assayed *in vitro* in the absence or presence of PNP (Figure 5.4b). TyrB and AspC were preincubated with PNP before αKG was added to initiate the reaction. Under these conditions, 5 μM and 50 μM PNP decreased AspAT activity of TyrB by ~30% and ~50%, respectively. Without preincubation, PNP had no significant effect on TyrB activity. PNP did not affect the activity of AspC when tested in the same assay conditions with 50 μM PNP. These data raised the possibility that PNP accumulation in a *yggS* mutant could compromise the AspAT activity of TyrB and contribute to the aspartate requirement of the *yggS aspC* mutant.

Exogenous α-keto acids phenocopy a *yggS* mutation. In *E. coli*, a *yggS* mutant accumulated ~5-fold more α-ketobutyrate (αKB) than the wild-type strain (10). We previously suggested YggS impacts transaminases, potentially resulting in imbalanced α-keto acid pools (9). Finally, in the presence of αKB, aspartate synthesis was compromised in *E. coli* (28) and *S. enterica* (29). This latter result appeared to link two metabolic features of a *yggS* mutant. To explore this connection, growth analysis focusing on the impact of αKB and αKG was performed. Growth of the wild type was delayed when αKB (1 mM) was added to minimal NCE gluconate (Figure 5.5a). Interestingly, αKB almost eliminated growth of an *aspC* strain (Figure 5.5a), phenocopying a *yggS aspC* double mutant (Figure 5.2a). Addition of aspartate restored growth of both wild-type and *aspC* strains, extending the correlation with a *yggS* mutation.

αKG is a key substrate in transamination reactions and a regulatory metabolite coordinating carbon and nitrogen metabolism (20), making it of particular interest in the context of *yggS.* In *S. enterica*, the *kgtP* gene, which encodes an αKG transporter (30), is not expressed in

minimal medium under laboratory conditions (31). However, dimethyl α-ketoglutarate (dmKG) can be used to increase endogenous pools of αKG, since this molecule can diffuse across the membrane and is converted to αKG by intracellular esterases (20). Addition of dmKG (10 mM) to the medium compromised growth of wild type, similar to αKB (Figure 5.5b). Significantly, this metabolite resulted in severely dampened growth of the *aspC* mutant, which was restored by addition of aspartate. Together, these data suggest the possibility that in a *yggS* background α-keto acids, particularly αKB and αKG, may interfere with aspartate synthesis via TyrB.

5.4 DISCUSSION

Studies in a variety of organisms have shown that a mutation in *yggS* or homologous genes can lead to pleiotropic consequences, ranging from observable defects to more subtle metabolic perturbations (6-14, 16, 18). In this work, we determined that a *yggS* mutation generates an aspartate requirement in an *aspC* background, and dissected its cause. While AspC is the major PLP-dependent aminotransferase involved in aspartate synthesis, TyrB catalyzes this reaction with lower efficiency (Table 5.2, Figure 5.4b), resulting in the near prototrophic growth of an *aspC* mutant (Figure 5.2). Data herein support the hypothesis that the AspAT activity of TyrB is compromised by the metabolic environment generated by lack of YggS. Consistent with our hypothesis, suppressors that restored growth of a *yggS aspC* mutant increased expression/activity of TyrB (Table 5.2). In addition, a lesion in *yggS* did not impact TyrB activity in crude extracts (Table 5.2), which eliminated a role for YggS in the transcription or translation of the *tyrB* gene.

Under the conditions tested, *in vitro* data showed that the AspAT activity of TyrB was inhibited by PNP (Figure 5.4b), a B_6 vitamer shown to accumulate in the absence of YggS (6-9). Assuming the cell volume and growth parameters of *S. enterica* are similar to those of *E. coli*,

intracellular PNP accumulation in an *S. enterica yggS* mutant is estimated to be ~16.5 μM (9, 32, 33), which is within the range of 5-50 μM PNP used in the *in vitro* assays described here. These data suggest the possibility that similar inhibition occurs *in vivo* and could contribute to the aspartate requirement of the *yggS aspC* mutant (Figure 5.2). Interestingly, inhibition was only observed when TyrB was preincubated with PNP prior to addition of αKG (Figure 5.4b). As aspartate was present in the preincubation reaction mixture, it is possible that the first half-reaction was able to proceed and PMP was generated during the preincubation period. Since PMP is not covalently bound to the active site, PNP could compete with PMP for binding to TyrB, leading to inhibition of the second half-reaction. This hypothesis is bolstered by the finding that among the three B_6 vitamers, TyrB homolog purified from rat liver exhibited the weakest affinity for PMP, which was ~2.5-fold and ~100-fold lower than that for PNP and PLP, respectively (34). AspC was insensitive to PNP inhibition (Figure 5.4b), consistent with the similar growth of the *tyrB* and *yggS tyrB* mutant pair (Figure 5.S1). This result may reflect the fact that *E. coli* AspC had a ~1.7-fold higher affinity for PMP compared to TyrB (35), suggesting PNP would have less access to the active site. In addition, growth analysis with *yggS*$^+$ and *yggS*$^-$ strains defective in AvtA (valine-pyruvate aminotransferase, EC 2.6.1.66) or IlvE (branched-chain-amino-acid aminotransferase, EC 2.6.1.42) did not detect a synthetic phenotype (Figure 5.S1), suggesting their overlapping activities were not compromised, unlike the case in a *yggS aspC* mutant. These data suggested that PNP sensitivity is not a general feature of PLP-dependent aminotransferases.

Previously, we suggested YggS had a general role in PLP/PMP recycling and impacted transamination reactions, which implied there might be metabolic consequences due to perturbed α-keto acid pools in a *yggS* mutant (9). Data presented here support this possibility and suggest that the synthetic phenotype of a *yggS aspC* mutant is one such consequence. Two significant α-

keto acids, αKB and αKG, phenocopied a *yggS* mutation when added exogenously to the growth medium of an *aspC* mutant (Figure 5.5). These data provided evidence of a physiological connection between the metabolic changes and the phenotypes of a *yggS* mutant. While addition of αKB could reduce TyrB and AspC activity *in vitro*, a concentration of ≥ 100 mM was required (Figure 5.S2) and thus direct inhibition by this metabolite was not deemed physiologically relevant.

The diverse phenotypes displayed by *yggS* mutants are likely to reflect indirect metabolic consequences caused by the lack of this highly conserved PLP-binding protein. The diversity of metabolic network structures among organisms suggests that in the absence of YggS, there will be both universal and organism-specific consequences for growth. For instance, while PNP is only present in a subset of organisms that encode a PNP/PMP oxidase (EC 1.4.3.5) (Ito *et al.*, unpublished), α-keto acids are universal metabolites that participate in a variety of processes, including transamination. Following this reasoning, and supported by the data herein, we suggest that YggS-dependent perturbations in α-keto acid levels are central to the functional role of YggS. Dissecting the molecular mechanism(s) that results in phenotypes of a *yggS* mutant is hampered by the complexity of interactions and regulatory roles described for α-keto acids *in vivo* (20, 36). In total, the results herein expand the base of knowledge that must be considered when models for the mechanism of YggS action are generated and tested. Continued characterization of consequences caused by a *yggS* mutation *in vivo* has the ability to focus efforts to define a biochemical activity for this protein that has been elusive thus far.

5.5 MATERIALS AND METHODS

Strains, plasmids, and primers. Strains and plasmids are listed in Table 5.S3 in the Supplementary Information. Primers used for strain/plasmid construction and transposon sequencing are presented as Table 5.S4. Bacterial strains are derivatives of *S. enterica* serovar Typhimurium LT2. Plasmids were propagated in *E. coli* DH5α (Invitrogen, Carlsbad, CA). Recombinant proteins were purified from *E. coli* BL21AI (Invitrogen, Carlsbad, CA).

Gene deletions were generated using phage λ Red recombination (37) adapted for *S. enterica* or using a pool of Tn*10*(d)Cm insertions. Mutations were transduced into appropriate strain backgrounds via phage P22 *HT105/1 int-201* (38), and phage-free transductants were isolated as described (39). In-frame deletions were confirmed by colony PCR. The locations of transposon insertions were determined using degenerate primers according to published method (40-42).

Expression plasmids were constructed by cloning *S. enterica yggS*, *aspC*, and *tyrB* into pCV1 (43) or pET28b(+).SapKO-CH.BspQI at the BspQI sites following described protocol (44). Constructed plasmids were confirmed by Sanger sequencing at Eton Bioscience (San Diego, CA). Plasmids were transformed into *E. coli* and *S. enterica* by electroporation.

Media and chemicals. *S. enterica* strains from cryo-stocks were grown on nutrient agar (8 g/liter Difco mix, 5 g/liter NaCl, 1.5% (wt/vol) agar) at 37ºC. Minimal medium was no-carbon E (NCE) medium supplemented with $MgSO_4$ (1 mM), trace elements (45), and one of the following as the sole carbon source: glucose (11 mM), gluconate (11 mM), sorbitol (11 mM), galactose (11 mM), mannose (11 mM), fructose (11 mM), xylose (13.2 mM), ribose (13.2 mM), arabinose (13.2 mM), succinate (20 mM), rhamnose (22 mM), glycerol (22 mM), citrate (22 mM), malate (40 mM),

oxaloacetate (40 mM), pyruvate (50 mM), fumarate (50 mM), or acetate (50 mM). Supplements included vitamin-free casamino acids (1% wt/vol), L-aspartate (1.8 mM), L-tyrosine (0.08 mM), L-phenylalanine (0.3 mM), L-isoleucine (0.3mM), αKB (1 mM), or dmKG (10 mM) as needed. Lysogeny broth (10 g/liter Bacto tryptone, 5 g/liter yeast extract, 5 g/liter NaCl) and super broth (32 g/liter Bacto tryptone, 20 g/liter yeast extract, 5 g/liter NaCl, 5 mM NaOH) were used to cultivate *E. coli* for protein purification. When appropriate, antibiotics were added as followed: kanamycin (Km, 50 μg/ml), chloramphenicol (Cm, 20 μg/ml), and ampicillin (Am, 150 μg/ml in rich medium and 15 μg/ml in minimal medium).

All chemicals were purchased from MilliporeSigma (formerly Sigma-Aldrich, St. Louis, MO) unless otherwise stated. *Taq* polymerase and restriction enzymes were purchased from New England BioLabs (Ipswich, MA). Primers were synthesized by Eton Bioscience (San Diego, CA). PNP was purified according to described protocol (42).

Growth analysis. *S. enterica* strains were precultured in 2 ml minimal NCE glucose supplemented with 1% casamino acids for 6-8 hours. Cells were pelleted by centrifugation and resuspended in an equal volume of 0.85% NaCl. Washed cultures were inoculated (2.5% vol/vol) into minimal NCE medium containing appropriate carbon sources and supplements as described above. Growth was monitored as a function of optical density at 650 nm (OD_{650}) over time in a 96-well plate using a BioTek ELx808 plate reader (BioTek Instruments, Winooski, VT). Data were visualized and statistical significance was determined using Prism 8.4.3 (GraphPad Software, La Jolla, CA).

Protein purification. *E. coli* BL21AI strains carrying expression plasmids (pDM1440 or pDM1441) were precultured in 10 ml lysogeny broth in duplicates at 37°C overnight and

subsequently used to inoculate two flasks containing 1.5 liters of super broth. Growth at 37ºC was monitored using a Spectronic 20D+ instrument (Thermo Fisher Scientific, Waltham, MA) until early-log phase (OD_{650} ~0.6-0.7). After addition of 0.02% (wt/vol) arabinose to induce expression, the temperature was shifted to 30ºC and growth continued in an Innova 44 shaking incubator (New Brunswick Scientific, Edison, NJ) at 200 rpm. Following a 20-hour incubation, cells were collected by centrifugation (7,000 × g, 15 min, 4°C) and stored at –80°C until purification.

All purification and buffer exchange steps for each protein were performed at 4ºC. Thawed cell pellet was resuspended at a concentration of ~2.5 ml/g wet weight in buffer A (100 mM potassium phosphate, 100 mM NaCl, 20 mM imidazole, 10% (vol/vol) glycerol, pH 8) containing lysozyme (1 mg/ml), DNase (0.25 mg/ml), and phenylmethylsulfonyl fluoride (1.5 mM). Cells were lysed at 18,000 psi using a Constant Systems Limited One Shot cell disruptor (Northants, United Kingdom). Cell lysate was clarified (48,000 × g, 45 min, 4°C), filtered (0.45-µm polyvinylidene difluoride), and loaded onto a 5-ml HisTrap HP Ni-Sepharose column (GE Healthcare, Chicago, IL) pre-equilibrated with 10 column volumes (CV) of buffer A using an NGC Quest 10 chromatography system (Bio-Rad, Hercules, CA). The loaded column was subsequently washed and eluded with 10 CV of buffer A, 5 CV of 4% buffer B (100 mM potassium phosphate, 100 mM NaCl, 500 mM imidazole, 10% glycerol, pH 8), a 10-CV gradient of 4-100% buffer B, and 4 CV of buffer B at a flow rate of 2 ml/min. After confirming on 14% SDS-PAGE gel, 100 µM PLP was added to the pooled fractions containing the target protein. The protein solution was concentrated using an Amicon Ultra-15 30K filter (MilliporeSigma, St. Louis, MO), exchanged into buffer C (100 mM potassium phosphate, 100 mM NaCl, 10% glycerol, pH 8) using a PD-10 desalting column (GE Healthcare, Chicago, IL), flash-frozen with liquid nitrogen, and stored at –80°C. Protein concentration was determined by Pierce bicinchoninic acid (BCA) protein assay

(Thermo Fisher Scientific, Waltham, MA) according to manufacturer's protocol using bovine serum albumin as a standard.

Aspartate aminotransferase (AspAT) assay. For AspAT assay using crude extracts, strains were precultured overnight in 2 ml minimal NCE glucose supplemented with 1% casamino acids in duplicates. Cells were then pelleted and resuspended in 0.85% NaCl as described. Aliquots of washed cultures were transferred (1% vol/vol) into 10 ml minimal NCE glucose supplemented with 1.8 mM aspartate. After reaching late-log phase (OD_{650} ~ 1.0-1.2) as determined by a Spectronic 20D+ instrument (Thermo Fisher Scientific, Waltham, MA), cells were centrifuged (7,000 × g, 10 min, 4°C), washed twice with 5 ml cold PBS, and stored at –80°C until assay. Frozen cell pellets were thawed in 1.5 ml 50 mM HEPES (pH 7.8) and lysed at 18,000 psi using a Constant Systems Limited One Shot cell disruptor (Northants, United Kingdom). Lysates were clarified (17,000 × g, 15 min, 4°C) and filtered (0.45-μm polyvinylidene difluoride) to obtain cell-free extracts.

AspAT activity was measured in the reverse direction using a coupled assay (46) with modifications. Briefly, reaction mixtures (200 μl) contained 50 mM HEPES (pH 7.8), 100 mM aspartate, 0.4 mM NADH, 5U porcine malate dehydrogenase, 100 μl cell-free extracts, and 5 mM αKG, which was added last to initiate the reaction. NADH oxidation was monitored spectrophotometrically at 340 nm (ε_{340} = 6220 M^{-1} cm^{-1}) in a 96-well quartz plate and normalized to 1-cm pathlength using a SpectraMax 398 Plus plate reader (Molecular Devices, Sunnyvale, CA). AspAT activity for each biological duplicate was measured with four technical replicates. Average specific activity from two independent experiments was reported as nanomoles of NADH oxidized

per minute per milligram of total protein. Protein concentration was determined by BCA assay as described.

AspAT assay mixtures using purified protein contained 50 mM HEPES (pH 7.8), 100 mM aspartate, 0.4 mM NADH, 5U porcine malate dehydrogenase, 2.5 μM PLP, 25 nM TyrB or AspC, 0-50 μM PNP, 0-500 mM αKB, and 1-5 mM αKG in a total volume of 200 μl as indicated in text. PNP (or 50 mM HEPES) was added to reaction mixtures and incubated for 0-10 minutes before the reaction was initiated by αKG addition. AspAT activity of TyrB and AspC (nmol NADH/min) was determined from two independent experiments using at least three technical replicates. Statistical tests were performed using Prism 8.4.3 (GraphPad Software, La Jolla, CA).

ACKNOWLEDGEMENTS

We thank Michael D. Paxhia and Jorge C. Escalante-Semerena for helpful discussions. We acknowledge Andrew J. Borchert for constructing plasmid pDM1440 and pDM1441. This work was supported by a competitive grant (GM095837) from the National Institutes of Health to DMD. The authors state that they have no conflicts of interest in presenting this work.

5.6 REFERENCES

1. Mittenhuber G. 2001. Phylogenetic analyses and comparative genomics of vitamin B_6 (pyridoxine) and pyridoxal phosphate biosynthesis pathways. Journal of Molecular Microbiology and Biotechnology. 3:1-20.

2. Tanaka T, Tateno Y, Gojobori T. 2004. Evolution of vitamin B_6 (pyridoxine) metabolism by gain and loss of genes. Molecular Biology and Evolution. 22:243-250.

3. Venegas A, Martial J, Valenzuela P. 1973. Active site-directed inhibition of *E. coli* DNA-dependent RNA polymerase by pyridoxal 5′-phosphate. Biochemical and Biophysical Research Communications. 55:1053-1059.

4. Bartzatt R, Beckmann JD. 1994. Inhibition of phenol sulfotransferase by pyridoxal phosphate. Biochemical Pharmacology. 47:2087-2095.

5. Vermeersch JJ, Christmann-Franck S, Karabashyan LV, Fermandjian S, Mirambeau G, Der Garabedian PA. 2004. Pyridoxal 5′-phosphate inactivates DNA topoisomerase IB by modifying the lysine general acid. Nucleic Acids Research. 32:5649-5657.

6. Prunetti L, El Yacoubi B, Schiavon CR, Kirkpatrick E, Huang L, Bailly M, El Badawi-Sidhu M, Harrison K, Gregory 3rd JF, Fiehn O. 2016. Evidence that COG0325 proteins are involved in PLP homeostasis. Microbiology. 162:694-706.

7. Ito T, Yamamoto K, Hori R, Yamauchi A, Downs DM, Hemmi H, Yoshimura T. 2019. Conserved pyridoxal 5′-phosphate-binding protein YggS impacts amino acid metabolism through pyridoxine 5′-phosphate in *Escherichia coli*. Applied and Environmental Microbiology. 85:e00430-19.

8. Ito T, Hori R, Hemmi H, Downs DM, Yoshimura T. 2020. Inhibition of glycine cleavage system by pyridoxine 5′-phosphate causes synthetic lethality in *glyA yggS* and *serA yggS* in *Escherichia coli*. Molecular Microbiology. 113:270-284.

9. Vu HN, Ito T, Downs DM. 2020. The role of YggS in vitamin B_6 homeostasis in *Salmonella enterica* is informed by heterologous expression of yeast *SNZ3*. Journal of Bacteriology. 202:e00383-20.

10. Ito T, Iimori J, Takayama S, Moriyama A, Yamauchi A, Hemmi H, Yoshimura T. 2013. Conserved pyridoxal protein that regulates Ile and Val metabolism. Journal of Bacteriology. 195:5439-5449.

11. Ito T, Yamauchi A, Hemmi H, Yoshimura T. 2016. Ophthalmic acid accumulation in an *Escherichia coli* mutant lacking the conserved pyridoxal 5′-phosphate-binding protein YggS. Journal of Bioscience and Bioengineering. 122:689-693.

12. Darin N, Reid E, Prunetti L, Samuelsson L, Husain RA, Wilson M, El Yacoubi B, Footitt E, Chong WK, Wilson LC. 2016. Mutations in *PROSC* disrupt cellular pyridoxal phosphate homeostasis and cause vitamin-B_6-dependent epilepsy. The American Journal of Human Genetics. 99:1325-1337.

13. Plecko B, Zweier M, Begemann A, Mathis D, Schmitt B, Striano P, Baethmann M, Vari MS, Beccaria F, Zara F. 2017. Confirmation of mutations in *PROSC* as a novel cause of vitamin B_6-dependent epilepsy. Journal of Medical Genetics. 54:809-814.

14. Tremiño L, Forcada-Nadal A, Rubio V. 2018. Insight into vitamin B_6-dependent epilepsy due to *PLPBP* (previously *PROSC*) missense mutations. Human Mutation. 39:1002-1013.

15. Shiraku H, Nakashima M, Takeshita S, Khoo CS, Haniffa M, Ch'ng GS, Takada K, Nakajima K, Ohta M, Okanishi T. 2018. *PLPBP* mutations cause variable phenotypes of developmental and epileptic encephalopathy. Epilepsia Open. 3:495-502.

16. Johnstone DL, Al-Shekaili HH, Tarailo-Graovac M, Wolf NI, Ivy AS, Demarest S, Roussel Y, Ciapaite J, van Roermund CW, Kernohan KD. 2019. PLPHP deficiency: clinical, genetic, biochemical, and mechanistic insights. Brain. 142:542-559.

17. Heath O, Pitt J, Mandelstam S, Kuschel C, Vasudevan A, Donoghue S. 2020. Early-onset vitamin B_6-dependent epilepsy due to pathogenic *PLPBP* variants in a premature infant: A case report and review of the literature. JIMD Reports. 58:3-11.

18. Labella JI, Cantos R, Espinosa J, Forcada-Nadal A, Rubio V, Contreras A. 2017. PipY, a member of the conserved COG0325 family of PLP-binding proteins, expands the cyanobacterial nitrogen regulatory network. Frontiers in Microbiology. 8:1244.

19. Tremiño L, Forcada-Nadal A, Contreras A, Rubio V. 2017. Studies on cyanobacterial protein PipY shed light on structure, potential functions, and vitamin B_6-dependent epilepsy. FEBS Letters. 591:3431-3442.

20. Doucette CD, Schwab DJ, Wingreen NS, Rabinowitz JD. 2011. α-Ketoglutarate coordinates carbon and nitrogen utilization via enzyme I inhibition. Nature Chemical Biology. 7:894.

21. Gelfand DH, Steinberg RA. 1977. *Escherichia coli* mutants deficient in the aspartate and aromatic amino acid aminotransferases. Journal of Bacteriology. 130:429-440.

22. Powell JT, Morrison JF. 1978. The purification and properties of the aspartate aminotransferase and aromatic-amino-acid aminotransferase from *Escherichia coli*. European Journal of Biochemistry. 87:391-400.

23. Harley CB, Reynolds RP. 1987. Analysis of *E. coli* promoter sequences. Nucleic Acids Research. 15:2343-2361.

24. Oliphant AR, Struhl K. 1988. Defining the consensus sequences of *E. coli* promoter elements by random selection. Nucleic Acids Research. 16:7673-7684.

25. Yang J, Camakaris H, Pittard J. 2002. Molecular analysis of tyrosine-and phenylalanine-mediated repression of the *tyrB* promoter by the TyrR protein of *Escherichia coli*. Molecular Microbiology. 45:1407-1419.

26. Yang J, Pittard J. 1987. Molecular analysis of the regulatory region of the *Escherichia coli* K-12 *tyrB* gene. Journal of Bacteriology. 169:4710-4715.

27. Sussman JK, Simons EL, Simons RW. 1996. *Escherichia coli* translation initiation factor 3 discriminates the initiation codon *in vivo*. Molecular Microbiology. 21:347-360.

28. Daniel J, Dondon L, Danchin A. 1983. 2-Ketobutyrate: a putative alarmone of *Escherichia coli*. Molecular and General Genetics MGG. 190:452-458.

29. Van Dyk TK, LaRossa RA. 1986. Sensitivity of a *Salmonella typhimurium aspC* mutant to sulfometuron methyl, a potent inhibitor of acetolactate synthase II. Journal of Bacteriology. 165:386-392.

30. Seol W, Shatkin AJ. 1991. *Escherichia coli kgtP* encodes an alpha-ketoglutarate transporter. Proceedings of the National Academy of Sciences. 88:3802-3806.

31. Yan D, Lenz P, Hwa T. 2011. Overcoming fluctuation and leakage problems in the quantification of intracellular 2-oxoglutarate levels in *Escherichia coli*. Applied and Environmental Microbiology. 77:6763-6771.

32. Cayley S, Lewis BA, Guttman HJ, Record Jr MT. 1991. Characterization of the cytoplasm of *Escherichia coli* K-12 as a function of external osmolarity: implications for protein-DNA interactions *in vivo*. Journal of Molecular Biology. 222:281-300.

33. Glazyrina J, Materne E-M, Dreher T, Storm D, Junne S, Adams T, Greller G, Neubauer P. 2010. High cell density cultivation and recombinant protein production with *Escherichia coli* in a rocking-motion-type bioreactor. Microbial Cell Factories. 9:1-11.

34. Voltattorni CB, Orlacchio A, Giartosio A, Conti F, Turano C. 1975. The binding of coenzymes and analogues of the substrate-coenzyme complex to tyrosine aminotransferase. European Journal of Biochemistry. 53:151-160.

35. Koehler E, Seville M, Jaeger J, Fotheringham I, Hunter M, Edwards M, Jansonius JN, Kirschner K. 1994. Significant improvement to the catalytic properties of aspartate aminotransferase: role of hydrophobic and charged residues in the substrate binding pocket. Biochemistry. 33:90-97.

36. LaRossa RA, Van Dyk TK. 1987b. Metabolic mayhem caused by 2-ketoacid imbalances. Bioessays. 7:125-130.

37. Datsenko KA, Wanner BL. 2000. One-step inactivation of chromosomal genes in *Escherichia coli* K-12 using PCR products. Proceedings of the National Academy of Sciences. 97:6640-6645.

38. Schmieger H. 1971. A method for detection of phage mutants with altered transducing ability. Molecular and General Genetics MGG. 110:378-381.

39. Chan RK, Botstein D, Watanabe T, Ogata Y. 1972. Specialized transduction of tetracycline resistance by phage P22 in *Salmonella typhimurium*: II. Properties of a high-frequency-transducing lysate. Virology. 50:883-898.

40. Chen P, Ailion M, Bobik T, Stormo G, Roth J. 1995. Five promoters integrate control of the *cob/pdu* regulon in *Salmonella typhimurium*. Journal of Bacteriology. 177:5401-5410.

41. Sun S, Berg OG, Roth JR, Andersson DI. 2009. Contribution of gene amplification to evolution of increased antibiotic resistance in *Salmonella typhimurium*. Genetics. 182:1183-1195.

42. Vu HN, Downs DM. 2021. An unexpected role for the periplasmic phosphatase PhoN in the salvage of B_6 vitamers in *Salmonella enterica*. Applied and Environmental Microbiology. 87:e02300-02320.

43. VanDrisse C, Escalante-Semerena J. 2016. New high-cloning-efficiency vectors for complementation studies and recombinant protein overproduction in *Escherichia coli* and *Salmonella enterica*. Plasmid. 86:1-6.

44. Galloway NR, Toutkoushian H, Nune M, Bose N, Momany C. 2013. Rapid cloning for protein crystallography using type IIS restriction enzymes. Crystal Growth and Design. 13:2833-2839.

45. Davis R, Botstein D, Roth J. 1980. Advanced bacterial genetics. Cold Spring Harbor Laboratory. New York.

46. Arnold PM, Parslow GR. 1995. Designing a coupled assay system for aspartate aminotransferase. Biochemical Education. 23:40-41.

47. Martínez-Chavarría LC, Sagawa J, Irons J, Hinz AK, Lemon A, Graça T, Downs DM, Vadyvaloo V. 2020. Putative horizontally acquired genes, highly transcribed during *Yersinia pestis* flea infection, are induced by hyperosmotic stress and function in aromatic amino acid metabolism. Journal of Bacteriology. 202:e00733-00719.

Table 5.1 – Cellular aspartate requirement is not impacted by a *yggS* mutation.

Aspartate concentration (mM)	Final OD_{650}[†]		*P* value[*]
	aspC tyrB	***yggS aspC tyrB***	
0	0.10 ± <0.01	0.10 ± <0.01	0.80
0.1	0.12 ± <0.01	0.12 ± <0.01	0.12
0.3	0.16 ± 0.01	0.17 ± <0.01	0.31
0.6	0.25 ± 0.01	0.26 ± <0.01	0.10
0.9	0.34 ± 0.01	0.36 ± 0.01	0.13
1.8	0.55 ± <0.01	0.55 ± 0.01	0.61

[†]Final OD_{650} was determined as the maximum optical density at 650 nm a strain achieved after 6-hour shaking incubation at 37°C in minimal NCE gluconate supplemented with 0.08 mM tyrosine, 0.3 mM phenylalanine, and 0-1.8 mM aspartate. Data were averaged from three biological replicates. Representative data from one of two independent experiments are shown.

[*]Statistical significance between growth of *aspC tyrB* and *yggS aspC tyrB* mutant for each condition was determined by two-tailed unpaired Student's *t* test.

Table 5.2 – AspAT activity in crude extracts is not affected by a lesion in *yggS*.

Strain[†]	AspAT activity[‡] (nmol NADH min^{-1} mg^{-1})	*P* value[*]
Wild type	389 ± 30	0.23
yggS	407 ± 54	
aspC	111 ± 25	0.99
yggS aspC	116 ± 27	
yggS aspC tyrB948p	516 ± 72	<0.0001
yggS aspC tyrB949p	186 ± 33	<0.0001
yggS aspC tyrB950p	169 ± 41	<0.005

[†]Strains were grown in minimal NCE glucose medium with aspartate (1.8 mM) and cell-free extracts were assayed for AspAT activity.

[‡]Average AspAT activity (in crude extracts) and standard deviation were determined from two independent experiments with biological duplicates, each of which was assayed with four technical replicates. Omitting aspartate from growth medium did not significantly affect AspAT activity in a wild-type strain (data not shown).

[*]Statistical significance between wild type and *yggS* mutant was determined by two-tailed unpaired Student's *t* test. One-way ANOVA followed by Dunnett's *post hoc* test was performed for the data set of the remaining strains with respect to *yggS aspC* mutant, and adjusted *P* values were reported.

Table 5.S1 – Growth of *aspC* (DM16150) and *yggS aspC* strain (DM16154) in minimal NCE with different carbon sources.

C source[†]		Lag time[‡] (h)		Doubling time (h)		Final OD_{650}[§]	
		aspC	*yggS aspC*	*aspC*	*yggS aspC*	*aspC*	*yggS aspC*
Non-permissive	Arabinose	3.5	NG	7.7 ± 0.7	NG	0.40 ± 0.01	0.15 ± <0.01
	Fructose	7.0	NG	3.9 ± 0.6	NG	0.55 ± 0.02	0.14 ± <0.01
	Galactose	4.5	NG	6.8 ± 0.4	NG	0.44 ± 0.01	0.14 ± <0.01
	Gluconate	5.0	NG	3.7 ± 0.2	NG	0.51 ± 0.01	0.16 ± <0.01
	Glucose	8.5	NG	6.7 ± 1.5	NG	0.47 ± 0.02	0.12 ± 0.01
	Mannose	8.0	NG	3.3 ± 0.5	NG	0.57 ± 0.02	0.13 ± <0.01
	Rhamnose	7.5	NG	3.2 ± 0.2	NG	0.64 ± <0.01	0.21 ± 0.01
	Ribose	6.5	NG	3.4 ± 0.2	NG	0.60 ± <0.01	0.15 ± <0.01
Semi-permissive	Acetate	13.5	24.5	5.6 ± 0.7	7.7 ± 0.3	0.68 ± 0.01	0.66 ± 0.01
	Glycerol	6.5	29.0	2.1 ± 0.1	3.4 ± 0.7	0.72 ± 0.02	0.62 ± <0.01
	Sorbitol	6.0	32.5	2.5 ± 0.1	3.2 ± 0.6	0.61 ± 0.01	0.52 ± 0.01
	Xylose	6.5	17.0	2.4 ± 0.1	5.0 ± 0.8	0.72 ± <0.01	0.63 ± <0.01
Permissive	Citrate	5.5	8.0	2.3 ± 0.1	2.8 ± 0.1	0.67 ± 0.01	0.68 ± 0.01
	Fumarate	5.0	6.5	2.2 ± 0.1	2.5 ± <0.1	0.82 ± <0.01	0.83 ± <0.01
	Malate	6.5	9.5	2.8 ± 0.2	3.5 ± 0.1	0.67 ± 0.01	0.65 ± 0.01
	Oxaloacetate	3.0	3.5	1.9 ± <0.1	2.7 ± 0.1	0.66 ± 0.01	0.59 ± 0.01
	Pyruvate	5.0	7.5	2.3 ± <0.1	2.9 ± 0.1	0.71 ± 0.01	0.66 ± <0.01
	Succinate	4.5	6.0	2.8 ± 0.1	3.2 ± <0.1	0.67 ± <0.01	0.67 ± <0.01

[†]Permissive carbon sources supported growth of the *yggS aspC* mutant with a lag time < 10 hours. Semi-permissive carbon sources allowed growth with a lag time > 15 hours. No detectable growth of the double mutant was observed after 40 hours in non-permissive carbon sources. Addition of 1.8 mM aspartate restored growth of both the *aspC* and *yggS aspC* strains to wild-type level (data not shown). Representative data from one of three independent experiments, each included three biological replicates, are shown.

[‡]Lag time is defined as the time required for a strain to reach ~$^1/_3$ of the final OD_{650}. NG: no growth.

[§]Final OD_{650} was determined as the maximum optical density at 650 nm a strain achieved after 40-hour shaking incubation at 37^{o}C.

Table 5.S2 – *yggS aspC* revertants isolated on minimal NCE glucose and gluconate.

C source[†]	Linkage to *tyrB*[‡]	Isolate[§]	Allele	Mutation	Effect	Doubling time (h)[¶]
Glucose	Yes	1-3	*tyrB948p*	NC_003197.2:g.4469253C>T	Increased TyrB activity ~4.4-fold	1.15 ± 0.02
		4, 5	*tyrB949p*	NC_003197.2:g.4469278T>A	Increased TyrB activity ~1.6-fold	1.17 ± 0.01
		6-8	*tyrB950p*	NC_003197.2:g.4469270C>T	Increased TyrB activity ~1.5-fold	1.44 ± 0.10
		9	ND[*]			2.20 ± 0.14
		10	*tyrB951p*	NC_003197.2:g.4469253C>A	ND	1.68 ± 0.02
Gluconate		11				
		12-17	*tyrB955*	NC_003197.2:g.4469319G>A	GTG→ATG start codon	1.80 ± 0.04
		18	*tyrB952p*	NC_003197.2:g.4469274T>G	ND	1.41 ± 0.02
		19	*tyrB953p*	NC_003197.2:g.4469245C>A		1.52 ± 0.04
		20	*tyrB954p*	NC_003197.2:g.4469303C>A		1.91 ± 0.11
	No	21	*tyrR956*	NC_003197.2:g.1776982del	Frameshift at Tyr245	2.72 ± 0.39
		22	*tyrR957*	NC_003197.2:g.1776917C>T	Pro267→Ser267	3.18 ± 0.27
		23	*nadR1101*	Tn*10*(d)Cm insertion	Loss of function	5.41 ± 0.38
		24	ND			2.64 ± 0.14
		25				5.57 ± 0.20
		26				3.45 ± 0.60

[†]Independent overnight cultures of *yggS aspC* strain (DM16154) were washed with 0.85% NaCl and 100 µl aliquot from each washed culture was plated on minimal NCE medium supplemented with glucose or gluconate as indicated in text. After 2-day incubation at 37ºC, spontaneous revertants were isolated and phenotypically confirmed before downstream analysis.

[‡]A mutation was genetically linked to *tyrB* if it was cotransducible with *tyrB* by phage P22.

[§]Each independently isolated suppressor was numbered.

¶Growth was determined in minimal NCE with the carbon source that the relevant revertants were isolated on. Representative growth from three biological replicates of one isolate for each mutation is shown.

*ND: not determined.

Table 5.S3 – Strains and plasmids used in this study.

Strain/plasmid	Description	Source
***S. enterica* LT2**		
DM15847	Wild type	(9)
DM15948	*yggS651*	(9)
DM15987	*avtA11*::*Cm*	This study
DM15988	*yggS651 avtA11*::*Cm*	This study
DM16150	*aspC789*::*Km*	(47)
DM16154	*yggS651 aspC789*::*Km*	This study
DM16356	*ilvE3220*::*Km*	This study
DM16357	*yggS651 ilvE3220*::*Km*	This study
DM16676	*tyrB947*::*Cm*	This study
DM16677	*yggS651 tyrB947*::*Cm*	This study
DM16678	*aspC789*::*Km tyrB947*::*Cm*	This study
DM16679	*yggS651 aspC789*::*Km tyrB947*::*Cm*	This study
DM17334	*yggS651 aspC789*::*Km tyrB948p* (NC_003197.2:g.4469253C>T)	This study
DM17335	*yggS651 aspC789*::*Km tyrB949p* (NC_003197.2:g.4469278T>A)	This study
DM17336	*yggS651 aspC789*::*Km tyrB950p* (NC_003197.2:g.4469270C>T)	This study
DM17337	*yggS651 aspC789*::*Km tyrB951p* (NC_003197.2:g.4469253C>A)	This study
DM17338	*yggS651 aspC789*::*Km tyrB952p* (NC_003197.2:g.4469274T>G)	This study
DM17339	*yggS651 aspC789*::*Km tyrB953p* (NC_003197.2:g.4469245C>A)	This study
DM17340	*yggS651 aspC789*::*Km tyrB954p* (NC_003197.2:g.4469303C>A)	This study
DM17341	*yggS651 aspC789*::*Km tyrB955* (NC_003197.2:g.4469319G>A)	This study
DM17343	*yggS651 aspC789*::*Km tyrR956* (NC_003197.2:g.1776982del)	This study
DM17344	*yggS651 aspC789*::*Km tyrR957* (NC_003197.2:g.1776917C>T)	This study
DM17345	*yggS651 aspC789*::*Km* revertant (isolate #24)	This study
DM17346	*yggS651 aspC789*::*Km* revertant (isolate #25)	This study
DM17347	*yggS651 aspC789*::*Km* revertant (isolate #26)	This study
DM17348	*yggS651 aspC789*::*Km* revertant (isolate #9)	This study
DM16618	*yggS651 aspC789*::*Km nadR1101*::Tn*10*(d)Cm	This study
DM16265	*yggS651 aspC789*::*Km* / pCV1	This study
DM16266	*yggS651 aspC789*::*Km* / pDM1575	This study
DM16267	*yggS651 aspC789*::*Km* / pDM1576	This study
DM16470	*yggS651 aspC789*::*Km* / pDM1583	This study
Plasmid		
pCV1	Modified pBAD24 (Am^R)	(43)
pDM1440	pET28b(+).SapKO-CH.BspQI expressing AspC-5xHis (Km^R)	This study
pDM1441	pET28b(+).SapKO-CH.BspQI expressing TyrB-5xHis (Km^R)	This study
pDM1575	pCV1 expressing AspC (Am^R)	This study
pDM1576	pCV1 expressing TyrB (Am^R)	This study
pDM1583	pCV1 expressing YggS (Am^R)	This study

Table 5.S4 – Primers used in this study.

Primer	Sequence (5' to 3')	Description
PR89	NNGCTCTTCNATGTTTGAGAACATAACCG	Construction of pDM1440
PR90	NNGCTCTTCNGTGCAGTACCGCGACA	
PR91	NNGCTCTTCNATGTTTCAAAAAGTTGAC	Construction of pDM1441
PR92	NNGCTCTTCNGTGCATGACAGCGGC	
PR1103	NNGCTCTTCNTTCATGTTTGAGAACATAACCGCC	Construction of pDM1575
PR1104	NNGCTCTTCNTTACAGTACCGCGACAATGG	
PR1105	NNGCTCTTCNTTCGTGTTTCAAAAAGTTGACGCC	Construction of pDM1576
PR1106	NNGCTCTTCNTTACATGACAGCGGCAAATG	
PR1158	NNGCTCTTCNTTCATGAACGATATCGCGCATAACC	Construction of pDM1583
PR1159	NNGCTCTTCNTTAATTTTTTGTGTAATCACGAGCACCA	
PR1114	GGTTATCCACTTTGACAGACAGTTCGATAGATCACCCGTTGTGTAGGCTGGAGCTGCTTC	Inactivation of *avtA*
PR1115	CTGAACGTCGTTCCGGCCTGCATGATGGCCGGAATAACCGCATATGAATATCCTCCTTAG	
PR1209	GTGTTATTTCCTGCCCTCTGTAAACCTGGAGAACCATCGCGTGTAGGCTGGAGCTGCTTC	Inactivation of *tyrB*
PR1210	TCAGGCCGGAGGGCACTGTTATCGCCGTCCGGCCTGAATACATATGAATATCCTCCTTAG	
TR_Cm	GGTGCGTAACGGCAAAAGCAC	Transposon sequencing (41)
TL_Cm	CCAGAGCCTGATAAAAACGGTTAC	
Tn10I	GACAAGATGTGTATCCACCTTAAC	
Arb1	GGCCACGCGTCGACTAGTACNNNNNNNNNNGATAT	
Arb6	GGCCACGCGTCGACTAGTACNNNNNNNNNNACGCC	

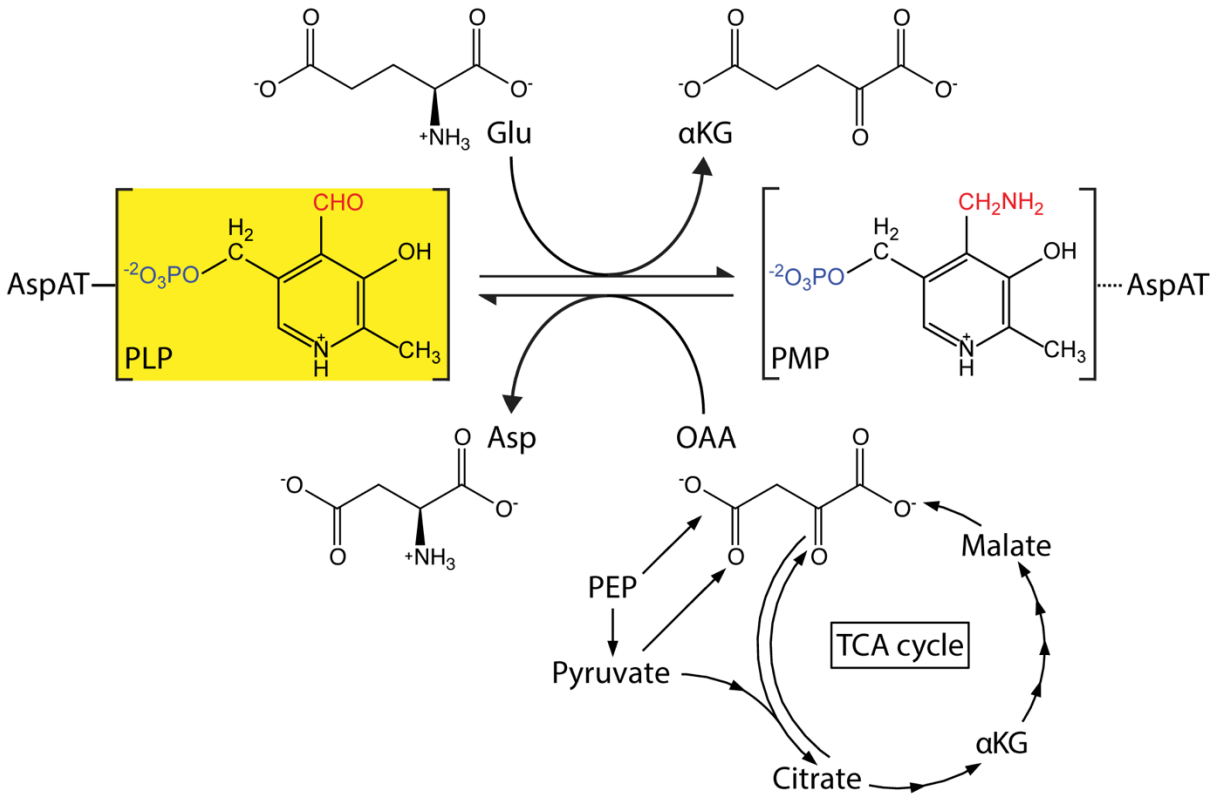

Figure 5.1 – Aspartate synthesis in *S. enterica* relies on PLP-dependent transamination reaction. In the first half-reaction of transamination, glutamate donates an amino group to PLP, generating α-ketoglutarate and PMP. In the second half-reaction, PMP is recycled back to PLP, transferring the amino group to oxaloacetate and producing aspartate. PLP is bound to the active site via a Schiff base linkage, while PMP is not covalently bound to the enzyme (indicated by a solid and dashed line, respectively). Oxaloacetate is synthesized from intermediates in glycolysis (PEP, pyruvate) or the TCA cycle (malate, citrate), as depicted. Abbreviations: AspAT, aspartate aminotransferase; PLP, pyridoxal 5′-phosphate; PMP, pyridoxamine 5′-phosphate; Glu, L-glutamate; αKG, α-ketoglutarate; Asp, L-aspartate; OAA, oxaloacetate; PEP, phosphoenolpyruvate; TCA, tricarboxylic acid.

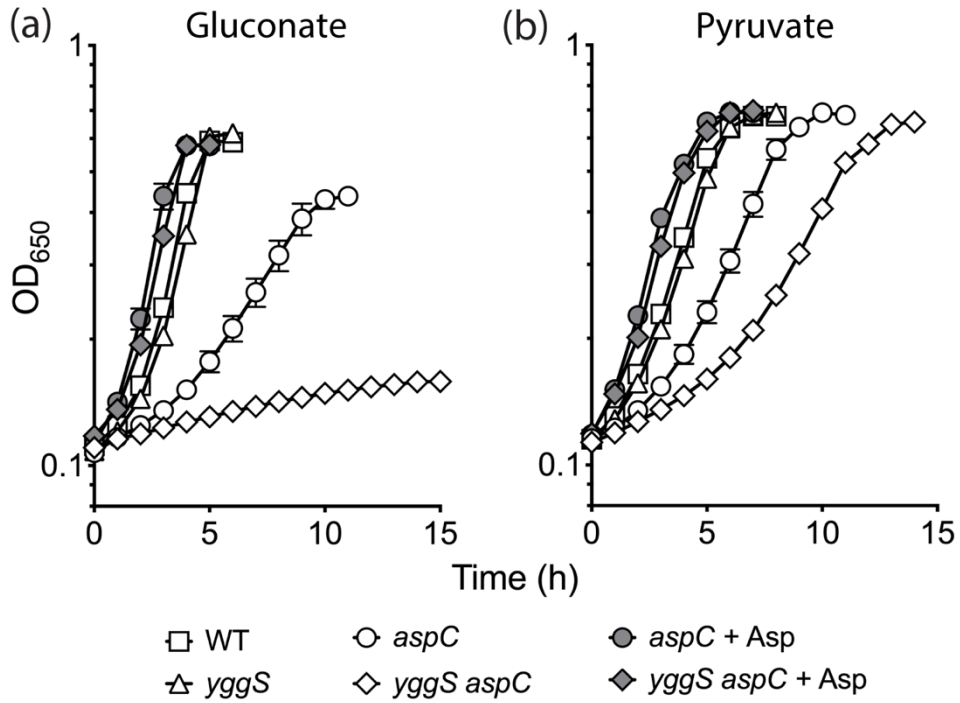

Figure 5.2 – Loss of *yggS* leads to aspartate limitation in an *aspC* background. *S. enterica* wild-type (DM15847, squares), *yggS* (DM15948, triangles), *aspC* (DM16150; circles), and *yggS aspC* (DM16154; diamonds) strains were grown in minimal NCE with (a) gluconate or (b) pyruvate as a sole carbon source in the absence (white symbols) or presence (gray symbols) of 1.8 mM aspartate. Representative data from three independent experiments, each with three biological replicates, are shown. Error bars depict standard deviation from the mean.

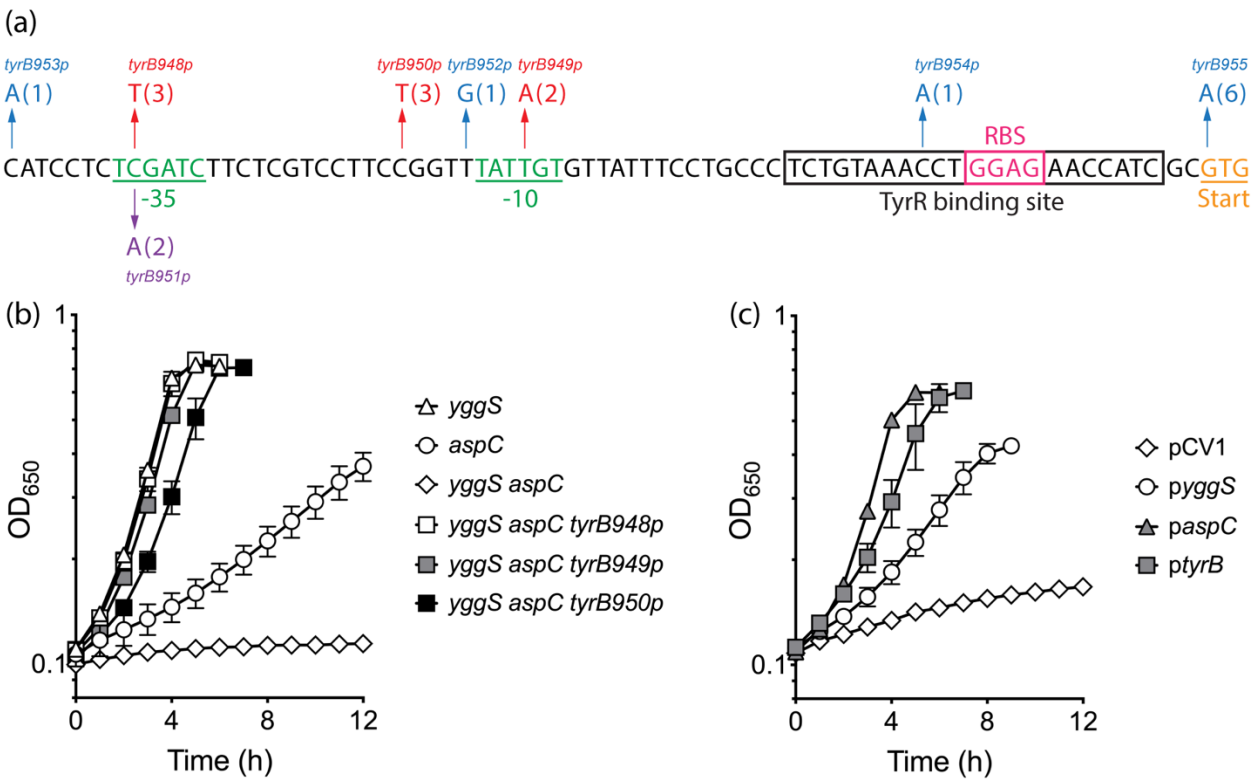

Figure 5.3 – Suppressors of aspartate requirement in a *yggS aspC* strain increase TyrB level.

(a) DNA sequence of the regulatory region of *tyrB*, including the -35 and -10 element of the promoter (green), the binding site of the transcriptional regulator TyrR (black box), the ribosomal binding site (pink box), and the start codon of *tyrB* (orange), is shown. Suppressor mutations linked to *tyrB* were isolated on minimal NCE glucose (red) or gluconate (blue). The allele in purple was isolated independently on glucose and on gluconate. The number of independent isolates of each substitution is indicated in parentheses. (b) Growth of representative *yggS aspC* revertants in minimal NCE glucose is depicted. (c) *yggS aspC* strains carrying empty vector control (pCV1, DM16265), vector expressing *yggS* (p*yggS*, DM16470), *aspC* (p*aspC*, DM16266), or *tyrB* (p*tyrB*, DM16267) were grown in minimal NCE gluconate without (white symbols) or with 0.02% arabinose (gray symbols) to induce expression of the respective gene. Data were obtained from

three biological replicates from two independent experiments, and error bars show standard deviation from the mean.

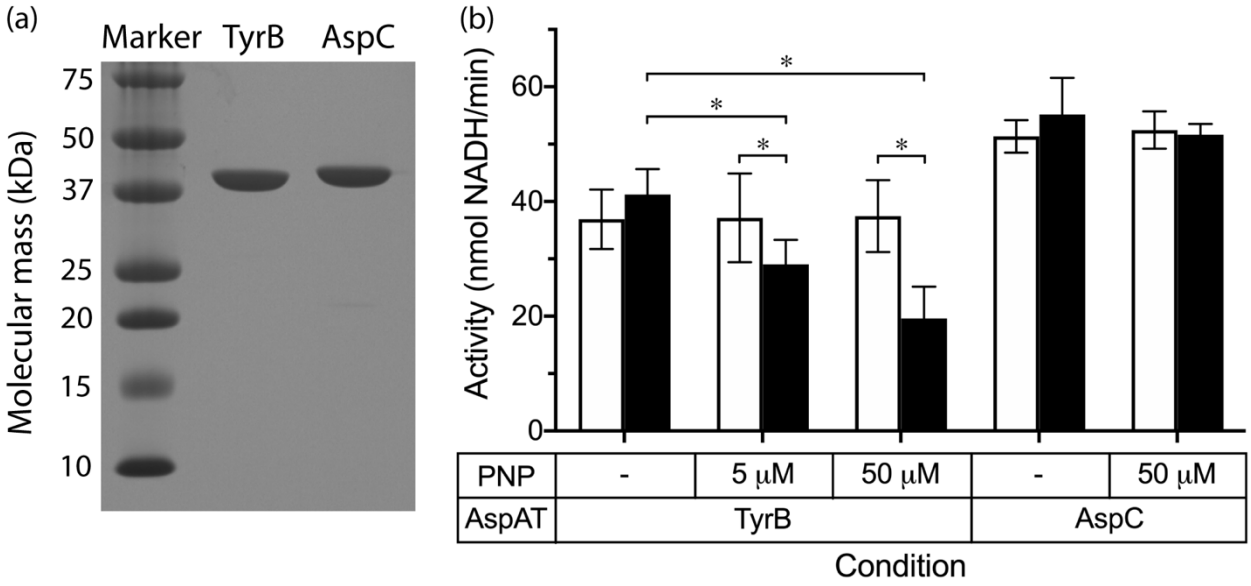

Figure 5.4 – PNP inhibits AspAT activity of TyrB *in vitro.* (a) After Ni-affinity purification, 2 μg of TyrB-5xHis and AspC-5xHis were separated on 14% SDS-PAGE gel and visualized with Coomassie blue staining. (b) AspAT activity was measured by a coupled assay as the rate of NADH oxidation when oxaloacetate (produced from aspartate and αKG by AspAT) was converted to malate. Assays were performed with (solid bars) or without (open bars) a 10-minute preincubation with PNP prior to initiating the reaction with αKG. Reaction mixtures contained 50 mM HEPES (pH 7.8), 25 nM TyrB or AspC, 100 mM Asp, 0.4 mM NADH, 5U malate dehydrogenase, 5 mM αKG, 2.5 μM PLP, and 0-50 μM PNP. Data were averaged from two independent experiments with at least three technical replicates each. Statistical significance was determined by One-way ANOVA followed by Bonferroni *post hoc* test for each AspAT. An asterisk indicates adjusted $P < 0.0001$. Abbreviations: AspAT, aspartate aminotransferase; PNP, pyridoxine 5′-phosphate.

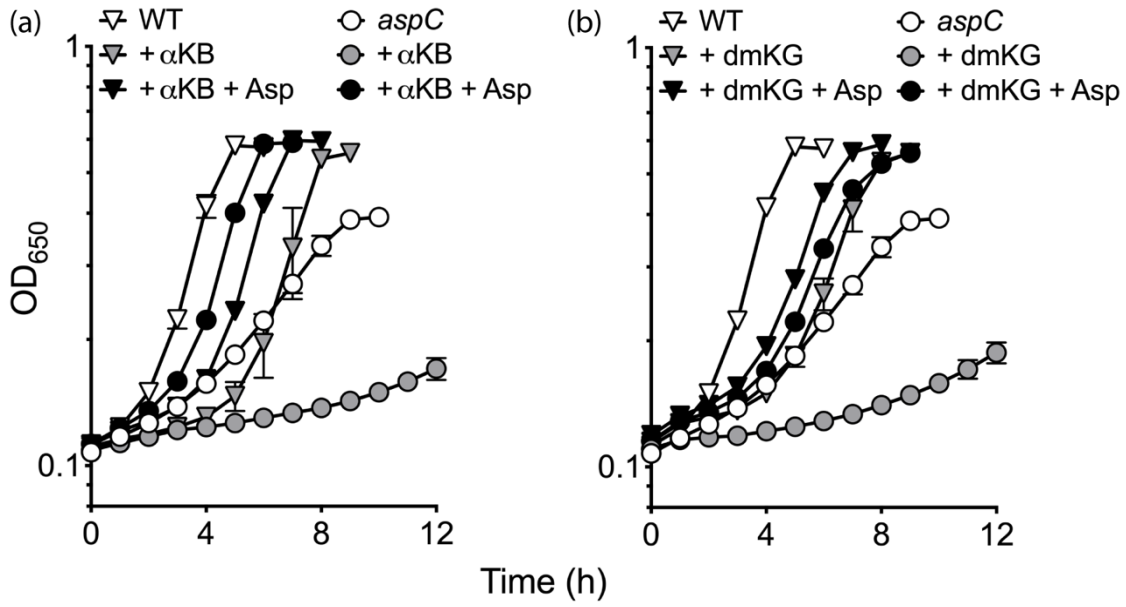

Figure 5.5 – Exogenous α-keto acids phenocopy a *yggS* mutation. Growth of wild type (DM15847) and *aspC* mutant (DM16154) in minimal NCE gluconate in the presence of (a) 1mM αKB or (b) 10 mM dmKG is shown. Addition of 1.8 mM aspartate restored growth of both strains. Average optical density at 650 nm (OD_{650}) and standard deviation of three biological replicates from two independent experiments are shown. Abbreviations: αKB, α-ketobutyrate; dmKG, dimethyl α-ketoglutarate; Asp, L-aspartate.

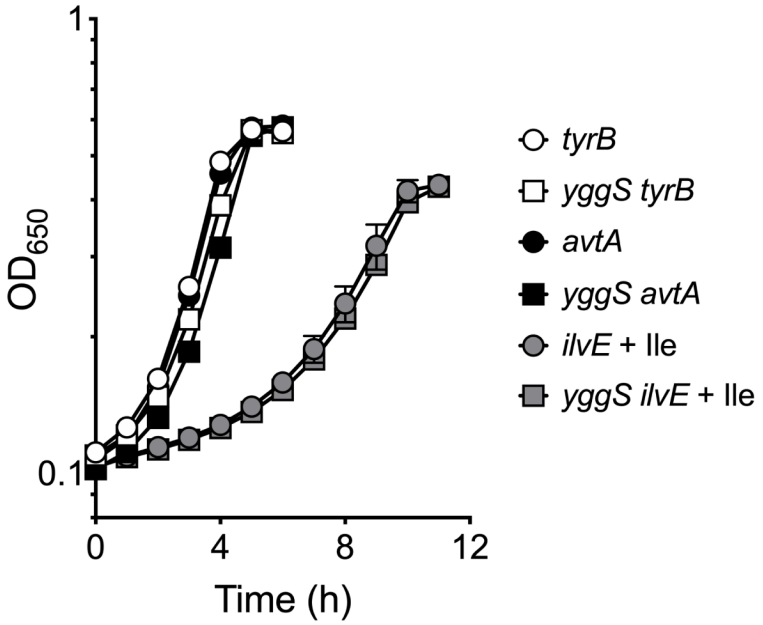

Figure 5.S1 – A mutation in *yggS* does not cause a synthetic phenotype in strains lacking other PLP-dependent aminotransferases. Growth of $yggS^+$ (circles) and $yggS^-$ (squares) strains were assessed in minimal NCE gluconate without or with 0.3 mM isoleucine (Ile). Data were obtained from three biological replicates from two independent experiments, and error bars show standard deviation from the mean.

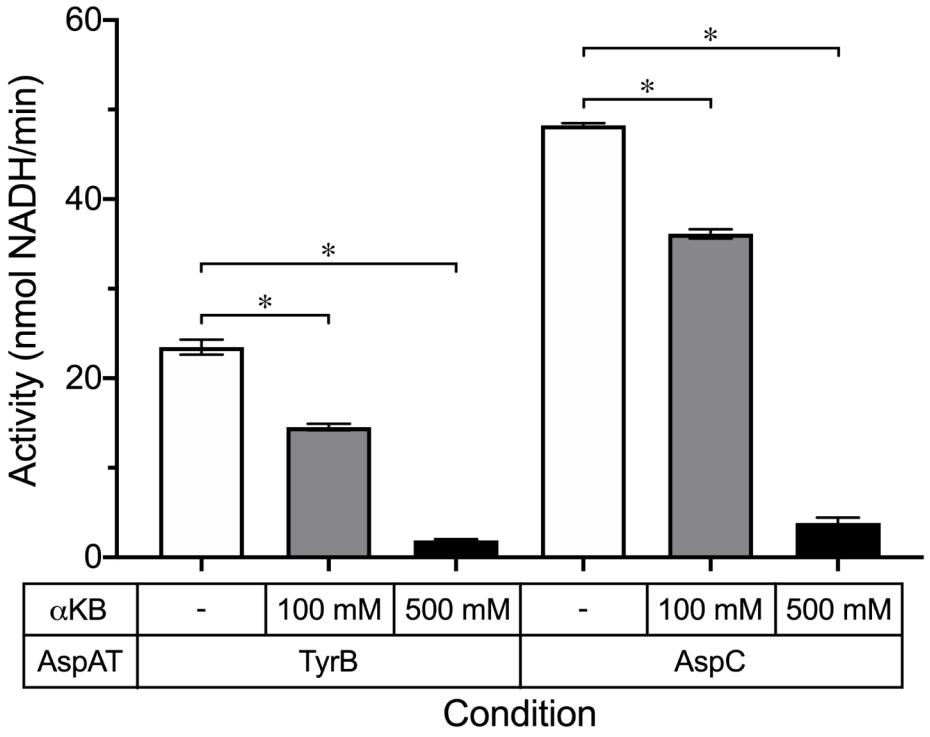

Figure 5.S2 – αKB at high concentrations inhibits AspAT activity *in vitro.* AspAT activity was determined by a coupled assay as described in Experimental Procedures. Assays were performed without (white bars) or with addition of 100 mM (gray bars) or 500 mM αKB (black bars). Reaction mixtures contained 50 mM HEPES (pH 7.8), 25 nM TyrB or AspC, 100 mM Asp, 0.4 mM NADH, 5U malate dehydrogenase, 1 mM αKG, 2.5 μM PLP, and 0-500 mM αKB. Representative data from two independent experiments with at least three technical replicates each are shown. Statistical significance was determined by One-way ANOVA followed by Dunnett's *post hoc* test for each AspAT. An asterisk indicates adjusted $P < 0.0001$. Abbreviations: AspAT, aspartate aminotransferase; αKB, α-ketobutyrate.

CHAPTER 6

CONCLUSIONS AND FUTURE DIRECTIONS

6.1 CONCLUSIONS

Enzyme promiscuity contributes to the robustness of vitamin B_6 metabolism. Chapter 2 identifies a moonlighting activity of the periplasmic acid phosphatase PhoN in the salvage of phosphorylated B_6 vitamers. Previously, the physiological role of PhoN in *S. enterica* was not established, despite available genetic and biochemical data. The absence of this enzyme in *E. coli*, a close relative of *S. enterica*, suggests that each species may refine and/or rewire components in a conserved pathway to suit its specific ecological niche. In addition, phenotypic analyses of mutants defective in *de novo* synthesis and salvage of PLP demonstrate the importance of enzyme promiscuity in contributing to robust metabolism of vitamin B_6 and organismal fitness.

Perturbations in vitamin B_6 metabolism have far-reaching consequences. Chapter 3 establishes a connection between vitamin B_6 metabolism and the synthesis of thiamine (vitamin B_1) and coenzyme A using dPN as a vitamin B_6 antagonist. Phenotypic and metabolite analyses show that dPN toxicity is dependent on phosphorylation to dPNP by PdxK. Results from nutritional supplementation using various genetic backgrounds suggest that dPNP targets the DXP-dependent PLP biosynthesis and PLP-dependent enzymes in the generation of one-carbon units, the latter of which leads to reduced flux to CoA and ThiC-dependent thiamine synthesis.

This work highlights the complexity and interconnection of metabolic networks in microbial physiology.

YggS affects homeostasis of B_6 vitamers. Chapter 4 and 5 examine the phenotypic and metabolic consequences of a *yggS* mutation, which was previously identified by our laboratory as a suppressor that allowed yeast Thi5p to function in an *S. enterica* thiamine auxotroph (1). Studies of YggS in different organisms suggested a role of this PLP-binding protein in vitamin B_6 homeostasis, though a precise mechanism has not been defined. My work shows that lack of YggS in *S. enterica* and *E. coli* leads to changes in intra- and extracellular pools of phosphorylated B_6 vitamers, which potentially is the cause of further downstream effects (Figure 6.1). In particular, accumulation of PNP and perturbations of α-keto acids are proposed to inhibit TyrB-dependent aspartate synthesis in an *S. enterica* strain lacking both *aspC* and *yggS*. When PNP accumulation in various *yggS* mutants is eliminated using a heterologous expression system for PLP synthesis, an epistatic role between YggS and PdxH in regulating PLP and PMP levels is uncovered, based on which a general model for YggS function is proposed. The work described in these two chapters serves as a foundation for future studies to elucidate the molecular mechanism of how YggS contributes to vitamin B_6 homeostasis.

6.2 FUTURE DIRECTIONS

Define the molecular mechanism of vitamin B_6 uptake. Although transporters for B_6 vitamers have been identified in a subset of bacteria, yeast, and plants (2-7), it is currently unclear if a homologous system is present in *S. enterica*. Work described in Chapter 3 opens the potential to

address this question using dPN resistance as a selection. If a B_6 transport system exists, mutations that prevent uptake of dPN, and presumably B_6 vitamers, are expected to be identified.

Spontaneous revertants of *S. enterica ptsJ* were independently isolated on minimal NCE media supplemented with 1-10 μM dPN and phenotypically confirmed. Growth and sequence analyses classify these suppressors into two categories. Twelve isolates carry mutations in *pdxK* and four with mutations elsewhere in the genome (Table 6.1). Based on the proposed mechanism of dPN toxicity (see Chapter 3), mutations in PdxK are predicted to decrease the activity and/or specificity of this enzyme toward dPN substrate, leading to a reduction in accumulated dPNP. To confirm this hypothesis, wild-type PdxK-6xHis and the V197G variant will be purified and their kinetic parameters with dPN and B_6 substrates determined *in vitro*. Interestingly, no mutation in *pdxK* was identified in the remaining four revertants (DM17449-DM17452) with Sanger sequencing method, suggesting at least another mechanism, rather than preventing dPN→dPNP conversion, exists to alleviate dPN toxicity. Thus, whole genome sequencing using Nanopore platform will be employed to identify potential mutations that may contribute to dPN resistance. To confirm which mutation(s) is causative, each will be reconstructed in the parental *ptsJ* background and growth with dPN will be assessed. Depending on the nature of the causative mutation, further approaches will be proposed to investigate the mechanism of dPN resistance.

How is PLP incorporated into apo-enzymes? Little is known about the fate of PLP molecules *in vivo* after *de novo* synthesis and salvage. PLP-dependent enzymes need to incorporate this cofactor into their tertiary structures for catalysis. Whether the incorporation of PLP occurs during or after protein folding, with or without the help of a chaperone(s), remains a topic of ongoing research. *In vitro* assays using purified PLP-dependent enzymes from different organisms showed

that apo-enzymes could be reactivated by addition of excess PLP, suggesting that PLP can access the active site of these folded enzymes in the absence of a chaperone under the conditions tested (8-11). Interestingly, when the experiment was done in crude extract to mimic the *in vivo* environment, the rate of reactivation significantly decreased compared to that in assay buffer (12), highlighting the need to reconcile results observed *in vitro* and their physiological relevance.

Preliminary data from my work with dPN hint at a potential role of the ClpXAP chaperone system in PLP incorporation and/or turnover. A *clpP* mutation prevented growth of an *S. enterica ptsJ* mutant at low dPN concentration, while the parental *ptsJ* and *clpP* single mutant showed mild and no growth defect, respectively (Figure 6.2). Minor growth delay associated with *ptsJ clpX* and *ptsJ clpA* strains in the presence of dPN was also detected (data not shown). ClpX was previously shown to accelerate the insertion of PLP to yeast apo-Hem1p (5-aminolevulinic acid synthase, EC 2.3.1.37) *in vitro* (13). In addition, protein trapping identified PLP-dependent enzymes such as GlyA (serine hydroxymethyltransferase, EC 2.1.2.1), IscS (cysteine desulfurase, EC 2.8.1.7), and TnaA (tryptophanase, EC 4.1.99.1) as targets for a $ClpXP^{trap}$ variant (14). Interestingly, GlyA is one of the two PLP-dependent enzymes proposed to be affected by dPNP accumulation (see Chapter 3). At this point, it is unclear if the ClpXAP system plays a direct or indirect role in alleviating dPN sensitivity. Protein trapping experiment with $ClpXP^{trap}$ variant described by Flynn *et al.* (14) can be performed using *ptsJ* strains grown in minimal NCE glucose without or with dPN supplementation. Comparing the proteomes identified by the $ClpXP^{trap}$ system between two conditions may reveal an enrichment for additional target enzymes associated with dPN toxicity.

Elucidate *in vivo* function of YggS. YggS is a conserved PLP-binding protein of unknown function implicated in vitamin B_6 homeostasis. Defining the molecular mechanism of YggS

function is crucial in understanding how levels of B_6 vitamers are regulated in the cells. Depending on purification method, YggS homologs and their variants from different organisms were reported to have monomeric or dimeric conformation (15-18). Determining which oligomeric state is physiologically relevant is an important step toward functional and biochemical characterization of this protein. To pursue this objective, rabbit polyclonal antibodies against purified *S. enterica* YggS were obtained according to manufacturer's protocol (Envigo, Indianapolis, IN). Western blot confirmed specific binding of the antibodies to purified YggS protein under denaturing condition (data not shown). To determine if *S. enterica* YggS exists as a monomer or dimer *in vivo*, Western blot will be performed using crude cell extracts from *yggS*$^+$ and *yggS*$^-$ strains run on native gels. Once confirmed, different purification schemes will be considered to purify YggS with the correct oligomeric state. Binding of potential substrates (B_6 vitamers, amino acids, α-keto acids, etc.) to YggS will be screened by monitoring the visible spectra of this protein. Compounds with detected spectral changes will be confirmed with isothermal titration calorimetry.

Analysis of variants is a useful approach to dissect the mechanism of enzyme catalysis. Many variants of YggS homologs have been isolated and their effects on physiology and protein properties reported (Figure 6.3 and Table 6.2). As knowledge on YggS activity is established, characterization of existing variants will be informative in understanding active site structure, cofactor/substrate binding, conformational changes, and so on. To expand the repertoire of YggS variants, genetic screens and/or selections can be used to isolate mutations in *yggS* with desired phenotypes in various backgrounds, such as *S. enterica thiC* p*THI5* (DM15176) and *yggS aspC* mutant (DM16154). Alternatively, site-directed mutagenesis can be employed to obtain more targeted mutations.

Phenotypic analysis is another powerful approach to probe the connection between YggS and other metabolic nodes. *S. enterica* strains lacking YggS showed no significant growth defect, unless additional mutations were introduced (19, 20). Many synthetic phenotypes observed in a *yggS* mutant are proposed to be downstream effects of accumulated PNP (Figure 6.1), thus employing a *yggS* background devoid of this vitamer, such as *S. enterica pdxJ yggS* p*SNZ3* (DM16712) and *B. subtilis ylmE* (DM16785), may prove informative. Using these PNP-free strains, transposon mutagenesis or TnSeq approach are proposed to identify mutations that reduce fitness of a *yggS* mutant but not a wild-type strain. Understanding how synthetic phenotypes are caused by these mutations in a *yggS* background may aid in elucidating the function of YggS.

Notably, whether YggS has a direct or indirect role in modulating PLP→PMP cycling (Figure 6.1) has not been determined. While the hypothesis that YggS catalyzes a PLP-dependent biochemical reaction is currently favored, it is formally possible that this protein simply acts as a carrier protein to quench excess free PLP. In this scenario, loss of YggS also leads to increased PLP levels, consistent with the proposed model on YggS function (Figure 6.1). Therefore, knowledge of the cellular amount of YggS, which can be determined using quantitative Western blot, will be helpful in assessing this model. The stoichiometry of YggS molecules per cell would be roughly in agreement with the amount of PLP that a *yggS* mutant excretes. In addition, expression of another PLP carrier protein would be able to compensate for loss of YggS. In *Saccharomyces cerevisiae*, Mtm1p has been proposed to bind and deliver PLP to the mitochondria (21). Mtm1p and YggS bind to PLP with approximately similar affinity (Mtm1p, K_D = 2-47 μM; YggS, K_D = 0.4-30 μM) (16, 17, 21), making the former a potential candidate to replace YggS. If *in trans* expression of yeast *MTM1* in strains lacking *yggS* can complement phenotypes associated

with a *yggS* mutation, this result will lend support for the hypothesis that YggS is a PLP carrier protein.

6.3 REFERENCES

1. Paxhia MD, Downs DM. 2021. Pyridoxal and α-ketoglutarate independently improve function of *Saccharomyces cerevisiae* Thi5 in the metabolic network of *Salmonella enterica*. Journal of Bacteriology. https://doi.org/10.1128/JB.00450-21.

2. Wang T, De Jesus AJ, Shi Y, Yin H. 2015. Pyridoxamine is a substrate of the energy-coupling factor transporter HmpT. Cell Discovery. 1:1-10.

3. Pan C, Zimmer A, Shah M, Huynh MS, Lai CC-L, Sit B, Hooda Y, Curran DM, Moraes TF. 2021. *Actinobacillus* utilizes a binding protein–dependent ABC transporter to acquire the active form of vitamin B_6. Journal of Biological Chemistry. https://doi.org/10.1016/j.jbc.2021.101046.

4. Stolz Jr, Vielreicher M. 2003. Tpn1p, the plasma membrane vitamin B_6 transporter of *Saccharomyces cerevisiae*. Journal of Biological Chemistry. 278:18990-18996.

5. Stolz Jr, Wöhrmann HJ, Vogl C. 2005. Amiloride uptake and toxicity in fission yeast are caused by the pyridoxine transporter encoded by *bsu1*$^+$ (*car1*$^+$). Eukaryotic Cell. 4:319-326.

6. Szydlowski N, Bürkle L, Pourcel L, Moulin M, Stolz J, Fitzpatrick TB. 2013. Recycling of pyridoxine (vitamin B_6) by PUP1 in *Arabidopsis*. The Plant Journal. 75:40-52.

7. Kato K, Shitan N, Shoji T, Hashimoto T. 2015. Tobacco NUP1 transports both tobacco alkaloids and vitamin B_6. Phytochemistry. 113:33-40.

8. Meister A, Sober HA, Peterson EA. 1954. Studies on the coenzyme activation of glutamic-aspartic apotransaminase. Journal of Biological Chemistry 206:89-100.

9. Mechanik M, Torchinsky YM, Florentiev V, Karpeisky MY. 1971. Interaction of the apoenzyme of L-glutamate decarboxylase with pyridoxal phosphate analogues. FEBS Letters. 13:177-18.

10. Oikonomakos N, Johnson L, Acharya K, Stuart D, Barford D, Hajdu J, Varvill K, Melpidou A, Papageorgiou T. 1987. Pyridoxal phosphate site in glycogen phosphorylase b: structure in native enzyme and in three derivatives with modified cofactors. Biochemistry. 26:8381-8389.

11. Brahatheeswaran B, Prakash V, Savithri HS, Rao NA. 1996. Interaction of sheep liver apo-serine hydroxymethyltransferase with pyridoxal-5′-phosphate: a physicochemical, kinetic, and thermodynamic study. Archives of Biochemistry and Biophysics. 330:363-372.

12. Yang ES, Schirch V. 2000. Tight binding of pyridoxal 5′-phosphate to recombinant *Escherichia coli* pyridoxine 5′-phosphate oxidase. Archives of Biochemistry and Biophysics. 377:109-114.

13. Kardon JR, Yien YY, Huston NC, Branco DS, Hildick-Smith GJ, Rhee KY, Paw BH, Baker TA. 2015. Mitochondrial ClpX activates a key enzyme for heme biosynthesis and erythropoiesis. Cell. 161:858-867.

14. Flynn JM, Neher SB, Kim Y-I, Sauer RT, Baker TA. 2003. Proteomic discovery of cellular substrates of the ClpXP protease reveals five classes of ClpX-recognition signals. Molecular Cell. 11:671-683.

15. Ito T, Iimori J, Takayama S, Moriyama A, Yamauchi A, Hemmi H, Yoshimura T. 2013. Conserved pyridoxal protein that regulates Ile and Val metabolism. Journal of Bacteriology. 195:5439-5449.

16. Prunetti L, El Yacoubi B, Schiavon CR, Kirkpatrick E, Huang L, Bailly M, El Badawi-Sidhu M, Harrison K, Gregory 3rd JF, Fiehn O. 2016. Evidence that COG0325 proteins are involved in PLP homeostasis. Microbiology. 162:694-706.

17. Tremiño L, Forcada-Nadal A, Contreras A, Rubio V. 2017. Studies on cyanobacterial protein PipY shed light on structure, potential functions, and vitamin B_6-dependent epilepsy. FEBS Letters. 591:3431-3442.

18. Fux A, Sieber SA. 2019. Biochemical and proteomic studies of human pyridoxal 5′-phosphate-binding Protein (PLPBP). ACS Chemical Biology. 15:254-261.

19. Ito T, Hori R, Hemmi H, Downs DM, Yoshimura T. 2020. Inhibition of glycine cleavage system by pyridoxine 5′-phosphate causes synthetic lethality in *glyA yggS* and *serA yggS* in *Escherichia coli*. Molecular Microbiology. 113:270-284.

20. Vu HN, Downs DM. 2021. Loss of YggS (COG0325) impacts aspartate metabolism in *Salmonella enterica*. Molecular Microbiology. https://doi.org/10.1111/mmi.14810.

21. Whittaker MM, Penmatsa A, Whittaker JW. 2015. The Mtm1p carrier and pyridoxal 5′-phosphate cofactor trafficking in yeast mitochondria. Archives of Biochemistry and Biophysics. 568:64-70.

22. Darin N, Reid E, Prunetti L, Samuelsson L, Husain RA, Wilson M, El Yacoubi B, Footitt E, Chong WK, Wilson LC. 2016. Mutations in *PROSC* disrupt cellular pyridoxal phosphate homeostasis and cause vitamin-B_6-dependent epilepsy. The American Journal of Human Genetics. 99:1325-1337.

23. Tremiño L, Forcada-Nadal A, Rubio V. 2018. Insight into vitamin B_6-dependent epilepsy due to *PLPBP* (previously *PROSC*) missense mutations. Human Mutation. 39:1002-1013.

24. Shiraku H, Nakashima M, Takeshita S, Khoo CS, Haniffa M, Ch'ng GS, Takada K, Nakajima K, Ohta M, Okanishi T. 2018. *PLPBP* mutations cause variable phenotypes of developmental and epileptic encephalopathy. Epilepsia Open. 3:495-502.

25. Johnstone DL, Al-Shekaili HH, Tarailo-Graovac M, Wolf NI, Ivy AS, Demarest S, Roussel Y, Ciapaite J, van Roermund CW, Kernohan KD. 2019. PLPHP deficiency: clinical, genetic, biochemical, and mechanistic insights. Brain. 142:542-559.

26. Jiao X, Xue J, Gong P, Wu Y, Zhang Y, Jiang Y, Yang Z. 2020. Clinical and genetic features in pyridoxine-dependent epilepsy: a Chinese cohort study. Developmental Medicine and Child Neurology. 62:315-321.

27. Plecko B, Zweier M, Begemann A, Mathis D, Schmitt B, Striano P, Baethmann M, Vari MS, Beccaria F, Zara F. 2017. Confirmation of mutations in *PROSC* as a novel cause of vitamin B_6-dependent epilepsy. Journal of Medical Genetics. 54:809-814.

28. Jensen KV, Frid M, Stödberg T, Barbaro M, Wedell A, Christensen M, Bak M, Ek J, Madsen CG, Darin N. 2019. Diagnostic pitfalls in vitamin B_6-dependent epilepsy caused by mutations in the *PLPBP* gene. JIMD Reports. 50:1-8.

29. Vu HN, Ito T, Downs DM. 2020. The role of YggS in vitamin B_6 homeostasis in *Salmonella enterica* is informed by heterologous expression of yeast *SNZ3*. Journal of Bacteriology. 202:e00383-20.

30. Zhao G, Winkler ME. 1995. Kinetic limitation and cellular amount of pyridoxine (pyridoxamine) 5′-phosphate oxidase of *Escherichia coli* K-12. Journal of Bacteriology. 177:883-891.

31. Barile A, Tramonti A, di Salvo ML, Nogués I, Nardella C, Malatesta F, Contestabile R. 2019. Allosteric feedback inhibition of pyridoxine 5′-phosphate oxidase from *Escherichia coli*. Journal of Biological Chemistry. 294:15593-15603.

32. Ito T, Yamamoto K, Hori R, Yamauchi A, Downs DM, Hemmi H, Yoshimura T. 2019. Conserved pyridoxal 5′-phosphate-binding protein YggS impacts amino acid metabolism through pyridoxine 5′-phosphate in *Escherichia coli*. Applied and Environmental Microbiology. 85:e00430-19.

33. Barak Ze, Chipman DM. 2012. Allosteric regulation in acetohydroxyacid synthases (AHASs)–different structures and kinetic behavior in isozymes in the same organisms. Archives of Biochemistry and Biophysics. 519:167-174.

34. Primerano DA, Burns R. 1982. Metabolic basis for the isoleucine, pantothenate or methionine requirement of *ilvG* strains of *Salmonella typhimurium*. Journal of Bacteriology. 150:1202-1211.

Table 6.1 – Initial characterization of *S. enterica ptsJ* revertants resistant to dPN.

Strain	DM #	Growth*				Mutation in *pdxK*
		dPN	PL	PN	PM	
ptsJ	17239	–	ND	ND	ND	None.
ptsJ pdxK	17168	+	ND	ND	ND	Gene deletion.
ptsJ pdxJK	17299	ND	+	–	–	Gene deletion.
ptsJ revertant	17439	+	+	–	–	AlaVal insertion between Glu181-Ala182.
	17440	+	+	+	+/–	UGA → UUA.
	17441	+/–	+	+	+/–	Val197 → Gly197.
	17442	+	+	–	–	Pro131 → Gln131.
	17443	+	+	–	–	T encoding Val214 deleted → frameshift.
	17444	+	+	–	–	Pro55-Val57 deletion.
	17445	+	+	+	+/–	IleVal insertion after Gly246.
	17446	+	+	+/–	–	Asp130 → Glu130.
	17447	+/–	+	+	+/–	Ser201→Arg201.
	17448	+/–	+	+	+/–	Gly70→Cys70.
	17449	+/–	+	+	+	Unknown.
	17450	+/–	+	+	+	Unknown.
	17451	+/–	+	+	+/–	Unknown.
	17452	+/–	+	+	+	Unknown.

*Growth with dPN was determined in liquid minimal NCE glucose supplemented with 1-10 μM dPN at 37°C. A *pdxJ666*::*Cm* allele was introduced into *ptsJ* revertants and growth of the corresponding strains were assessed by spotting 5 μl of 1 mM PL, PN, and PM on soft agar overlay of minimal NCE glucose. + indicates growth; – indicates no growth, +/– indicates intermediate growth after ~20-hour incubation at 37°C. ND: not determined.

Table 6.2 – Reported YggS variants and their effects in different organisms.

Organism	Variant	Effect	Source
E. coli	K36A	Abolishes PLP binding.	(15)
S. enterica	G83D	Spontaneous mutation that allows yeast Thi5p function in *S. enterica thiC*; PLP excretion observed in bioassay.	Laboratory collection
	K137A	Site-directed mutation located on a conserved loop. Fails to rescue PN sensitivity of an *E. coli yggS* or complement growth of an *S. enterica yggS aspC* on gluconate.	
S. elongatus	P63L	No effects on protein yield, thermal stability, folding or PLP content	(17)
	R210Q	Lower protein yield; decreased thermal stability; little to no PLP bound to purified protein.	
Human	P87L	Rescues PN sensitivity in *E. coli yggS.*	(22)
		Decreased solubility; variant still binds PLP.	(23)
	R241Q	Exacerbated PN sensitivity in *E. coli yggS.*	(22)
		Decreased solubility and thermal stability, no PLP bound.	(23)
		Reduced protein yield; protein can bind PLP at high concentration and exists as monomeric and dimeric form.	(18)
	L175P	Fails to complement PN sensitivity in *E. coli yggS.*	(22)
		Purified protein misfolds.	(23)
	P40L R205Q	Decreased thermal stability; protein still binds PLP.	
	Y69C	Decreased PLP accessibility and content; dimerization observed.	
		Reduced protein yield; purified protein has slight increase in thermal stability and exists as monomeric form.	(18)
	E67K	Seizure and other symptoms.	(24)
	E67L T116I I94F H275D	Predicted to affect PLP binding.	(25)
	G224A	Disrupted loop 15 and orientation of PLP binding residues.	
	D124Ter	Protein truncation.	
	S78Ter Q71Ter	Protein truncation.	(22)
	C15Ter	Protein truncation.	(26)
	M113T	Seizure; nearly normal neurodevelopment.	
	ΔS84	Deletion of Ser84; predicted effect on barrel fold.	(27)
	R41W	Hyperglyceridemia, hyperlactatemia and other symptoms.	(28)
	R41Q	Reduced protein yield and stability.	(18)
	V45D	Reduced protein yield and thermal stability. No PLP binding observed for purified protein, which can be reconstituted at high concentration; monomeric form.	

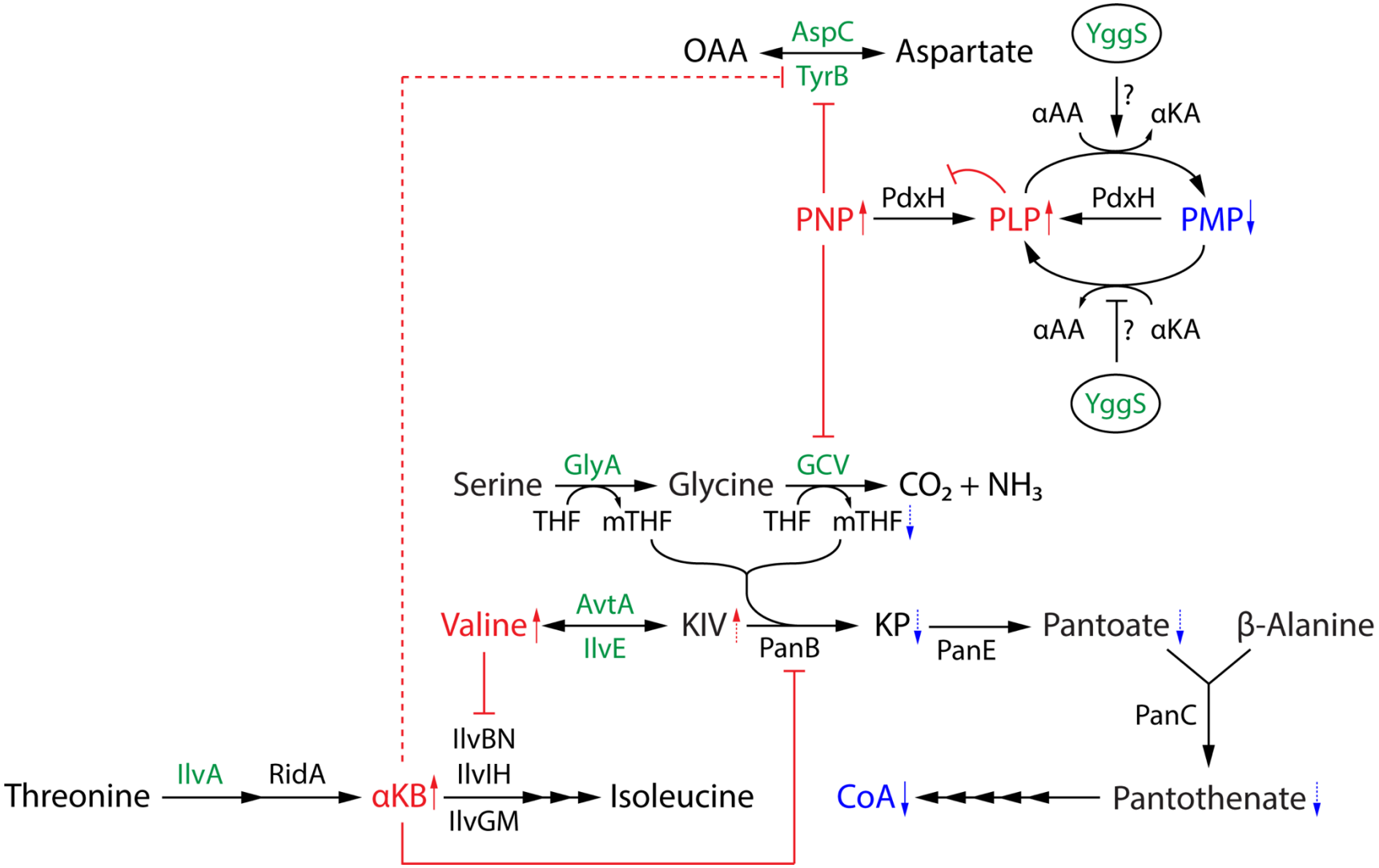
OAA
AspC
TyrB
Aspartate
YggS
?
αAA
αKA
PNP
PdxH
PLP
PdxH
PMP
αAA
?
αKA
YggS
Serine
GlyA
THF
mTHF
Glycine
GCV
THF
mTHF
CO2 + NH3
Valine
AvtA
IlvE
KIV
PanB
KP
PanE
Pantoate
β-Alanine
PanC
IlvBN
Threonine
IlvA
RidA
αKB
IlvIH
IlvGM
Isoleucine
CoA
Pantothenate

Figure 6.1 – Working model of YggS function and how lack of this protein impacts the metabolic network of *S. enterica* and *E. coli*. YggS is predicted to directly or indirectly facilitate PLP→PMP or dampen PMP→PLP conversion. A mutation in *yggS* results in decreased PMP and increased PLP pools (29), the latter of which inhibits PdxH activity (30, 31), leading to accumulation of the PNP substrate (16, 19, 29, 32). PNP accumulation can inhibit PLP-dependent enzymes such as GcvP of the GCV system (19) and TyrB (20). Inhibition of the GCV system leads to reduced mTHF level, which limits the rate of KIV→KP conversion catalyzed by PanB, subsequently lowering flux through CoA synthesis (15) and accumulating the KIV substrate. Increased KIV leads to higher production of valine, which can inhibit IlvBN and IlvIH (33) and cause αKB accumulation in *E. coli yggS* mutant (15). Accumulated αKB further dampens activity of PanB (34) and TyrB (20). Green highlight shows PLP-dependent enzymes/proteins. Red (↑), blue (↓), solid, and dashed arrows indicate increased, decreased, experimentally shown, and predicted metabolite levels, respectively, of a *yggS* mutant compared to wild type. Red solid lines represent direct inhibition, whereas dashed red lines represent indirect inhibitory effects. Abbreviations: PNP, pyridoxine 5′-phosphate; PLP, pyridoxal 5′-phosphate; PMP, pyridoxamine 5′-phosphate; αAA, α-amino acid; αKA, α-keto acid; OAA, oxaloacetate; GCV, glycine-cleavage system; THF, tetrahydrofolate; mTHF, 5,10-methylenetetrahydrofolate; KIV, α-ketoisovalerate; KP, ketopantoate; αKB, α-ketobutyrate.

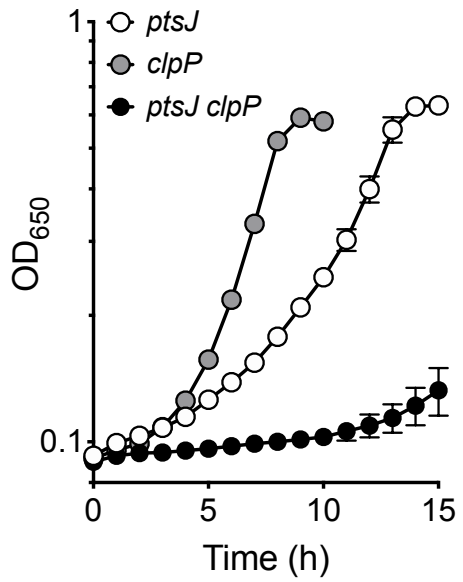

Figure 6.2 – Mutation in *clpP* leads to a synthetic dPN sensitivity in a *ptsJ* mutant. *S. enterica ptsJ* (DM17239), *clpP* (DM17166), and *ptsJ clpP* (DM17250) were grown in minimal NCE glucose supplemented with 0.5 μM dPN. Data were obtained from three biological replicates. Error bars show standard deviations from the mean value.

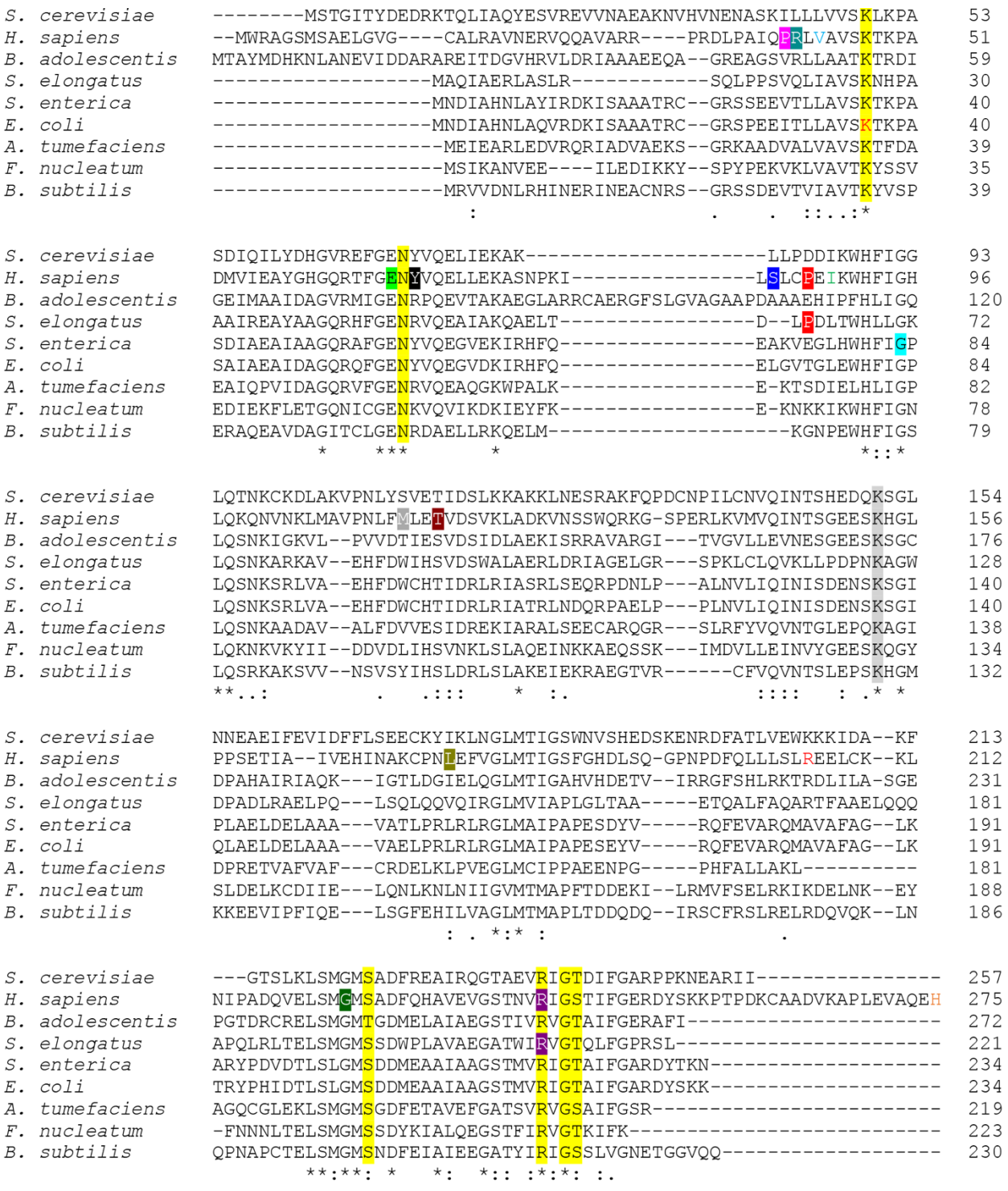

Figure 6.3 – Conservation of isolated YggS variants. Sequences of YggS homologs from *Saccharomyces cerevisiae*, *Homo sapiens* (human), *Bifidobacterium adolescentis*, *Synechococcus elongatus*, *Salmonella enterica*, *Escherichia coli*, *Agrobacterium tumefaciens*, *Fusobacterium*

nucleatum, and *Bacillus subtilis* were aligned using Clustal Omega (v1.2.4). Yellow highlight shows residues forming the putative active site. Other highlighted residues indicate reported YggS variants from different organisms (see Table 6.2 for more details). A star represents a fully conserved residue. A colon and a period represent conservation between residues with strongly and weakly similar properties, respectively.